AN ABSTRACT OF THE DISSERTATION OF

Krista Longnecker for the degree of Doctor of Philosophy in Oceanography presented on July 2, 2004.

Title: Bacterioplankton in the Oregon Upwelling System: Distribution, Cell-specific Leucine Incorporation, and Diversity

Abstract approved:

Redacted for privacy

Barry F. Sherr

Marine bacterioplankton play an important role in global elemental cycles because they return carbon dioxide and nutrients to the biosphere as they reduce organic matter. Furthermore, marine bacterioplankton are not uniformly active, and subpopulations of the in situ community may be more or less active at any given time. Defining whether or not a cell is 'active' is not without difficulty, and the result varies depending on the assay used, since different assays examine different physiological processes within a cell. Linking the level of activity of a cell with its phylogenetic identity is an additional important step in examination of the role of marine prokaryotes in global elemental cycles. In this project, flow cytometry was used in two ways to examine relative cell-specific metabolic activity in bacterioplankton cells: as relative cell-specific nucleic acid content via staining with SYBR Green I, and as ability to reduce sufficient 5-cyano-2,3-ditolyl tetrazolium chloride (CTC) to be identified as having an active electron transport system. Based on flow cytometric sorting of cells labeled with ^{3}H-leucine, the high nucleic acid (HNA) cells had higher cell-specific leucine incorporation rates than the low nucleic acid (LNA) cells. The HNA cells were also responsible for proportionately more of the leucine incorporation by the total heterotrophic population. While the CTC-positive cells had higher average cell-specific leucine incorporation rates than the HNA cells, their low abundances meant that they were responsible for less than 15% of the total leucine incorporation. The diversity of *Bacteria* observed within the HNA and LNA assemblages was

examined using phylogenetic analysis based on the V3-V4-V5 variable regions of 16S rRNA genes. Most of the phylogenetic groups of *Bacteria* identified in this study were present in both the HNA and LNA assemblage and had, at times, an active electron transport system (i.e., were able to reduce CTC). Finally, non-metric multidimensional scaling was presented as a new method to analyze DNA sequence data in conjunction with measured environmental parameters.

Bacterioplankton in the Oregon Upwelling System: Distribution, Cell-specific Leucine Incorporation, and Diversity

by

Krista Longnecker

A DISSERTATION

submitted to

Oregon State University

in partial fulfillment of

the requirements for the

degree of

Doctor of Philosophy

Presented July 2, 2004

Commencement June 2005

Doctor of Philosophy dissertation of Krista Longnecker presented on July 2, 2004

APPROVED:

Redacted for privacy

Major Professor, representing Oceanography

Redacted for privacy

Dean of the College of Oceanic and Atmospheric Sciences

Redacted for privacy

Dean of Graduate School

I understand that my dissertation will become part of the permanent collection of Oregon State University libraries. My signature below authorizes release of my dissertation to any reader upon request.

Redacted for privacy

Krista Longnecker, Author

ACKNOWLEDGMENTS

I greatly appreciate the guidance I have received from Barry Sherr and Evelyn Sherr, guidance which began at the very start of my time at COAS. Barry has shown me that crazy ideas are possible and valid ways to address questions, while Ev's consideration of this project in light of other research in the area is very much appreciated. My other committee members (Kate Field, Steve Giovannoni, Wayne Huber, and Ricardo Letelier) have also asked intriguing and insightful questions about the research and I appreciate their input into this project.

Oregon State University, and in particular COAS, has been a tremendous place to be a graduate student, because of the faculty, the other students, and the behind the scenes support of different parts of the administration. I thank Charlie Miller for making me raise questions about other people's research and my own research. Bruce McCune of the botany department gave me an excellent grounding in multivariate statistics through his class and by patiently answering questions even after the end of the term.

I was lucky to arrive at COAS with a great cohort of students. Perhaps some day there will be a new research institute representing the range of scientific questions that can be answered by Mark Baumgartner, Lisa Eisner, Jaime Gómez-Gutiérrez, Sam Laney, Daniel Palacios, and Malinda Sutor. Certainly I have enjoyed both the science and non-science discussions with this group and their significant others, and I look forward to working with all of them in the future.

Along the way towards obtaining my degree, I received help and ship time from other people which I greatly appreciate. The ground work for the research presented in Chapters Two and Four was initially conducted in 2001 on a series of day-long cruises on the RV *Elakha*. I would like to thank Tim Cowles' lab for the opportunity to participate on those cruises. Two undergraduates, Maike Lichtenberg and Delfina Homen, were extremely helpful, and I would still working in the lab if not for their help. Finally, all of the data presented here were generated from samples collected during a 2002 cruise on the RV *Wecoma*. I thank the captain, crew, and marine technicians of the RV *Wecoma* for their assistance during the cruise and the

other cruise participants. The opportunity to participate on a cruise with a group of researchers interested in answering the same question, but using different methods, was wonderful. I also enjoyed the discussions during and following the cruise, and think that the broader implications of this project became much clearer thanks to their input.

This research was funded by NSF OCE-0002236 and OCE-0240785 to B.F.S. and E.B.S., and additional support for laboratory equipment came from an OSU Research Equipment Reserves Fund grant.

CONTRIBUTION OF AUTHORS

Drs. Barry Sherr and Evelyn Sherr contributed to the collection of the data, its analysis, and the editing of Chapters Two and Four of this dissertation.

TABLE OF CONTENTS

TABLE OF CONTENTS (CONTINUED)

TABLE OF CONTENTS (CONTINUED)

TABLE OF CONTENTS (CONTINUED)

LIST OF FIGURES

LIST OF FIGURES (CONTINUED)

Figure Page

LIST OF FIGURES (CONTINUED)

Figure Page

LIST OF TABLES

LIST OF APPENDIX TABLES

LIST OF APPENDIX FIGURES

LIST OF APPENDIX FIGURES (CONTINUED)

Bacterioplankton in the Oregon Upwelling System: Distribution, Cell-specific Leucine Incorporation, and Diversity

1 Introduction

1.1 Background

> "Though often invaluable for estimating the total number of microorganisms in certain materials, direct microscopic counts give very little information concerning the nature of the microorganisms, often failing to distinguish inactive or dead cells from living ones." (ZoBell 1946, page 41)

Although fifty years have passed since ZoBell noted the difficulty in determining if a cell is inactive or dead, there are still disagreements among marine microbial ecologists about how to determine if a cell is dead or alive. Even defining cell death in prokaryotes is not without controversy. The level of activity in marine prokaryotes is important because on global scales of space and time, the amount of carbon dioxide they produce essentially balances primary production. Thus, one role of heterotrophic bacterioplankton is to return carbon dioxide and nutrients to the biosphere. Although the global carbon cycle is not the immediate focus of this research, on a larger scale it drives the questions for my research interests due to the importance of the global carbon cycle and the recent interest in quantifying changes in atmospheric carbon dioxide levels.

Currently, there is no consensus on what 'activity' means for prokaryotic cells. Furthermore, the assays used to identify 'active' cells rely on different proxies that interact with different components of the cells' metabolic machinery. During unbalanced growth, the different components of a cell may be uncoupled, which further complicates interpretation of different assays. That these factors lead to a lack of consensus among methods is not surprising. Several studies support the idea that marine bacterial cells are not uniformly active; instead sub-populations of the bacterial assemblage are more or less active at any one time (del Giorgio and Bouvier 2002;

Cottrell and Kirchman 2003; Smith and del Giorgio 2003). In oligotrophic environments, bacteria may be in a starvation-survival mode when insufficient energy is present to allow growth or reproduction (Morita 1997). Even after months of starvation, isolates from marine systems are able to respond to nutrient additions (Amy and Morita 1983). This suggests that the starvation-survival mode is a viable, cellular state, and may be one strategy marine bacterioplankton use to respond to periods with low nutrient and carbon input.

1.1.1 Methods used to identify cells as 'active'

There are a variety of methods used to identify metabolically 'active' cells and each has resulted in different conclusions about which cells are 'active' and what proportion of the community the 'active' cells represent. Some of this may be caused by variations between the protocols used for each method. However, each method measures different physiological properties of a cell; thus, lack of agreement in the results between assays may represent varying responses of a cell to each assay. The result is little agreement about how to measure 'activity' and what is the best method to use.

1.1.1.1 Examining a cell's ability to exclude specific compounds

One broad class of assays relies on cells' ability to prevent molecules from entering the cell. Cells with intact membranes are able to exclude large compounds, such as rhodamine and propidium iodide (PI). Thus if a cell is stained with rhodamine or PI, it has a compromised membrane and may not be a viable cell. Cultures incubated with antibiotics chosen on a species-specific basis to inhibit growth, show an increase in intracellular PI over time (Suller and Lloyd 1999). PI has also been used in a dual staining method with SYBR Green to examine differences between the abilities of high nucleic acid (HNA) and low nucleic acid (LNA) cells to exclude PI (Grégori et al. 2001). While all of the HNA cells were able to exclude PI, only 68% of the LNA cells were able to exclude PI (Grégori et al. 2001). In the single seawater

sample tested in this study, around one-third of the LNA community had a compromised membrane (Grégori et al. 2001).

Cells can also let in molecules due to the depolarization of their membrane, which can indicate a decrease in a cell's viability. The compound bis-(1,3-dibutylbarbituric acid) trimethine oxonol ($DiBAC_4(3)$) will enter cells with depolarized membranes and bind to lipid-containing intracellular components (Jepras et al. 1995; Beck and Huber 1997; Novo et al. 1999). There are examples of using $DiBAC_4(3)$ in laboratory cultures with *E. coli* and *Salmonella* (Jepras et al. 1995; Novo et al. 1999), or using $DiBAC_4(3)$ to label non-viable cells to avoid when choosing cells with optical tweezers for further culturing efforts (Beck and Huber 1997). Cultures stressed with either antibiotics (Suller and Lloyd 1999) or starvation (López-Amorós et al. 1997) show increases in the number of cells containing $DiBAC_4(3)$. In starved cells, these increases occur concurrently with decreases in abundance of cells able to reduce 5-cyano-2,3-ditolyl tetrazolium chloride (CTC). While the addition of nutrients to the starved cultures causes a subsequent decrease in the number of cells stained with $DiBAC_4(3)$, the number of CTC-positive cells does not increase, suggesting that the cells enter a state without respiratory activity, although their membranes can return to a polarized state (López-Amorós et al. 1997).

SYTOX is a another stain which will enter cells with depolarized membranes, although it differs from $DiBAC_4(3)$ as it binds to nucleic acids within the cells (Roth et al. 1997). In starved *E. coli* and *Salmonella* cultures, although there are initial differences in the SYTOX fluorescence between the live and heat-killed cells, over time the SYTOX fluorescence histograms of the starved, but presumed live, cells more closely resemble the starved, heat-killed controls (Lebaron et al. 1998). Thus the application of SYTOX to examine 'activity' of heterotrophic communities has to be considered with caution. SYTOX has been used to examine viability in phytoplankton cells after infection with viral particles (Brussaard et al. 2001), and in a field study examining the range of phytoplankton viability in samples from the North Atlantic (Veldhuis et al. 2001). To my knowledge, there are no examples of using SYTOX to examine viability of heterotrophic bacterioplankton in marine systems.

Oligonucleotide probes targeting the ribosomal RNA of a cell have also proven useful in marine microbial ecology. Fluorescent in situ hybridizations (FISH) can be used to identify prokaryotes through the use of oligonucleotide probes designed to target known regions of the 16S rRNA gene or the 23S rRNA gene (Olsen et al. 1986; DeLong et al. 1989; Amann 1995). FISH relies on the presence of target sites within the ribosomes; therefore, changes in the cellular abundance of ribosomes changes the observed fluorescence within the cell (Kerkhof and Ward 1993; Oda et al. 2000). The RNA content of cells is correlated with growth rate (DeLong et al. 1989; Kemp et al. 1993; Poulsen et al. 1993). However, there are large differences between different isolates; therefore the method may only be useful when applied to a single species (Kemp et al. 1993). In addition to changes in growth rate, a decrease in fluorescence from the EUB338 probe (Amann et al. 1990) is hypothesized to be due to increased cellular stress in the mixing zone of an estuary (del Giorgio and Bouvier 2002).

The Vital Stain and Probe method (VSP) uses a combination of FISH and physiological stains to identify four different types of cells: 1) live and active, 2) live, with low or no activity, 3) dead, and 4) dead but recently active (Williams et al. 1998; Howard-Jones et al. 2001; Howard-Jones et al. 2002). VSP uses FISH to identify cells with sufficient ribosomal RNA contents to be labeled with the probes; labeled cells are considered 'active' cells. An additional staining step uses PI to identify cells with a permeable membrane; cells that allow the PI stain to enter the cell are considered dead. Use of this method in the Arctic suggested that live, but low activity cells are the most abundant component of the ecosystem (Howard-Jones et al. 2002).

1.1.1.2 Identifying cells with an active electron transport system

Cells with an active electron transport system (ETS) have been identified through uptake of the fluorogenic dye 5-cyano-2,3-ditolyl tetrazolium chloride (CTC), which, when reduced in the cell's ETS, will fluorescence red due to its conversion into insoluble, fluorescent formazan crystals (Rodriguez et al. 1992; Smith and McFeters 1997). Laboratory experiments with *Escherichia coli* K-12 indicate that CTC is reduced by aerobic dehydrogenases (succinate and NAD(P)H) in the respiratory chain

of whole cells (Smith and McFeters 1997). The use of CTC as a proxy for identifying metabolically 'active' cells is controversial because of questions about (1) the toxicity of CTC, (2) whether all cells can reduce CTC, and (3) the lower proportion of active cells identified through the use of CTC (Ullrich et al. 1996; Karner and Fuhrman 1997; Yamaguchi and Nasu 1997; Ullrich et al. 1999). However, in one study, all of the marine heterotrophic cultures tested were capable of CTC reduction (Sherr et al. 1999a). In another study, the addition of organic substrates resulted in increases in the abundance of CTC-positive cells (Choi et al. 1999).

The use of CTC in aquatic systems is supported by the positive correlation between the abundance of CTC-positive cells with whole water respiration rates (Smith 1998). The abundance of CTC-positive cells is also positively correlated with volumetric incorporation rates of ^{3}H-leucine or ^{3}H-thymidine (del Giorgio et al. 1997; Sherr et al. 1999a; Sherr et al. 1999b) and the CTC-positive cells are, on average, larger than the bulk heterotrophic bacterial community (Gasol et al. 1995; Søndergaard and Danielsen 2001). Thus the CTC assay seems to identify the most 'highly active' cells within a bacterial assemblage (Sherr et al. 1999a; Nielsen et al. 2003). Denaturing gradient gel electrophoresis (DGGE) of a variable region of the 16S rRNA gene has been used to compare the diversity of cells capable of CTC reduction with the total bacterial community (Bernard et al. 2000b; Bernard et al. 2001). The diversity of bands in the CTC-positive community included *Roseobacter* and a sequence clustering with agg58 within the *Bacteroidetes* (Bernard et al. 2000b). However, the water samples were incubated with yeast extract for 24 hours prior to conducting the CTC assay. Therefore, the differences between the CTC-positive community and the in situ community need to be considered cautiously in this study.

1.1.1.3 Variability in nucleic acid content and DNA synthesis

Flow cytometric analysis has identified two major groups of bacterial cells based on cell-specific nucleic acid content: high or low nucleic acid cells (HNA and LNA cells, respectively; Li et al. 1995; Jellett et al. 1996; Gasol and del Giorgio 2000). In cultures, the majority of cells in exponential phase growth are HNA cells,

while the LNA cell numbers increase in late stationary phase (Jellett et al. 1996). These early data on the differences in the HNA and LNA cell abundance patterns led to the hypothesis that the HNA cells are the active, and dynamic, members of the community (Li et al. 1995; Jellett et al. 1996; Gasol et al. 1999); conversely the LNA cells have been thought to be dead or dying cells, or cells with lower cell-specific metabolic activity (Zubkov et al. 2001b; Smith and del Giorgio 2003). Some mesocosm experiments support this hypothesis since the abundance of HNA cells increases over the incubation period while there is little or no change in the abundance of the LNA cells (Li 1995; Gasol et al. 1999; Flaten et al. 2003; Wetz and Wheeler 2004). The presence of heterotrophic nanoflagellates (HNF) results in no net growth in the HNA cells and a concurrent decrease in the LNA cell abundance, suggesting the HNF are grazing the larger, more active cells (Gasol et al. 1999), as Gonzalez and colleagues (1993) and Sherr and colleagues (1992) also observed. Conversely, LNA cells are more abundant in oligotrophic systems (Li 1995; Casotti et al. 2000; Jochem 2001; Vaqué et al. 2001; Andrade et al. 2003), indicating they may play a larger role in more oligotrophic systems or may be composed of a phylogenetically different group of microorganisms.

Whether the diversity of LNA cells is different from the HNA cells has not been adequately explored. One possible explanation for the changes in HNA cell numbers is that the LNA cells change into HNA cells. Servais and colleagues (2003) used single-strand conformation polymorphism fingerprinting (SSCP) to show that the HNA and LNA cell assemblages were very similar in samples collected from the Mediterranean coast; however, data using FISH and clone libraries on samples from the North Sea revealed that the HNA and LNA cell assemblages are dominated by different *Bacteria* (Zubkov et al. 2001a; Zubkov et al. 2001b; Zubkov et al. 2002). The differences between these two sets of results could either be due to differences in the ecosystems sampled, or to methodological differences. The diversity of cells stained with nucleic acid stains has also been examined using DGGE for different size classes of cells, where the size classes were arbitrary divisions along the side scatter axis on cytograms of side scatter versus green fluorescence (Bernard et al. 2000a). There were

DGGE bands common to all the size classes; however, the diversity of *Bacteria* was greater for the smaller size classes (Bernard et al. 2000a).

The phylogenetic diversity of cells synthesizing DNA has also been examined through detection of cells incorporating bromodeoxyuridine (BrdU, Urbach et al. 1999; Pernthaler et al. 2002). BrdU is structurally similar to thymidine and is incorporated into cells synthesizing DNA. Fluorescent antibodies for this molecule are then used to quantify the amount of BrdU which has been incorporated into the cell's DNA, and paramagnetic beads can be used to separate the BrdU-labeled portion of the community. However, there is disagreement regarding whether all marine microorganisms can incorporate BrdU (Urbach et al. 1999; Pernthaler et al. 2002; Hamasaki et al. 2004). In a series of inlets in Washington, the diversity of the total community did not vary, although the diversity of BrdU incorporating bacterioplankton did vary between inlets (Evans et al. 2004).

Flow cytometric detection of HNA and LNA cell populations has been used on samples incubated with radioactively-labeled compounds to address differences in cell-specific incorporation rates (Servais et al. 1999; Lebaron et al. 2001; Zubkov et al. 2001b; Servais et al. 2003). In both discrete samples and samples from a mesocosm enriched with nitrogen and phosphorus, HNA cells were responsible for a larger fraction of leucine incorporation than LNA cells (Servais et al. 1999; Lebaron et al. 2001; Servais et al. 2003). However, in the Celtic Sea, LNA cells had higher biomass specific rates in the surface waters than HNA cells, although in the pycnocline and deeper waters, LNA cells incorporated less ^{35}S labeled methionine than HNA cells when incorporation was normalized to biomass (Zubkov et al. 2001b). Furthermore, CTC-positive cells incubated with ^{3}H-leucine contributed < 60% of the total incorporation (Servais et al. 2001). While these studies examined incorporation rates of radioactively-labeled compounds in different ecosystems, no environmental parameters were included in analysis of the data from the few marine samples analyzed.

1.1.1.4 Identification of cells incorporating radioactively-labeled metabolic precursors

Another method to examine cell-specific incorporation rates combines FISH and microautoradiography, and was concurrently developed by several groups (Lee et al. 1999; Ouverney and Fuhrman 1999; Cottrell and Kirchman 2000). This method has the advantage of being able to determine the diversity of microorganisms actually incorporating the radioactively-labeled substrate. Thus far the method has provided evidence that marine *Archaea* can incorporate amino acids (Ouverney and Fuhrman 2000), different phylogenetic groups of *Bacteria* utilize different sources of organic matter (Cottrell and Kirchman 2000), and the utilization of dimethylsulfoniopropionate (DMSP) is not restricted to the *Alphaproteobacteria* (Malmstrom et al. 2004). Furthermore, using the size of the silver grains obtained from the microautoradiography as a proxy for relative cell-specific activity, there was variability in the single-cell activity between the different phylogenetic groups identified by FISH in the Delaware Bay estuary (Cottrell and Kirchman 2003).

1.1.2 Using 16S rRNA genes to identify marine prokaryotes

Since the advent of the use of molecular techniques to identify microorganisms (Olsen et al. 1986), they have been widely applied to the identification of the prokaryotic community in marine systems (for review see: Giovannoni and Rappé 2000). As sequencing technology has improved, larger portions of genomes have been examined through the sequencing of entire genomes from some marine cultures (Palenik et al. 2003; Rocap et al. 2003), to the sequencing of the entire metagenome of a given ecosystem (Venter et al. 2004). Analysis based on the 16S rRNA gene from samples collected off the Oregon coast has revealed no major differences from bacterial communities studied in other marine systems (Rappé et al. 2000). Sequences obtained from clone libraries created from samples collected off the Oregon coast include *Gammaproteobacteria*, *Alphaproteobacteria* (SAR116, SAR11, *Roseobacter*), Marine Group A / SAR406, *Actinobacteria* (Marine Gram-positives) and *Betaproteobacteria* (Rappé et al. 2000). The 16S rRNA gene clone libraries of the

prokaryotic community in the vicinity of the Columbia River plume has identified many of the same *Bacteria* found in marine waters off the Oregon coast (Crump et al. 1999). However, there are differences in the Columbia River samples between sequences found attached to particles and sequences obtained from the free-living community (Crump et al. 1999).

1.1.3 Analysis of DNA sequence data in an ecological context

Analysis of ecological data collected from studies such as those conducted off the Oregon coast must consider the interactions between biotic and abiotic factors. One method particularly suited to environmental studies is non-metric multidimensional scaling (NMS). Since NMS is a non-parametric technique, the data are not expected to meet requirements of multivariate normality. NMS is a form of multivariate statistical analysis that can be used to examine the differences (or similarities) between samples by reducing the comparisons between samples from a multidimensional space to fewer dimensions, preferably two or three. NMS has been used to compare samples being examined visually, microscopically, or with molecular techniques (see for example: van Hannen et al. 1999; Peterson et al. 2002). To my knowledge, there has been no attempt at using NMS to systematically compare individual DNA sequences. DNA sequence data are traditionally analyzed through the calculation of distance matrices using nucleotide substitution models to examine the differences between pairs of DNA sequences. The data are then visually presented as trees calculated using one of several available optimality criteria. The best tree is chosen from a set of trees, and the level of support of grouping within the tree is evaluated by bootstrapping or jackknifing. In Chapter Three, I have proposed using NMS to analyze DNA sequence data and explored how to evaluate the use of NMS for sequence data. As an example, NMS is used to examine the diversity of sequences obtained from a subset of the Oregon coast samples in conjunction with the concurrently measured environmental parameters.

1.2 Research objectives and summary of results

The underlying goal of this dissertation was to apply a subset of assays to examine differences in activity, diversity, and distribution of metabolically active cells within the heterotrophic prokaryotic community from a set of samples collected off the Oregon coast in the spring of 2002. Chapter Two focuses on cell-specific leucine incorporation in whole seawater samples and in subpopulations of these same samples. These subpopulations were defined based on cell-specific nucleic acid content, which allowed the samples to be sorted by flow cytometry into HNA and LNA assemblages. An additional subpopulation was defined based on cells' ability to reduce CTC. The differences in cell-specific leucine incorporation and total leucine incorporation for each of the subpopulations were examined for three sampling stations, different depths, and against measured environmental parameters. The abundances of the cytometrically-defined groups, both photoautotrophic and heterotrophic, were examined for ten sampling stations, and revealed that the shelf station samples at the time of the cruise were composed of different cytometrically-defined groups than the slope and offshore samples.

Chapter Three presents a new method of analyzing DNA sequence data in conjunction with measured environmental parameters. This chapter compares the results from NMS analysis with neighbor joining trees and discusses the correlation with environmental parameters. The NMS results were comparable to the results from the neighbor joining trees calculated using the same DNA sequences. The correlations with measured environmental parameters were low, indicating that the temporal and / or spatial scale of measured environmental and biological parameters might not have been appropriate to explain the differences between the DNA sequences.

The goal of Chapter Four was to address two hypotheses regarding the diversity of the flow cytometrically-defined groups. The first hypothesis was that the phylogenetic diversity of the HNA cells was the same as the diversity of LNA cells. The second hypothesis was that the diversity of the CTC-positive cells would only reflect the diversity of a subset of the entire heterotrophic community at the time of sampling. In the samples from the Oregon coast, most of the phylogenetic groups

could be present in either the HNA or the LNA population, or both. Furthermore, all but one of the phylogenetic groups identified from the sorted populations were also obtained in the CTC-positive sorts, indicating that the ability to reduce CTC was widespread throughout the *Bacteria*.

The dissertation concludes with a summary of the results presented in the previous chapters and suggestions for future research to address some of the questions raised by this project. Finally, the appendix includes information about the calibrations conducted following the *Wecoma* cruise, details on defining the CTC-positive cells and the photoautotrophic cells using the flow cytometer, and the trees used to place the sequences obtained from the DGGE bands in a phylogenetic context.

There are two different conventions regarding the use of the term 'bacteria' in this dissertation. In chapter Four, the term *Bacteria* (capital 'B' and italicized) is used to indicate one of the two domains of prokaryotic life, the other being the *Archaea*. However, in the chapter discussing the cell-specific leucine incorporation, the term 'bacteria' was used to broadly discuss heterotrophic prokaryotes and does not specifically refer to microorganisms within the domain *Bacteria*. Furthermore, the nomenclature presented in the second edition of *Bergey's Manual of Systematic Bacteriology* is used throughout the dissertation. Therefore *Alphaproteobacteria* is used rather than □-*Proteobacteria* (similarly for the other classes of *Proteobacteria*), and phylum *Bacteroidetes* includes the classes *Bacteroidetes*, *Flavobacteria*, and *Sphingobacteria* rather than using the terms '*Cytophaga-Flavobacterium*' or '*Cytophaga*-like' (Kirchman 2002).

All the samples discussed in this dissertation were collected during a cruise off the Oregon coast in April/May of 2002, and therefore the data represent a single snapshot in space and time. After the cruise, we learned that 2002 data from the GLOBEC project revealed increased transport of colder, fresher water from the subarctic Pacific to the region encompassed by the Newport Hydrographic line relative to the previous five years of data collected during the GLOBEC project (Barth 2003; Murphree et al. 2003; Strub and James 2003). Wheeler and colleagues (2003) proposed that the increase in primary production in the colder, fresher water would be

accompanied by an increase in respiration in the water column. Thus, the data presented here from 2002 may not be indicative of average conditions off the Oregon coast since we also observed the colder, fresher water at two stations in the later part of the cruise. Regardless of the presence of the anomalous water mass, the data from this cruise present an interesting examination of differences among the proxies used to define heterotrophic cells' metabolic activity, and the differences in the phylogenetic diversity and distribution patterns of each cytometrically-defined group.

1.3 Literature cited

Amann, R.I. (1995). Fluorescently labelled, rRNA-targeted oligonucleotide probes in the study of microbial ecology. *Molecular Ecology* **4**: 543-554.

Amann, R.I., L. Krumholz and D.A. Stahl (1990). Fluorescent-oligonucleotide probing of whole cells for determinative, phylogenetic, and environmental studies in microbiology. *Journal of Bacteriology* **172**: 762-770.

Amy, P.S. and R.Y. Morita (1983). Starvation-survival patterns of sixteen freshly isolated open-ocean bacteria. *Applied and Environmental Microbiology* **45**: 1109-1115.

Andrade, L., A.M. Gonzalez, F.V. Araujo and R. Paranhos (2003). Flow cytometry assessment of bacterioplankton in tropical marine environments. *Journal of Microbiological Methods* **55**: 841-850.

Barth, J.A. (2003). Anomalous southward advection during 2002 in the Northern California Current: evidence from lagrangian surface drifters (doi:10.1029/2003GL017511). *Geophysical Research Letters* **30**: 8024.

Beck, P. and R. Huber (1997). Detection of cell viability in cultures of hyperthermophiles. *FEMS Microbiology Letters* **147**: 11-14.

Bernard, L., C. Courties, C. Duperray, H. Schäfer, G. Muyzer and P. Lebaron (2001). A new approach to determine the genetic diversity of viable and active bacteria in aquatic ecosystems. *Cytometry* **43**: 314-321.

Bernard, L., C. Courties, P. Servais, M. Troussellier, M. Petit and P. Lebaron (2000a). Relationships among bacterial cell size, productivity, and genetic diversity in aquatic environments using cell sorting and flow cytometry. *Microbial Ecology* **40**: 148-158.

Bernard, L., H. Schäfer, F. Joux, C. Courties, G. Muyzer and P. Lebaron (2000b). Genetic diversity of total, active and culturable marine bacteria in coastal seawater. *Aquatic Microbial Ecology* **23**: 1-11.

Brussaard, C.P.D., D. Marie, R. Thyrhaug and G. Bratbak (2001). Flow cytometric analysis of phytoplankton viability following viral infection. *Aquatic Microbial Ecology* **26**: 157-166.

Casotti, R., C. Brunet, B. Aronne and M. Ribera d'Alcala (2000). Mesoscale features of phytoplankton and planktonic bacteria in a coastal area as induced by external water masses. *Marine Ecology Progress Series* **195**: 15-27.

Choi, J.W., B.F. Sherr and E.B. Sherr (1999). Dead or alive? A large fraction of ETS-inactive marine bacterioplankton cells, as assessed by reduction of CTC, can become ETS-active with incubation and substrate addition. *Aquatic Microbial Ecology* **18**: 105-115.

Cottrell, M.T. and D.L. Kirchman (2000). Natural assemblages of marine Proteobacteria and members of the *Cytophaga-Flavobacter* cluster consuming low- and high-molecular-weight dissolved organic matter. *Applied and Environmental Microbiology* **66**: 1692-1697.

Cottrell, M.T. and D.L. Kirchman (2003). Contribution of major bacterial groups to bacterial biomass production (thymidine and leucine incorporation) in the Delaware estuary. *Limnology and Oceanography* **48**: 168-178.

Crump, B.C., E.V. Armbrust and J.A. Baross (1999). Phylogenetic analysis of particle-attached and free-living bacterial communities on the Columbia River, its estuary, and the adjacent coastal ocean. *Applied and Environmental Microbiology* **65**: 3192-3204.

del Giorgio, P.A. and T.C. Bouvier (2002). Linking the physiologic and phylogenetic successions in free-living bacterial communities along an estuarine salinity gradient. *Limnology and Oceanography* **47**: 471-486.

del Giorgio, P.A., Y.T. Prairie and D.F. Bird (1997). Coupling between rates of bacterial production and the number of metabolically active cells in lake bacterioplankton, measured using CTC reduction and flow cytometry. *Microbial Ecology* **34**: 144-154.

DeLong, E.F., G.S. Wickham and N.R. Pace (1989). Phylogenetic stains: ribosomal RNA-based probes for the identification of single cells. *Science* **243**: 1360-1363.

Evans, C.T., B. Van Mooy, R.G. Keil, C. Greengrove and G. Chin-Leo (2004). Isolation of DNA from actively growing heterotrophic bacteria using 5-bromo-2'-deoxyuridine (BrdU). *American Society of Limnology and Oceanography / The Oceanography Society Ocean Research Conference*, Honolulu, HI.

Flaten, G.A.F., T. Castberg, T. Tanaka and T.F. Thingstad (2003). Interpretation of nutrient-enrichment bioassays by looking at sub-populations in a marine bacterial community. *Aquatic Microbial Ecology* **33**: 11-18.

Gasol, J.M. and P.A. del Giorgio (2000). Using flow cytometry for counting natural planktonic bacteria and understanding the structure of planktonic bacterial communities. *Scientia Marina* **64**: 197-224.

Gasol, J.M., P.A. del Giorgio, R. Massana and C.M. Duarte (1995). Active versus inactive bacteria: size-dependence in a coastal marine plankton community. *Marine Ecology Progress Series* **128**: 91-97.

Gasol, J.M., U.L. Zweifel, F. Peters, J.A. Fuhrman and Å. Hagström (1999). Significance of size and nucleic acid content in heterogeneity as measured by flow cytometry in natural planktonic bacteria. *Applied and Environmental Microbiology* **65**: 4475-4483.

Giovannoni, S.J. and M. Rappé (2000). Evolution, diversity, and molecular ecology of marine prokaryotes. *Microbial Ecology of the Oceans*. D.L. Kirchman (Ed). New York, Wiley-Liss, Inc.: 47-84.

González, J.M., E.B. Sherr and B.F. Sherr (1993). Differential feeding by marine flagellates on growing vs starving, and on motile vs non-motile, bacterial prey. *Marine Ecology Progress Series* **102**: 257-267.

Grégori, G., S. Citterio, A. Ghiani, M. Labra, S. Sgorbati, S. Brown and M. Denis (2001). Resolution of viable and membrane-compromised bacteria in freshwater and marine waters based on analytical flow cytometry and nucleic acid double staining. *Applied and Environmental Microbiology* **67**: 4662-4670.

Hamasaki, K., R.A. Long and F. Azam (2004). Individual cell growth rates of marine bacteria, measured by bromodeoxyuridine. *Aquatic Microbial Ecology* **35**: 217-227.

Howard-Jones, M.H., V.D. Ballard, A.E. Allen, M.E. Frischer and P.G. Verity (2002). Distribution of bacterial biomass and activity in the marginal ice zone of the central Barents Sea during summer. *Journal of Marine Systems* **38**: 77-91.

Howard-Jones, M.H., M.E. Frischer and P.G. Verity (2001). Determining the physiological status of individual bacterial cells. *Methods in Microbiology*. J.H. Paul (Ed), Academic Press Ltd. **30:** 175-206.

Jellett, J.F., W.K.W. Li, P.M. Dickie, A. Boraie and P.E. Kepkay (1996). Metabolic activity of bacterioplankton communities assessed by flow cytometry and single carbon substrate utilization. *Marine Ecology Progress Series* **136**: 213-225.

Jepras, R.I., J. Carter, S.C. Pearson, F.E. Paul and M.J. Wilkinson (1995). Development of a robust flow cytometric assay for determining numbers of viable bacteria. *Applied and Environmental Microbiology* **61**: 2696-2701.

Jochem, F.J. (2001). Morphology and DNA content of bacterioplankton in the northern Gulf of Mexico: analysis by epifluorescence microscopy and flow cytometry. *Aquatic Microbial Ecology* **25**: 179-194.

Karner, M. and J.A. Fuhrman (1997). Determination of active marine bacterioplankton: a comparison of universal 16S rRNA probes, autoradiography, and nucleoid staining. *Applied and Environmental Microbiology* **63**: 1208-1213.

Kemp, P.F., S. Lee and J. LaRoche (1993). Estimating growth rate of slowly growing marine bacteria from RNA content. *Applied and Environmental Microbiology* **59**: 2594-2601.

Kerkhof, L. and B.B. Ward (1993). Comparison of nucleic acid hybridization and fluorometry for measurement of the relationship between RNA/DNA ratio and growth rate in a marine bacterium. *Applied and Environmental Microbiology* **59**: 1303-1309.

Kirchman, D.L. (2002). The ecology of *Cytophaga-Flavobacteria* in aquatic environments. *FEMS Microbiology Ecology* **39**: 91-100.

Lebaron, P., P. Catala and N. Parthuisot (1998). Effectiveness of SYTOX green stain for bacterial viability assessment. *Applied and Environmental Microbiology* **64**: 2697-2700.

Lebaron, P., P. Servais, H. Agogué, C. Courties and F. Joux (2001). Does the high nucleic acid content of individual bacterial cells allow us to discriminate between active cells and inactive cells in aquatic systems? *Applied and Environmental Microbiology* **67**: 1775-1782.

Lee, N., P. Halkjær, K.H. Andreasen, S. Juretschko, J.L. Nielsen, K.-H. Schleifer and M. Wagner (1999). Combination of fluorescent in situ hybridization and microautoradiography—a new tool for structure-function analyses in microbial ecology. *Applied and Environmental Microbiology* **65**: 1289-1297.

Li, W.K.W. (1995). Composition of ultraphytoplankton in the central North Atlantic. *Marine Ecology Progress Series* **122**: 1-8.

Li, W.K.W., J.F. Jellett and P.M. Dickie (1995). DNA distributions in planktonic bacteria stained with TOTO or TO-PRO. *Limnology and Oceanography* **40**: 1485-1495.

López-Amorós, R., S. Castel, J. Comas-Riu and J. Vives-Rego (1997). Assessment of *E. coli* and *Salmonella* viability and starvation by confocal laser microscopy and flow cytometry using rhodamine 123, DiBAC4(3), propidium iodide, and CTC. *Cytometry* **28**: 298-305.

Malmstrom, R.R., R.P. Kiene and D.L. Kirchman (2004). Identification and enumeration of bacteria assimilating dimethylsulfoniopropionate (DMSP) in the North Atlantic and Gulf of Mexico. *Limnology and Oceanography* **49**: 597-606.

Morita, R.Y. (1997). *Bacteria in Oligotrophic Environments*. New York, Chapman and Hall.

Murphree, T., S.J. Bograd, F.B. Schwing and B. Ford (2003). Large scale atmosphere-ocean anomalies in the northeast Pacific during 2002 (doi:10.1029/2003GL017303). *Geophysical Research Letters* **30**: 8026.

Nielsen, J.L., M. Aquino de Muro and P.H. Nielsen (2003). Evaluation of the redox dye 5-cyano-2,3-tolyl-tetrazolium chloride for activity studies by simultaneous use of microautoradiography and fluorescence in situ hybridization. *Applied and Environmental Microbiology* **69**: 641-643.

Novo, D., N.G. Perlmutter, R.H. Hunt and H.M. Shapiro (1999). Accurate flow cytometric membrane potential measurement in bacteria using diethyloxacarbocyanine and a ratiometric technique. *Cytometry* **35**: 55-63.

Oda, Y., S.-J. Slagman, W.G. Meijer, L.J. Forney and J.C. Gottschall (2000). Influence of growth rate and starvation on fluorescent in situ hybridization of *Rhodopseudomonas palustris*. *FEMS Microbiology Ecology* **32**: 205-213.

Olsen, G.J., D.L. Lane, S.J. Giovannoni, N.R. Pace and D.R. Stahl (1986). Microbial ecology and evolution: A ribosomal RNA approach. *Annual Review of Microbiology* **40**: 337-366.

Ouverney, C.C. and J.A. Fuhrman (1999). Combined microautoradiography-16S rRNA probe technique for determination of radioisotope uptake by specific microbial cell types in situ. *Applied and Environmental Microbiology* **65**: 1746-1752.

Ouverney, C.C. and J.A. Fuhrman (2000). Marine planktonic *Archaea* take up amino acids. *Applied and Environmental Microbiology* **66**: 4829-4833.

Palenik, B., B. Brahamsha, F.W. Larimer, M. Land, L. Hauser, P. Chain, J. Lamerdin, W. Regala, E.E. Allen, J. McCarren, I. Paulsen, A. Dufresne, F. Partensky, E.A. Webb and J. Waterbury (2003). The genome of a motile marine *Synechococcus*. *Nature* **424**: 1037-1042.

Pernthaler, A., J. Pernthaler, M. Schattenhofer and R. Amann (2002). Identification of DNA-synthesizing bacterial cells in coastal North Sea plankton. *Applied and Environmental Microbiology* **68**: 5728-5736.

Peterson, W.T., J.E. Keister and L.R. Feinberg (2002). The effects of the 1997-1999 El Niño/La Niña events on the hydrography and zooplankton off the central Oregon coast. *Progress in Oceanography* **54**: 381-398.

Poulsen, L.K., G. Ballard and D.A. Stahl (1993). Use of rRNA fluorescence in situ hybridization for measuring the activity of single cells in young and established biofilms. *Applied and Environmental Microbiology* **59**: 1354-1360.

Rappé, M.S., K. Vergin and S.J. Giovannoni (2000). Phylogenetic comparisons of a coastal bacterioplankton community with its counterparts in open ocean and freshwater systems. *FEMS Microbiology Ecology* **33**: 219-232.

Rocap, G., F.W. Larimer, J. Lamerdin, S. Malfatti, P. Chain, N.A. Ahlgren, A. Arellano, M. Coleman, L. Hauser, W.R. Hess, Z.I. Johnson, M. Land, D. Lindell, A.F. Post, W. Regala, M. Shah, S.L. Shaw, C. Steglich, M.B. Sullivan, C.S. Ting, A. Tolonen, E.A. Webb, E.R. Zinser and S.W. Chisholm (2003). Genome divergence in two *Prochlorococcus* ecotypes reflects oceanic niche differentiation. *Nature* **424**: 1042-1047.

Rodriguez, G.G., D. Phipps, K. Ishiguro and H.F. Ridgway (1992). Use of a fluorescent redox probe for direct visualization of actively respiring bacteria. *Applied and Environmental Microbiology* **58**: 1801-1808.

Roth, B.L., M. Poot, S.T. Yue and P.J. Millard (1997). Bacterial viability and antibiotic susceptibility testing with SYTOX green nucleic acid stain. *Applied and Environmental Microbiology* **63**: 2421-2431.

Servais, P., H. Agogué, C. Courties, F. Joux and P. Lebaron (2001). Are the actively respiring cells (CTC+) those responsible for bacterial production in aquatic environments? *FEMS Microbiology Ecology* **35**: 171-179.

Servais, P., E.O. Casamayor, C. Courties, P. Catala, N. Parthuisot and P. Lebaron (2003). Activity and diversity of bacterial cells with high and low nucleic acid content. *Aquatic Microbial Ecology* **33**: 41-51.

Servais, P., C. Courties, P. Lebaron and M. Troussellier (1999). Coupling bacterial activity measurements with cell sorting by flow cytometry. *Microbial Ecology* **38**: 180-189.

Sherr, B.F., P. del Giorgio and E.B. Sherr (1999a). Estimating abundance and single-cell characteristics of respiring bacteria via the redox dye CTC. *Aquatic Microbial Ecology* **18**: 117-131.

Sherr, B.F., E.B. Sherr and J. McDaniel (1992). Effect of protozoan grazing on the frequency of dividing cells in bacterioplankton assemblages. *Applied and Environmental Microbiology* **58**: 2381-2385.

Sherr, E.B., B.F. Sherr and C.T. Sigmon (1999b). Activity of marine bacteria under incubated and *in situ* conditions. *Aquatic Microbial Ecology* **20**: 213-223.

Smith, E.M. (1998). Coherence of microbial respiration rate and cell-specific bacterial activity in a coastal planktonic community. *Aquatic Microbial Ecology* **16**: 27-35.

Smith, E.M. and P.A. del Giorgio (2003). Low fractions of active bacteria in natural aquatic communities? *Aquatic Microbial Ecology* **31**: 203-208.

Smith, J.J. and G.A. McFeters (1997). Mechanisms of INT (2-(4-iodophenyl)-3-(4-nitrophenyl)-5-phenyl tetrazolium chloride), and CTC (5-cyano-2,3-ditolyl tetrazolium chloride) reduction in *Escherichia coli* K-12. *Journal of Microbiological Methods* **29**: 161-175.

Søndergaard, M. and M. Danielsen (2001). Active bacteria (CTC+) in temperate lakes: temporal and cross-system variations. *Journal of Plankton Research* **23**: 1195-1206.

Strub, P.T. and C. James (2003). Altimeter estimates of anomalous transports into the northern California Current during 2000–2002 (doi:10.1029/2003GL017513). *Geophysical Research Letters* **30**: 8025.

Suller, M.T.E. and D. Lloyd (1999). Fluorescence monitoring of antibiotic-induced bacterial damage using flow cytometry. *Cytometry* **35**: 235-241.

Ullrich, S., B. Karrasch and H.-G. Hoppe (1999). Is the CTC dye technique an adequate approach for estimating active bacterial cells? *Aquatic Microbial Ecology* **17**: 207-209.

Ullrich, S., B. Karrasch, H.-G. Hoppe, K. Jeskulke and M. Mehrens (1996). Toxic effects on bacterial metabolism of the redox dye 5-cyano-2,3-ditolyl tetrazolium chloride. *Applied and Environmental Microbiology* **62**: 4587-4593.

Urbach, E., K.L. Vergin and S.J. Giovannoni (1999). Immunochemical detection and isolation of DNA from metabolically active bacteria. *Applied and Environmental Microbiology* **65**: 1207-1213.

van Hannen, E.J., W. Mooij, M.P. van Agterveld, H.J. Gons and H.J. Laanbroek (1999). Detritus-dependent development of the microbial community in an experimental system: qualitative analysis by denaturing gradient gel electrophoresis. *Applied and Environmental Microbiology* **65**: 2478-2484.

Vaqué, D., E.O. Casamayor and J.M. Gasol (2001). Dynamics of whole community bacterial production and grazing losses in seawater incubations as related to the changes in the proportions of bacteria with different DNA content. *Aquatic Microbial Ecology* **25**: 163-177.

Veldhuis, M.J.W., G.W. Kraay and K.R. Timmermans (2001). Cell death in phytoplankton: correlation between changes in membrane permeability, photosynthetic activity, pigmentation and growth. *European Journal of Phycology* **36**: 167-177.

Venter, J.C., K. Remington, J.F. Heidelberg, A.L. Halpern, D. Rusch, J.A. Eisen, D. Wu, I. Paulsen, K.E. Nelson, W. Nelson, D.E. Fouts, S. Levy, A.H. Knap, M.W. Lomas, K. Nealson, O. White, J. Peterson, J. Hoffman, R. Parsons, H. Baden-Tillson, C. Pfannkoch, Y.-H. Rogers and H.O. Smith (2004). Environmental genome shotgun sequencing of the Sargasso Sea. *Science* **304**: 66-74.

Wetz, M.S. and P.A. Wheeler (2004). Response of bacteria to simulated upwelling phytoplankton blooms. *Marine Ecology Progress Series* **272**: 49-57.

Wheeler, P.A., A. Huyer and J. Fleischbein (2003). Cold halocline, increased nutrients and higher chlorophyll off Oregon in 2002 (doi:10.1029/2003GLO17395). *Geophysical Research Letters* **30**: 8021.

Williams, S.C., Y. Hong, D.C.A. Danavall, M.H. Howard-Jones, D. Gibson, M.E. Frischer and P.G. Verity (1998). Distinguishing between living and nonliving bacteria: evaluation of the vital stain propidium iodide and its combined use with molecular probes in aquatic samples. *Journal of Microbiological Methods* **32**: 225-236.

Yamaguchi, N. and M. Nasu (1997). Flow cytometric analysis of bacterial respiratory and enzymatic activity in the natural aquatic environment. *Journal of Applied Microbiology* **83**: 43-52.

ZoBell, C.E. (1946). *Marine Microbiology*. Waltham, MA, Chronica Botanica.

Zubkov, M.V., B.M. Fuchs, S.D. Archer, R.P. Kiene, R. Amann and P.H. Burkill (2001a). Linking the composition of bacterioplankton to rapid turnover of dissolved dimethylsulphoniopropionate in an algal bloom in the North Sea. *Environmental Microbiology* **3**: 304-311.

Zubkov, M.V., B.M. Fuchs, P.H. Burkill and R. Amann (2001b). Comparison of cellular and biomass specific activities of dominant bacterioplankton groups in stratified waters of the Celtic Sea. *Applied and Environmental Microbiology* **67**: 5210-5218.

Zubkov, M.V., B.M. Fuchs, G.A. Tarran, P.H. Burkill and R. Amann (2002). Mesoscale distribution of dominant bacterioplankton groups in the northern North Sea in early summer. *Aquatic Microbial Ecology* **29**: 135-144.

2 High nucleic acid, low nucleic acid, and CTC-positive bacterial cells in an upwelling ecosystem: distribution and cell-specific leucine incorporation

2.1 Abstract

The distribution of metabolic activity among subpopulations of marine bacterioplankton is not well understood. To address this problem, water samples were collected from a series of stations along a transect from mesotrophic shelf waters to oligotrophic waters off the Oregon coast. Whole seawater bacterial leucine incorporation rates and cell-specific leucine incorporation rates were determined for different groups of bacterioplankton sorted with a flow cytometer based on (1) cell-specific nucleic acid content: high nucleic acid (HNA), low nucleic acid (LNA), and total cells (both HNA and LNA cells combined, autotrophic cells excluded); or (2) intracellular accumulation of reduced 5-cyano-2,3-ditolyl tetrazolium chloride (CTC), an indicator of an active electron transport system. The cell-specific rates of leucine incorporation were generally higher for HNA cells and CTC-positive cells compared to total cells and LNA cells. HNA cells accounted for most of the volumetric ^{3}H-leucine incorporation rates by the bacterial assemblage. The proportion of the volumetric leucine incorporation attributable to LNA cells was higher at an offshore, basin station. A high nitrate concentration accompanied the increased role of the LNA cells at the surface of this station. The lower cell abundances of CTC-positive cells caused this component of the bacterial assemblage to be responsible for only 5-13% of volumetric leucine incorporation. Nonmetric multidimensional scaling of the flow cytometrically-defined cells revealed the shelf stations clustered separately from the slope and offshore stations, primarily due to differing abundances of the photoautotrophic community.

2.2 Introduction

Heterotrophic bacterioplankton play important roles in marine biogeochemical cycles. Yet questions remain about the cell-specific distribution of metabolic activity in marine bacterioplankton assemblages in any given hydrological regime, time, or

depth in the water column. Although a variety of assays have been used to assess cell-specific activity in heterotrophic bacterioplankton, there is no consensus on the meaning of the results from these assays (Karner and Fuhrman 1997; Sherr et al. 1999; Smith and del Giorgio 2003). A main goal of this study was to compare data from three different assays used to distinguish levels of cell-specific metabolic activity: rate of incorporation of radioactively-labeled leucine, cell-specific nucleic acid content, and the ability of a cell's electron transport system to reduce the fluorogenic dye 5-cyano-2,3-ditolyl tetrazolium chloride (CTC).

The incorporation of metabolic precursors, such as amino acids or nucleotides, has been used as a measure of volumetric (net community) rates of bacterial activity. These measurements are usually based on whole seawater incubations, and therefore include the entire bacterial assemblage. Recent studies support the idea that marine bacterial cells are not uniformly active, rather sub-populations of the bacterial assemblage are more or less active at any one time (del Giorgio and Bouvier 2002; Cottrell and Kirchman 2003; Smith and del Giorgio 2003). Flow cytometric analysis has revealed the presence of two major groups of bacterial cells based on nucleic acid content: high or low nucleic acid cells (HNA and LNA cells, respectively; Li et al. 1995; Jellett et al. 1996; Gasol and del Giorgio 2000). HNA cells have been proposed to be active cells, while LNA cells may be dead or dying cells (Li et al. 1995; Jellett et al. 1996; Gasol et al. 1999), or cells with reduced cell-specific metabolic activity (Zubkov et al. 2001; Smith and del Giorgio 2003).

The relationship between incorporation of metabolic precursors and cell-specific nucleic acid content has been examined by flow cytometric sorting of HNA and LNA cells to determine the cell-specific incorporation rates of radioactively-labeled metabolic precursors (Servais et al. 1999; Bernard et al. 2000; Lebaron et al. 2001; Zubkov et al. 2001; Servais et al. 2003). In both discrete samples and samples from a mesocosm enriched with nitrogen and phosphorus, HNA cells are responsible for a larger fraction of leucine incorporation than LNA cells (Servais et al. 1999; Lebaron et al. 2001; Servais et al. 2003). However, in the Celtic Sea, LNA cells have higher biomass specific rates in the surface waters than HNA cells, although in the

pycnocline and deeper waters, LNA cells incorporate less ^{35}S labeled methionine than HNA cells when incorporation is normalized to biomass (Zubkov et al. 2001). Given the observed differences in the phylogenetic diversity of HNA and LNA cells (Zubkov et al. 2001; Zubkov et al. 2002), we do not yet know how differences in diversity of HNA and LNA cells will change estimates of cell-specific 'activity' in different marine ecosystems.

Bacterial cells with an active electron transport system have been identified through the use of the fluorogenic dye 5-cyano-2,3-ditolyl tetrazolium chloride (CTC) (Rodriguez et al. 1992), which is reduced by primary aerobic dehydrogenases in the cell's electron transport system (Smith and McFeters 1997). The abundance of CTC-positive cells is positively correlated with whole water respiration rates (Smith 1998), and with volumetric incorporation rates of ^{3}H-leucine or ^{3}H-thymidine (del Giorgio et al. 1997; Sherr et al. 1999). CTC is an indicator of respiration and not growth; therefore if balanced growth is not occurring, CTC may not correlate with leucine or thymidine incorporation. These observations have led to the hypothesis that CTC reduction may indicate the most highly active cells in a bacterial assemblage (Sherr et al. 1999; Nielsen et al. 2003). However, in one previous study in which CTC-positive cells were incubated with ^{3}H-leucine and sorted on a flow cytometer to measure bacterial leucine incorporation, the CTC-positive cells contributed < 60% of the incorporation by the total population (Servais et al. 2001).

Since the Oregon upwelling system provides a wide range of environmental conditions within relatively short geographic distances (Chavez et al. 2002; Huyer et al. 2002; Peterson et al. 2002), it is an excellent system in which to examine variability in the cell-specific metabolic activity and distribution of bacterioplankton. Bacterial leucine incorporation rates in these waters vary over three orders of magnitude, with rates decreasing from the mesotrophic zone to subsurface depths, and with increasing distance from shore (Sherr et al. 2001). Furthermore, the abundance of HNA cells is positively correlated to bacterial leucine incorporation and chlorophyll *a* in some (Li et al. 1995), but not all (Jellett et al. 1996), ecosystems. Conversely the abundance of LNA cells can be greater in oligotrophic systems (Li et al. 1995, Casotti et al. 2000,

Jochem 2001, Vaqué et al. 2001), indicating that the distribution of HNA and LNA cells varies between ecosystems.

In this study, we examined both volumetric and cell-specific leucine incorporation rates of heterotrophic prokaryotes in seawater samples collected in late April/early May 2002. At each station, all samples were incubated with ^{3}H-leucine; a subset of the samples was subsequently incubated with CTC. After the cruise, separate aliquots of each sample were either processed to obtain whole seawater bacterial leucine incorporation rates, or sorted with a flow cytometer into groups of cells based on nucleic acid content or CTC-fluorescence. We compared the cell-specific leucine incorporation rates of the sorted groups of cells with each other, to whole seawater bacterial leucine incorporation, and in relation to measured physical, chemical, and other biological oceanographic parameters.

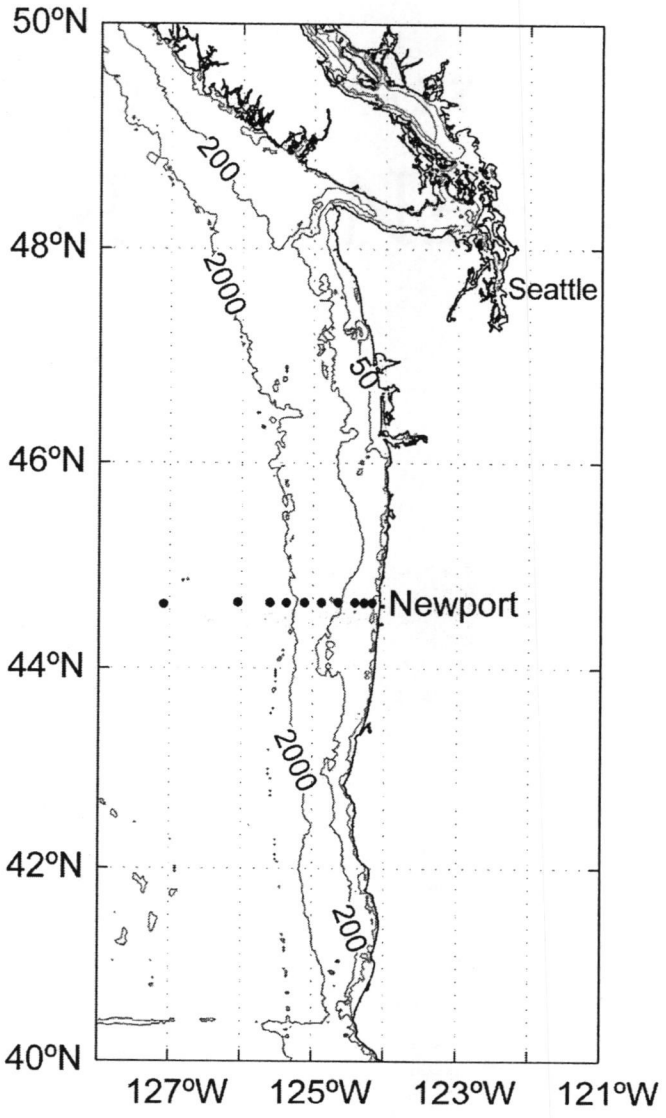

Figure 2-1. Regional map of the sampling area with contour lines indicating the 50 m, 200 m, and 2000 m isobaths. Ten stations were sampled repeatedly along the Newport Hydrographic line which runs west of Newport, OR (Table 2-1).

2.3 Materials and Methods

2.3.1 Sample collection and oceanographic parameters

Samples were collected using General Oceanics 5 L niskin bottles mounted on a rosette equipped with a SeaBird SBE 911+ CTD, a SeaTech fluorometer, a Biospherical PAR sensor, and a SeaTech 25 cm transmissometer. Ten stations were chosen along the Newport Hydrographic line extending westward from Newport,

Oregon: three stations on the shelf, three stations on the slope, and four basin stations above the abyssal plain (Figure 2-1, Table 2-1). The water depths at these stations increase from 60 m at the innermost station to over 2900 m at the basin stations.

Table 2-1. Summary of sampling stations along the Newport Hydrographic line, stations are grouped by region. Multiple casts were conducted at each sampling station during the period from April 26 to May 20, 2002. Samples labeled with ^{3}H-leucine and sorted on the flow cytometer were collected from NH5, NH35, and NH127.

Region	Station Name	Distance from shore (km)	Maximum depth (m)	Latitude (°N)	Longitude (°W)
Shelf	NH5	9	60	44.65	124.17
	NH10	18	80	44.65	124.28
	NH15	28	90	44.65	124.40
Slope	NH25	46	300	44.65	124.63
	NH35	65	450	44.65	124.88
	NH45	84	700	44.65	125.10
Basin	NH55	102	2900	44.65	125.37
	NH65	120	2900	44.65	125.58
	NH85	157	2900	44.65	126.05
	NH127	249	2900	44.65	127.10

2.3.2 Environmental parameters

For chlorophyll concentration, discrete water samples were filtered through a GF/F filter and kept frozen at -80°C for up to one month before processing. 90% HPLC grade acetone was added to the filters and allowed to extract overnight at -20°C. Chlorophyll *a* and pheopigment concentrations were determined using a Turner Designs 10-AU fluorometer (Strickland and Parsons 1972). Nutrient samples were collected into 60 ml high-density polyethylene (HDPE) bottles and frozen at sea (-20 °C). The analyses for phosphate, nitrate plus nitrite (N+N), nitrite, and silicic acid (silicate) were performed using a hybrid Technicon AutoAnalyzerII™ and Alpkem RFA300™ system following protocols modified from Gordon et al. (1994). Nitrate

concentrations were determined by subtracting nitrite from the N+N value. Results were reported in units of micromoles per liter (μM). The estimated precision for each element is: PO_4 (0.008 μM), N+N (0.15 μM), NO_2 (0.01 μM), silicic acid (0.3 μM).

2.3.3 Determining cell abundance using the flow cytometer

Water samples in 3 ml aliquots were fixed with 0.2% w/v paraformaldehyde (final concentration), stored in the dark for at least 10 min at room temperature to harden cells, and quick-frozen in liquid nitrogen. Samples were then stored at -80°C until sample processing on shore. A Becton-Dickinson FACSCalibur flow cytometer was used to enumerate the heterotrophic and photoautotrophic cells. A known concentration of fluorescent microspheres (1 μm for heterotrophic cells, 3 μm for photoautotrophic cells; Polysciences, Warrington, PA) was added to each sample to determine sample volume processed in the flow cytometer, and thus cell abundance from cytometric counts. The concentration of the working stock of microspheres was pre-determined using Becton-Dickinson TrueCount Beads (Franklin Lakes, NJ). Photoautotrophic cells were enumerated using unstained aliquots of the water sample. Cytograms of FL3 (red) fluorescence versus FL2 (orange) fluorescence were used to count *Synechococcus* and picoeukaryotes, while cytograms of side scatter versus FL3 fluorescence were used to count diatoms. The larger cells were presumed to be diatoms, as visual inspection of the high chlorophyll *a* shelf waters showed that diatoms dominated the phytoplankton. *Prochlorococcus* cells were not observed in any of the samples. The aperture size on the sample injection port is 180 μm, therefore larger cells, particularly diatom chains, would not be counted by the flow cytometer.

For heterotrophic cells, subsamples were stained with 1x SYBR Green I (Molecular Probes, Eugene, OR; diluted from the 10,000x stock solution) and 25 mM potassium citrate for 15 min following a protocol modified from Marie et al. (1997). Logical gating in the Cell Quest software (Becton-Dickinson, Franklin Lakes, NJ) was used to exclude cyanobacteria, based on orange fluorescence, from the abundance counts of heterotrophic prokaryotes. Regions were established on the cytograms to define bacterial cells with high nucleic acid content (HNA) and low nucleic acid

content (LNA) (Figure 2-2). The regions for the HNA and LNA cells were adjusted in between each sample when needed; in general these two groups of cells were distinct, as has been observed by others (Li et al. 1995; Jellett et al. 1996; Gasol and del Giorgio 2000). Mean cell-specific SYBR fluorescence was obtained for HNA and LNA cells along with abundance of cells within each group. The fluorescence data from the HNA and LNA regions were normalized to the fluorescence of the beads prior to any further analysis.

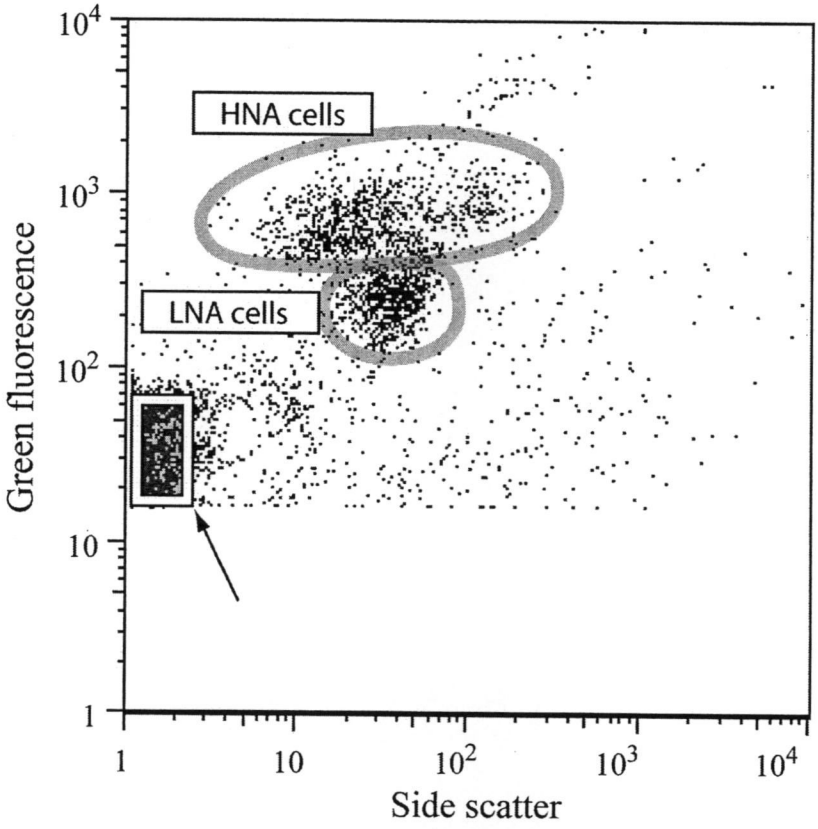

Figure 2-2. Cytogram of side scatter versus green (SYBR) fluorescence with two sort regions outlined. Cells within the region of higher fluorescence are high nucleic acid cells (HNA cells), while cells with lower fluorescence are the low nucleic acid cells (LNA cells). Total cells were sorted separately as the region encompassed by both the HNA cells and the LNA cells, with any autotrophic cells excluded. The box marked with an arrow at the X-Y origin of the cytogram contains the non-cellular particles sorted to obtain each sample's background radioactivity level.

2.3.4 Abundance of cells with an active electron transport system

Water samples were incubated with 5-cyano-2,3-ditolyl tetrazolium chloride (CTC) (Polysciences, Warrington, PA) immediately following collection to identify cells with an active electron transport system. Three ml subsamples were incubated with 2.5 mM CTC for one hour in the dark at 10°C. Previous studies off the Oregon coast had shown no difference in flow cytometric detection and incorporation of 2.5 mM CTC compared to 5 mM CTC (data not shown). Incubations were stopped by the addition of 0.2% w/v paraformaldehyde (final concentration). Samples were kept in the dark at room temperature for at least 10 min to harden cells before freezing at -80°C. Samples were thawed immediately prior to determination of CTC-positive cell abundance via flow cytometry (del Giorgio et al. 1997).

2.3.5 Whole seawater volumetric leucine incorporation

Incorporation rates of ^{3}H-leucine into whole seawater samples were assayed following the protocol of Smith and Azam (1992). For each water sample, 1.5 ml aliquots were pipetted into four 2-ml plastic microcentrifuge tubes containing ^{3}H-leucine (Perkin Elmer Life Science Products, specific activity 170 Ci mmol^{-1}) to yield 20 nM final concentration. One of the four aliquots served as a killed control, with 5% (final concentration) of trichloroacetic acid (TCA) immediately added to the tube. The aliquots were incubated for one hour in the dark at the in situ water temperature. The labeled samples were then killed with 5% TCA (final concentration), and stored frozen at -20°C. Samples were returned to shore and processed no more than three weeks after the sampling date. Prior experiments with radioactively-labeled samples frozen for up to one month showed no difference in leucine incorporation rates compared to unfrozen samples processed immediately (data not shown). Activity was determined using a Wallac 1141 liquid scintillation counter (LSC). The activity of the killed control was subtracted from the values for the three live aliquots.

2.3.6 Flow cytometric sorting of cells labeled with ^{3}H-leucine

Water samples from three stations, NH5, NH35, and NH127, were sorted to determine rates of cell-specific leucine incorporation. The samples were incubated immediately after collection with 40 nM of ^{3}H-leucine (specific activity 170 Ci mmol^{-1}) in the dark for one hour at 10°C, which was within 1.5°C of the average in situ water temperature. Due to the cost of the isotope, killed controls were not incubated along with the live samples. A higher concentration of leucine was used for samples to be sorted to ensure sufficient radiolabeling of cells. However, saturation curve experiments carried out during the cruise showed that whole seawater samples incubated with 20 nM leucine or 40 nM leucine had similar volumetric leucine incorporation rates, therefore the lower leucine concentration was used for the whole seawater volumetric leucine incorporation incubations. Following the initial 1-hour incubation, a subset of the sample tubes was incubated with 2.5 mM of CTC for an additional hour in the 10°C water bath. Samples were fixed with 0.2% w/v paraformaldehyde (final concentration), allowed to sit for at least 10 min in the dark, and then quick-frozen and stored in liquid nitrogen. After the return to shore, samples were transferred to a -80°C freezer for storage until sample processing.

Prior to sorting, aliquots of each thawed sample were incubated in the dark with 2x concentration of SYBR Green I, diluted from the 10,000x stock solution, for 15 minutes. All sorts were run on low flow using the Single Cell Option of the Becton-Dickinson Cell Quest software. Bacterial cells were sorted using four different sort criteria, three of which were based on SYBR-stained cells. Sorting regions for HNA and LNA cells were defined in a cytogram of side scatter versus green fluorescence (Figure 2-2); a separate sort for total cells (heterotrophic prokaryotes only) was conducted with the sort region as the combined HNA and LNA cell regions. Cells were sorted onto 25 mm, 0.2 μm cellulose acetate membranes using a Becton-Dickinson cell concentrator unit attached to the flow cytometer's sort line. A total of 1.0×10^5 cells were sorted for each region. Fading of the SYBR fluorescence was observed during sorting; to counteract this, twice the normal concentration of SYBR was used and a freshly-stained aliquot of the sample was placed on the flow

cytometer's sample injection port every 15 minutes. Over 140 sorts were done from the 35 samples that were collected. As a control, an aliquot of each sample was stained with SYBR Green I as above and 1.0×10^5 of low-fluorescent (non-cell) particles at the X-Y origin of the cytogram (Figure 2-2) were sorted and processed for background radioactivity.

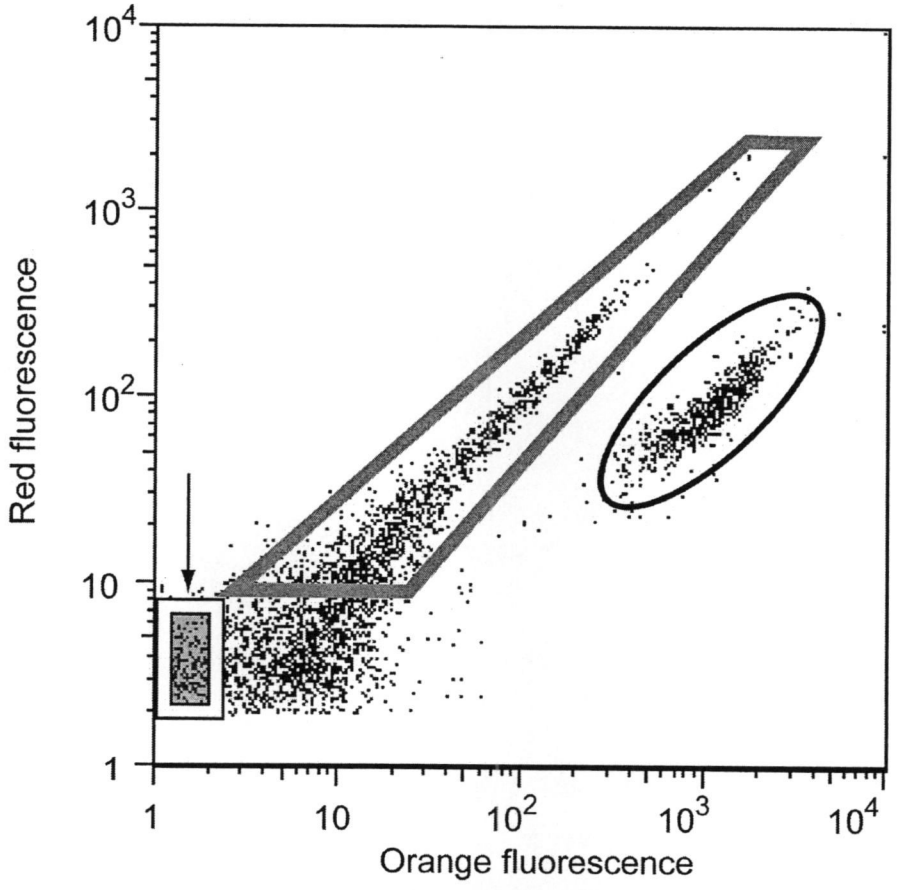

Figure 2-3. Cytogram of orange fluorescence versus red fluorescence with the sort region for the CTC-positive cells outlined in grey. The area below the sort region was determined to be noise based on cytograms of side scatter versus orange fluorescence. See text for details and discussion of the noise region in the identification of CTC-positive cells. The black oval marks *Synechococcus* cells which were excluded from the CTC sorts. The box marked with an arrow at the X-Y origin of the cytogram contains the non-cellular particles sorted to obtain each sample's background radioactivity level.

CTC-positive cells were sorted within a defined region in cytograms of orange fluorescence versus red fluorescence (Figure 2-3). The lower threshold for sorting was determined by examination of the side scatter versus orange fluorescence cytogram for each sample (figure not shown). As for the SYBR Green-stained samples, a region near the origin of the cytogram with non-cellular particles was sorted for each CTC sample and used as a measurement of background radioactivity on the filters.

In order to exclude *Synechococcus* from the cell sorts, logical gating was used for the HNA, LNA, and total heterotrophic cell regions. For CTC sorts, we determined that cyanobacterial cells fell into an area outside of the CTC-positive cell region (Figure 2-3). We also intentionally sorted cyanobacteria that were present in high numbers in two of the radioactively-labeled samples, and determined that *Synechococcus* was not incorporating ^{3}H-leucine at a measurable rate.

After the desired number of cells had been collected, the filter was removed from the cell concentrator unit, transferred to a filter manifold, and processed following the method of Kirchman (1993), which has previously been shown to result in similar values to the centrifugation method (Smith and Azam 1992). The filter was washed twice with cold 5% TCA and twice with cold 80% ethanol. After washing, the filter was folded into a 7 ml scintillation vial and allowed to dry. Ethyl acetate (0.5 ml) was added to the scintillation vial to dissolve the filter, followed by 3 ml of scintillation cocktail. The samples were allowed to sit for two days before counting on a Wallac LSC. For each sample, the disintegrations per minute (DPM) of the background filter (non-cell sort) was subtracted from the DPM values of the cell sorts for that sample. Cell-specific rates of leucine incorporation were obtained by dividing the molar leucine incorporation rate determined for each filter by the number of cells sorted for that sample. The volumetric leucine incorporation rate for each sorted group was calculated by multiplying the abundance of cells within each sorted region by the cell-specific leucine incorporation rate for that group. This later calculation will be referred to as sorted volumetric leucine incorporation to distinguish it from the whole seawater volumetric leucine incorporation rates obtained from the non-sorted samples.

2.3.7 Nonmetric multidimensional scaling

Nonmetric multidimensional scaling (NMS, Kruskal 1964; Mather 1976) was used to examine the spatial distribution of the photoauto- and heterotrophic cells along the transect. The abundances of the following cytometrically-defined groups were used in the NMS analysis: total cells (the combination of all autotrophic and heterotrophic cells), total heterotrophic cells, HNA cells, LNA cells, diatoms, *Synechococcus*, and picoeukaryotes. The relative Sorensen distance measure was used; therefore differences in absolute cell abundances between the samples are removed since the samples are standardized by the number of cells within each sample. The NMS analysis was started with random configuration and run using the 'slow and thorough' settings in the autopilot mode. Forty runs were done with real data, and Monte Carlo simulations were conducted with 50 runs of randomized data which were then compared to the output from the real data. The p-values were calculated as the proportion of randomized runs with stress less than or equal to the observed stress. The dimensionality of the data set was assessed by comparison of NMS runs with real data compared to the Monte Carlo simulations. Additional axes were added if the addition of the axis resulted in a significant improvement over the randomized data (at $p \leq 0.05$), and the reduction in stress was greater than five. The proportion of variation represented by each axis was assessed by calculating the coefficient of determination (r^2) between distances in the ordination space and distance in the original space. Joint plots showing the relationship between the environmental data and the ordination scores were overlaid on the NMS plot; the angle and length of the line indicates the direction and strength of the relationship. Joint plots were calculated for the following environmental variables: temperature, salinity, depth, phosphate, silicate, nitrate, nitrite, whole seawater volumetric leucine incorporation, chlorophyll *a*, and % transmission. Joint plots with r^2 values below 0.2 on either axis are not plotted.

2.3.8 Statistical analysis

Calculations of mixed layer depth were modified from Kara et al. (2000). Statistical analyses were conducted in SPSS v. 11.5 (SPSS, Inc.), Matlab 6.5

(Mathworks), or PC-ORD v. 4.19 (MjM Software Design). For the NMS analysis, the abundance data were transformed using a square root transformation to reduce the skewness and coefficient of variation of the data. The other data were log transformed to improve normality. Analyses performed included Spearman rank correlations, partial correlations controlling for one variable, one-way ANOVAs, paired t-tests, and Kruskal-Wallis tests. All relationships were significant at the $p < 0.01$ level unless otherwise noted.

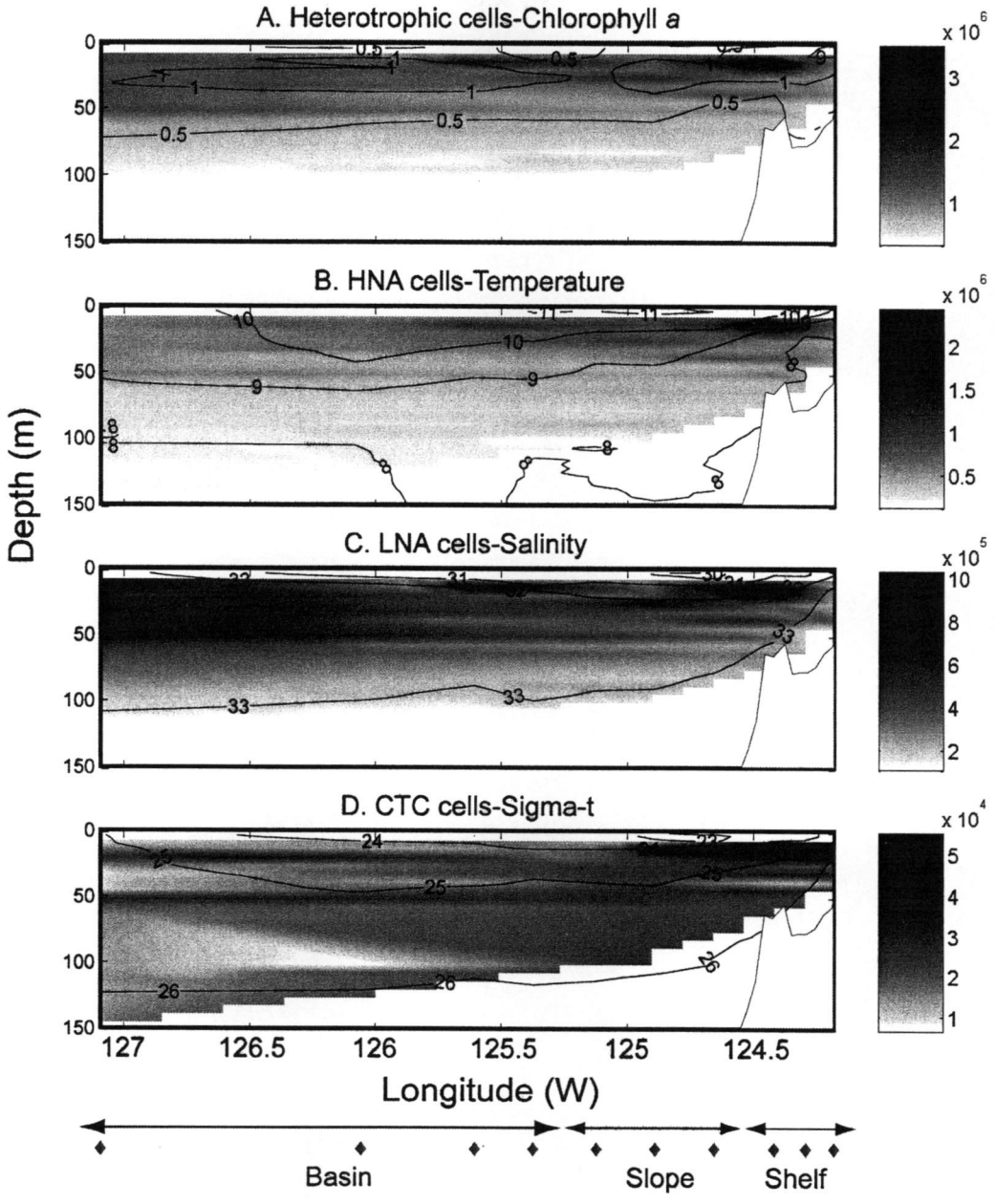

Figure 2-4. Contour plots of physical parameters overlain on plots of cell abundance (A) abundance of heterotrophic cells (cells ml^{-1}) compared to chlorophyll *a* ($\mu g\ L^{-1}$, contour lines) (B) HNA cell abundance (cells ml^{-1}) and temperature (°C, contour lines) (C) LNA cell abundance (cells ml^{-1}) and salinity (contour lines) (D) CTC-positive cell abundance (cells ml^{-1}) with sigma-t (contour lines). Data are from the whole cruise. At the bottom of the figure, diamonds indicate the location of individual sampling stations, and the bars cluster the stations into shelf, slope or basin region. The physical parameters were averaged into 1-m bins at all ten sampling stations; therefore, there is one data point for every meter of depth.

2.4 Results

2.4.1 Regional hydrography during sampling

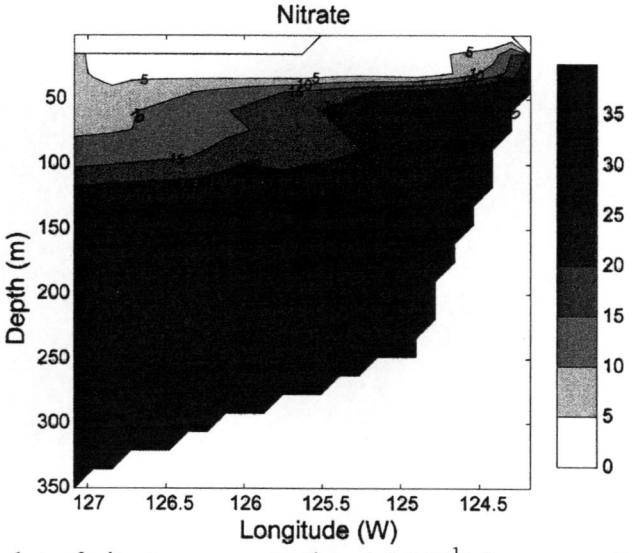

Figure 2-5. Contour plot of nitrate concentration ($\mu M\ L^{-1}$) from samples collected over the entire cruise. Silicate and phosphate concentrations showed the same pattern of increasing in nutrient concentrations with depth.

Around the slope stations, the physical data revealed a lens of low salinity water due to Columbia River outflow from the north (Figure 2-4C). The isopycnals sloped towards the surface at the shelf stations, indicating upwelling due to the presence of northerly winds (wind data not shown). The surface water at the most westward station, NH127, was colder, saltier, and therefore denser, when compared to the other basin stations. Nutrient concentrations were highest in the deep water samples and on the shelf where the upwelled water had higher nutrient concentrations (Figure 2-5).

The patterns for phosphate and silicate were similar to the nitrate concentrations shown in Figure 2-5. Nitrate depletion was observed in the surface samples while measurable levels of phosphate were still present (Figure 2-6A). However, the samples from NH127, the station furthest from the coast, had measurable levels of nitrate, phosphate, and silicate in surface waters (Figure 2-6B). In samples with measurable nitrate and phosphate, the N:P ratio was 16.4:1. In samples

with nitrate concentrations less than 35 μM L^{-1}, the silicate:phosphate ratio was 17.1:1. This ratio was higher in deep water samples below the mixed layer due to larger increases in the silicate concentration. Chlorophyll *a* levels were highest close to shore at the subsurface chlorophyll maxima, and decreased with increasing depths and distance from shore (Figure 2-4A).

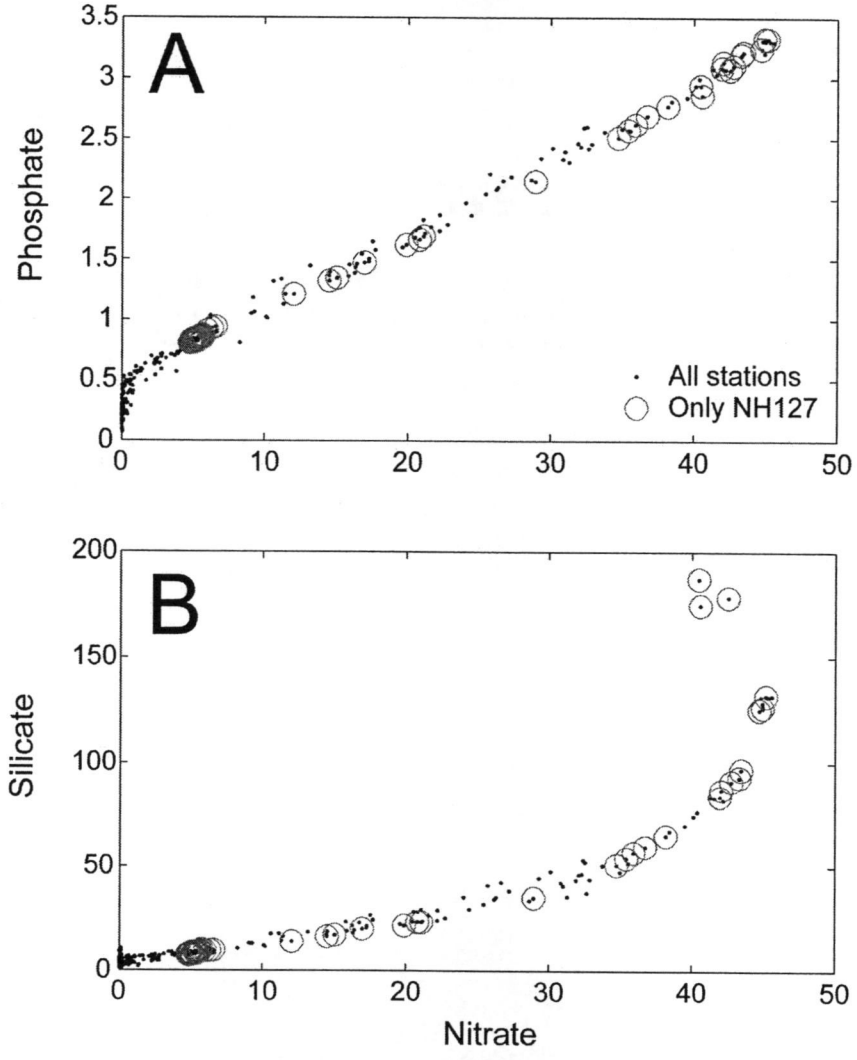

Figure 2-6. Nutrient concentrations (in μM L^{-1}) for all the samples collected where (A) is nitrate vs. phosphate, and (B) shows nitrate vs. silicate. The samples from the station furthest from shore, NH127, have been indicated with a gray circle.

2.4.2 Cell abundance data – heterotrophic and photoautotrophic cells

The highest abundance of total heterotrophic bacterial cells was in the surface waters of the shelf and slope stations, although the sampling station closest to shore (NH5) had relatively lower abundances (Figure 2-4A). The abundance of HNA cells was similar to the pattern described for the total heterotrophic cells. In contrast, the LNA abundances were elevated in the upper 50 m of the basin stations compared to the slope and shelf stations. The abundance of HNA cells relative to the total heterotrophic cell abundance was higher at the surface of all stations except NH127. The samples from NH127 exhibited a pattern not observed elsewhere in the region: in 35% of the samples from this station, the abundance of LNA cells was greater than the abundance of HNA cells. At the other stations, the abundance of LNA cells was greater than HNA cell abundance in less than 15% of the samples. The abundances of total heterotrophic cells, HNA cells and LNA cells were positively correlated to each other, and to temperature, whole seawater volumetric bacterial leucine incorporation, and chlorophyll *a*, based on Spearman rank correlation analyses. Conversely, negative correlations were observed with depth, salinity, and nutrient concentrations (Spearman rank correlations).

The abundance of photoautotrophic cells was higher in the mixed layer; however, there were subsurface peaks in the abundance of diatoms, *Synechococcus*, and picoeukaryotes (Figure 2-7). Picoeukaryotes and *Synechococcus* were abundant from the slope stations and extending offshore to NH127, while the diatoms reached maximum abundance close to shore in the upwelling region.

The abundance of CTC-positive cells was highest in the shelf region, reaching a maximum of 1.13×10^5 cells ml^{-1}, and lowest at the basin stations (Figure 2-4D). The abundance of CTC-positive cells relative to the total heterotrophic bacterial cells was higher in deeper samples from the slope and basin stations, and lowest in the surface samples of the basin and slope stations. The abundance of CTC-positive cells was positively correlated to chlorophyll *a* and temperature; significant negative

correlations were observed with depth, salinity, and nutrient concentrations (Spearman rank correlations).

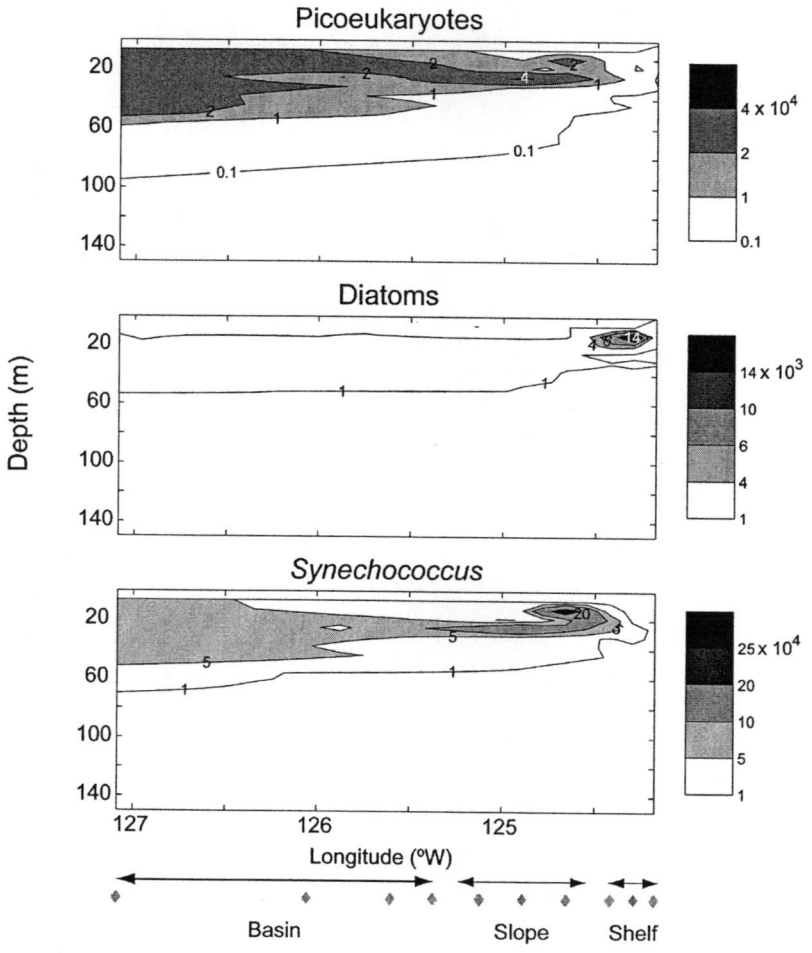

Figure 2-7. Abundance of photoautotrophic cells counted by the flow cytometer. Abundance of picoeukaryotes, diatoms and *Synechococcus* are given in cells ml^{-1}. *Prochlorococcus* was not detected in any of the samples processed.

Non-metric multidimensional scaling (NMS) was used to explore differences in the distribution of the flow cytometrically-defined cell populations among the different hydrographic regions and sampling depths. The goal of the NMS was to examine the extent of similarity among the samples based on the relative abundances of the microbial community measured for each sample. A two-dimensional solution was found to best explain the differences between the samples (Figure 2-8). Each point within Figure 2-8 represents the composite of all the cytometrically-defined

cells. Points which are closer together represent samples which have a similar community of organisms present, where community is defined in terms of the flow cytometrically-defined subpopulations. The final solution was the result of 101 iterations with a final stress of 4.17 and a final instability of 1×10^{-5}. The ordination was rotated to maximize the correlation with whole seawater volumetric leucine incorporation. The cumulative proportion of variation explained by the final two-dimensional solution was 0.99, with 0.87 and 0.13 on Axis 1 and Axis 2, respectively. Therefore, most of the variability between the samples was explained by the distribution of samples along Axis 1. The ordination revealed that the slope and basin stations had greater similarity than the shelf stations (Figure 2-8), largely due to the increased abundances of *Synechococcus* and picoeukaryotes in the offshore regions. However, the deep samples from NH127, the station furthest from shore, clustered within the shelf samples.

One advantage of NMS is the ability to examine the physical and chemical data concurrently with the abundance data from the samples. Joint plots overlaid on the ordination show the correlation between the environmental data and the ordination scores (Figure 2-8). The joint plots indicate Axis 1 was positively correlated with whole seawater volumetric leucine incorporation, and negatively correlated with the percent transmission of the water, a measure of the amount of particulate matter in the water. Axis 2 was negatively correlated with temperature, and positively correlated with salinity and nutrient concentrations. Therefore, samples which are separated along Axis 1 were influenced primarily by biological factors, while samples along Axis 2 were influenced more by physical and chemical parameters.

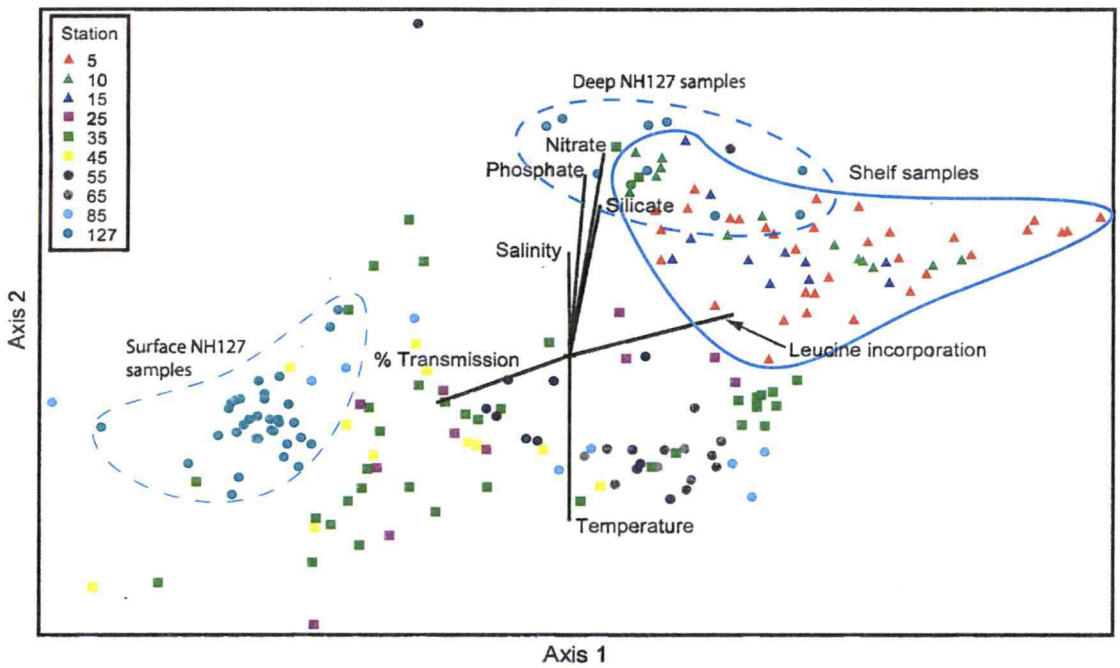

Figure 2-8. Non-metric multidimensional scaling (NMS) analysis showing the distribution of samples based on differences between the relative abundances of flow cytometrically-defined groups of photoauto- and heterotrophic cells. The shelf samples are outlined with the solid line. The samples from NH127 are outlined with a dotted line highlighting the separation of the surface samples from the deep samples. The joint plots are overlaid in black on top of the ordination results. The length of each line indicates the strength of the correlation with the axis. Joint plots with r^2 values below 0.2 on either axis are not plotted.

2.4.3 Whole seawater volumetric leucine incorporation

The whole seawater volumetric leucine incorporation rates, as determined from the 1.5 mL incubations, were highest at the sampling stations closest to shore, and reached a maximum value of 570 pM Leu hr^{-1} in a sample collected above the chlorophyll maxima at NH10. The lowest whole seawater volumetric leucine incorporation rates were obtained from deep samples at the slope and basin stations. The whole seawater volumetric leucine incorporation rates were positively correlated with chlorophyll *a*, abundance of total cells, heterotrophic cells, HNA and LNA cells, diatoms, CTC-positive cells, and temperature. Negative correlations were observed with depth, salinity, and nutrient concentrations (phosphate, nitrate, and silicate) (Spearman rank correlation coefficients, significant at the $p<0.05$ level).

The positive correlation between whole seawater volumetric leucine incorporation and absolute abundance was strongest for HNA cells and weakest for LNA cells ($r = 0.76$ and $r = 0.13$ for HNA and LNA cells, respectively). The abundances of HNA and LNA cells relative to the total heterotrophic cell abundance were also significantly linearly related to whole seawater volumetric leucine incorporation ($r = 0.61$ and $r = -0.65$ for HNA and LNA cells, respectively). Whole seawater volumetric leucine incorporation was significantly, positively correlated to HNA cells' mean FL1 fluorescence ($r = 0.34$). No significant correlation was observed with the LNA cells' mean FL1 fluorescence.

The abundance of CTC-positive cells was positively correlated to whole seawater volumetric leucine incorporation for all stations ($r = 0.49$). The significance of this correlation was driven by the broad range of data for the shelf stations, and the correlation was not significant when just considering the data for the slope or basin stations. There was no significant correlation between the relative abundance of CTC-positive cells (the ratio of CTC-positive cells to the total heterotrophic cell abundance) and whole seawater volumetric leucine incorporation. Finally, the mean FL3 fluorescence of the CTC-positive cells was negatively correlated to whole seawater volumetric leucine incorporation ($r = -0.47$).

2.4.4 Cell-specific leucine incorporation rates

At one station each from the shelf, slope, and basin regions, samples from multiple depths were radioactively labeled and flow cytometrically sorted into total cells (HNA cells and LNA cells combined), HNA cells, LNA cells, and CTC-positive cells. As a control, we sorted particles from a region of the cytogram which was primarily noise. The highest leucine incorporation rate obtained from the non-cell sort regions was 9 pM Leu hr^{-1}, which represented about 2% of the cell-specific leucine incorporation rate of the total cell population for that sample. At all three stations, the cell-specific leucine incorporation rate for all the sorts decreased with depth (Figure 2-9). The trend in cell-specific rates with depth shown for total cells (Figure 2-9) was similar to the other sorted groups, although the range of cell-specific leucine

incorporation rates varied for each group (Figure 2-10, Table 2-2). Cell-specific leucine incorporation rates were generally higher for HNA cells than for LNA cells (two-sided $p < 0.001$, paired t-test). The cell-specific leucine incorporation rates for the total cells were less than for the HNA cells (two-sided $p < 0.001$, paired t-test), but greater than for the LNA cells (two-sided $p = 0.002$, paired t-test). There were four instances when the cell-specific leucine incorporation rate for the LNA cells was greater than the rate for the HNA cells (Figure 2-11). In one surface sample from the slope station, the cell-specific leucine incorporation rate for the LNA cells was seven times higher than the rate for the HNA cells. This sample was sorted twice to confirm these results.

There was variability in the cell-specific incorporation rates between casts at each of the sampling stations (Figure 2-11). The ratio of cell-specific leucine incorporation for HNA cells relative to the rate for total cells was greater than one in all but three samples (Figure 2-11B), while the ratio of cell-specific leucine incorporation for the LNA cells relative to the rate for total cells was less than one in all but seven of the samples (Figure 2-11C). The mean fluorescence for the HNA or LNA cells within a sample was measured on the same sub-samples used to determine cell abundances. There was a significant, positive correlation between the cell-specific leucine incorporation rates for the HNA cells and their mean green fluorescence ($r = 0.61$, Spearman rank correlation coefficient, $p<0.001$). The relationship between cell-specific leucine incorporation and mean green fluorescence of the LNA cells was not significant.

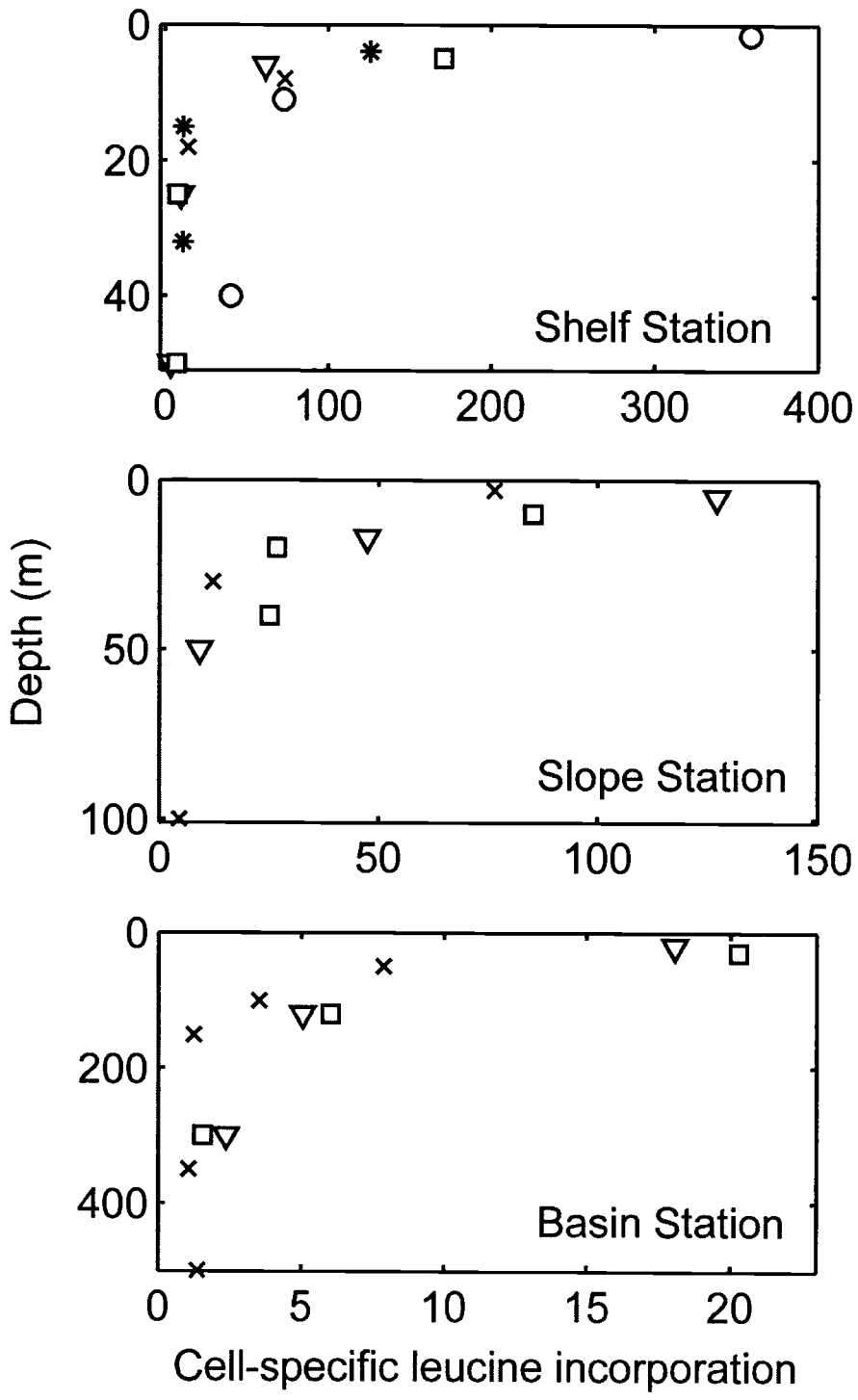

Figure 2-9. Cell-specific leucine incorporation rates for total cells (units are 10^{-21} Mol leucine $cell^{-1}$ hr^{-1}) plotted against depth. A different scale is shown for each sampling station. The different symbols denote water samples collected during different casts.

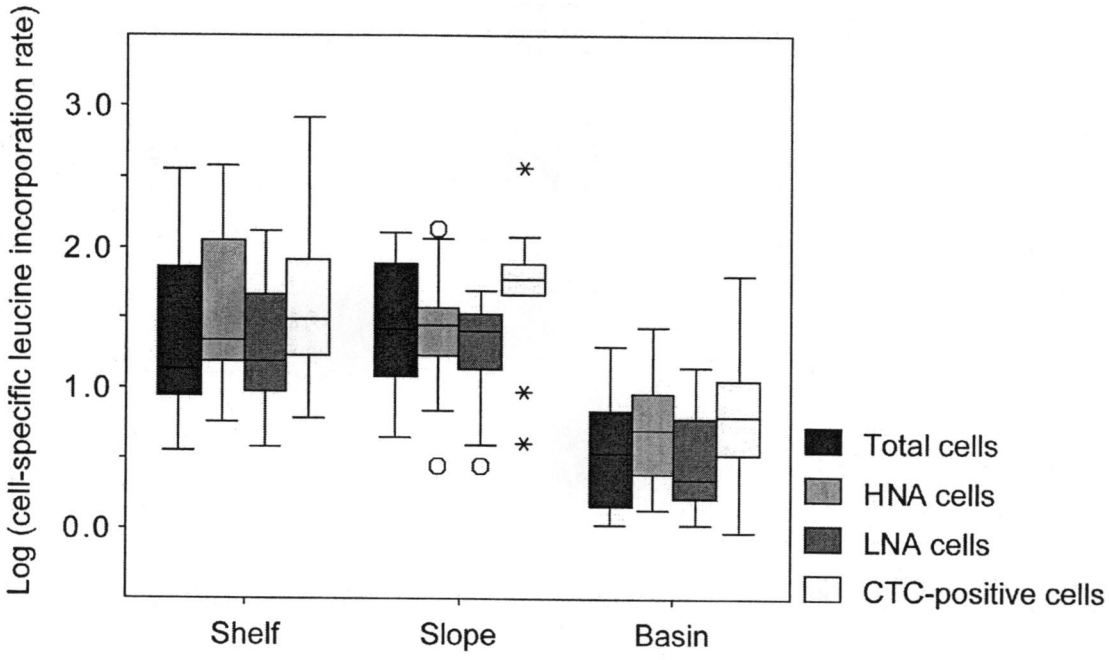

Figure 2-10. Box plots of the cell-specific leucine incorporation rates (log-transformed data) across the three sampling stations. Four separate sorts were done for each sample: total cells, HNA cells, LNA cells, and CTC-positive cells. The box represents the middle 50% of the cell-specific leucine incorporation rates, or the inter-quartile range (IQR) of the data. The whiskers extend to include data within 1.5 IQRs of the box. Outliers, marked with a circle, are defined as cell-specific leucine incorporation rates between 1.5 and 3 IQRs away from the box; extreme outliers, marked with an asterisk, are greater than 3 IQRs away from the box.

Table 2-2. Summary, by sampling region, of cell-specific leucine incorporation rates (in 10^{-21} Mol leu $cell^{-1}$ hr^{-1}). Values are the mean values (± standard deviation) for each region. Four separate sorts were conducted for each sample, and the data are for total cells, HNA cells, LNA cells, and CTC-positive cells.

Region	**Sampling depths (m)**	**Cell-specific incorporation rate (10^{-21} Mol leu $cell^{-1}$ hr^{-1})**			
		Total Cells	**HNA**	**LNA**	**CTC**
Shelf	2-50	65 (± 95)	86 (± 110)	33 (± 36)	130 (± 236)
Slope	3-100	46 (± 42)	45 (± 48)	24 (± 16)	90 (± 109)
Basin	20-500	6 (± 7)	9 (± 9)	5 (± 5)	14 (± 19)

2.4.5 Cell-specific leucine incorporation by CTC-positive cells

As found for the SYBR-stained cells, the cell-specific leucine incorporation rates of CTC-positive cells were highest at the surface and decreased with depth. A point-to-point comparison showed cell-specific leucine incorporation rates for CTC-positive cells were generally higher than rates found for total cells (two-sided $p < 0.0001$, paired t-test). In one-third of the samples, the cell-specific leucine incorporation rates for CTC-positive cells were 1% to 50% (average of 28%) lower than the rates for total cells (Figure 2-11D).

For the whole data set, the cell-specific leucine incorporation rate for the CTC-positive cells was not significantly greater than the cell-specific leucine incorporation rates for the HNA cells (two-sided $p = 0.150$, paired t-test), but was significantly greater than the cell-specific leucine incorporation rate for the LNA cells (two-sided $p < 0.0001$, paired t-test). The cell-specific leucine incorporation rates for the CTC-positive cells was usually greater than the cell-specific leucine incorporation rate for total cells; however, there were instances at all three sampling stations where the cell-specific leucine incorporation rate of the CTC-positive cells was less than the rate for total cells (Figure 2-11D). There was no relationship between CTC-positive cells' cell-specific leucine incorporation rates and mean red fluorescence of the CTC-positive cells.

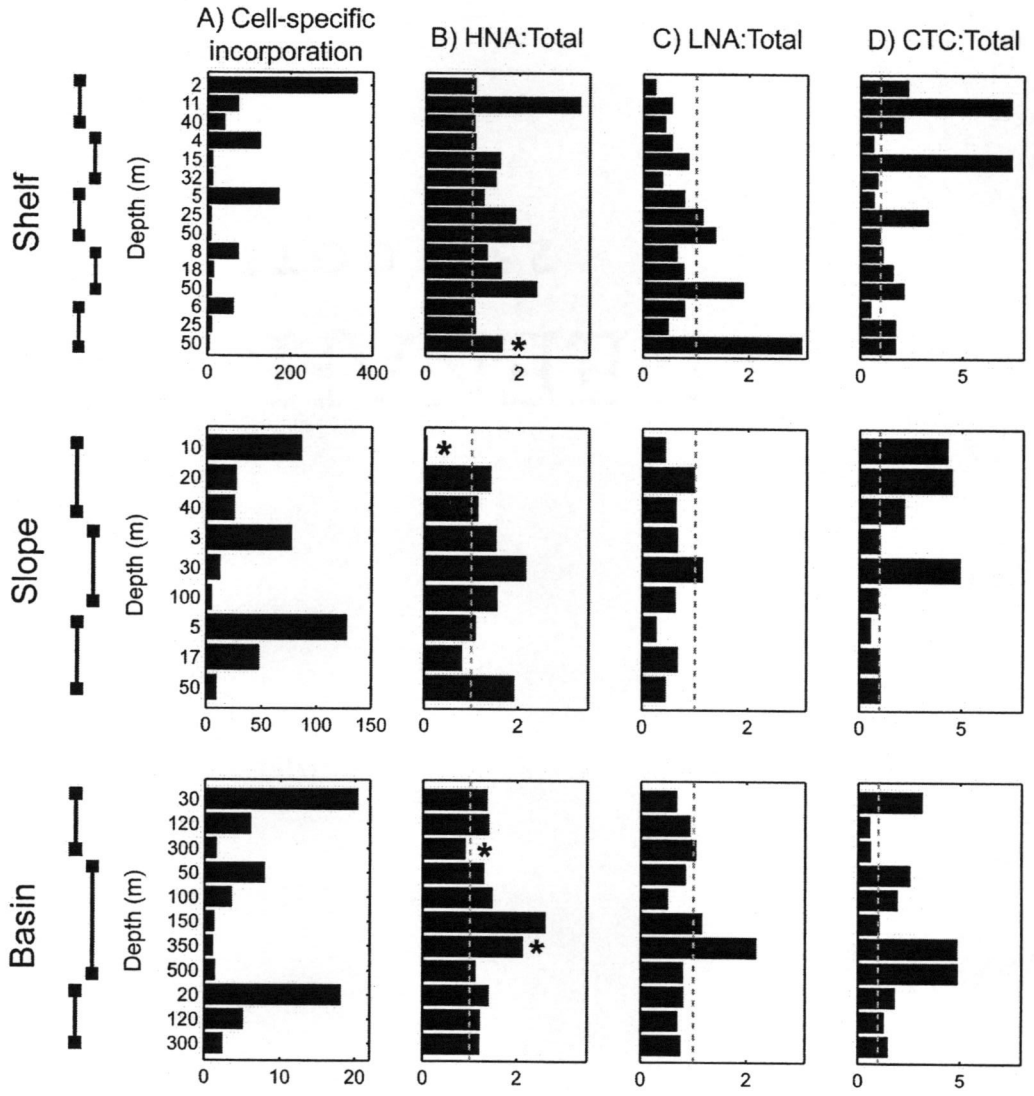

Figure 2-11. Bar graphs of the cell-specific leucine incorporation rates and the variability in the cell-specific leucine incorporation rates from all the samples. (A) shows the cell-specific leucine incorporation rates of the total cells for each sample collected at the shelf, slope and basin station. (B) shows the ratio of the cell-specific leucine incorporation for HNA cells relative to the cell-specific leucine incorporation rate for total cells. (C) shows the rate for LNA cells relative to that for total cells. (D) shows the rate for CTC-positive cells relative to the total cells' rate. The lines on plots B-D are to indicate where the ratio between the two values would be equal to one. An * in the row of bar graphs with the HNA:total cell ratio highlights the samples in which the cell-specific leucine incorporation rate for the LNA cells was greater than the rate for the HNA cells. Sampling depths are given to the left of the bar graphs. The vertical lines to the left of the sampling depths indicate samples collected during the same cast.

2.4.6 Sorted volumetric leucine incorporation rates

Table 2-3. Mean of the sorted volumetric leucine incorporation rate for total cells and the proportional contribution of the HNA cells, LNA cells, and CTC-positive cells to the total sorted volumetric leucine incorporation rate. Values in parentheses for the total cells' sorted volumetric leucine incorporation rate are the standard deviation, while the values in parentheses for the proportion of sorted volumetric leucine incorporation are the 95% confidence intervals. See text for details on the calculations to determine the percent of volumetric leucine incorporation by the HNA, LNA, and CTC-positive populations.

Sampling region	Total cells' sorted volumetric leucine incorporation rate (pM Leu hr^{-1})	Percent of sorted volumetric leucine incorporation rate by:		
		HNA cells	LNA cells	CTC-positive cells
Shelf	81 (± 128)	116% (84–147%)	25% (14–36%)	7% (3–10%)
Slope	53 (± 50)	71% (44–99%)	25% (15–35%)	7% (3–12%)
Basin	7 (± 11)	82% (58–106%)	38% (26–51%)	14% (2–27%)

We calculated the sorted volumetric leucine incorporation for each of the four groups sorted on the flow cytometer by multiplying the cell-specific leucine incorporation rate by the abundance of cells of each type found in the sample (Table 2-3). The percent of sorted volumetric leucine incorporation attributable to the HNA, LNA, and CTC-positive populations was calculated by dividing the sorted volumetric leucine incorporation rate for each population by the sorted volumetric leucine incorporation rate of the total cells. The sorted volumetric leucine incorporation rates of the total cells showed a strong, positive correlation to whole seawater volumetric bacterial leucine incorporation values ($r = 0.93$, Spearman rank correlation coefficient, $p<0.001$, Figure 2-12). Furthermore, the total cells' sorted volumetric leucine incorporation rate was also highly correlated to the sum of the sorted volumetric incorporation rates for the HNA and LNA populations ($r = 0.94$, Spearman rank correlation coefficient, $p<0.001$, Figure 2-12). Therefore, although there were samples

where the HNA and LNA cell-specific leucine incorporation rates were less than the total cell's incorporation rate, in general the sum of the HNA and LNA incorporation rate was equal to the total cell's incorporation rate.

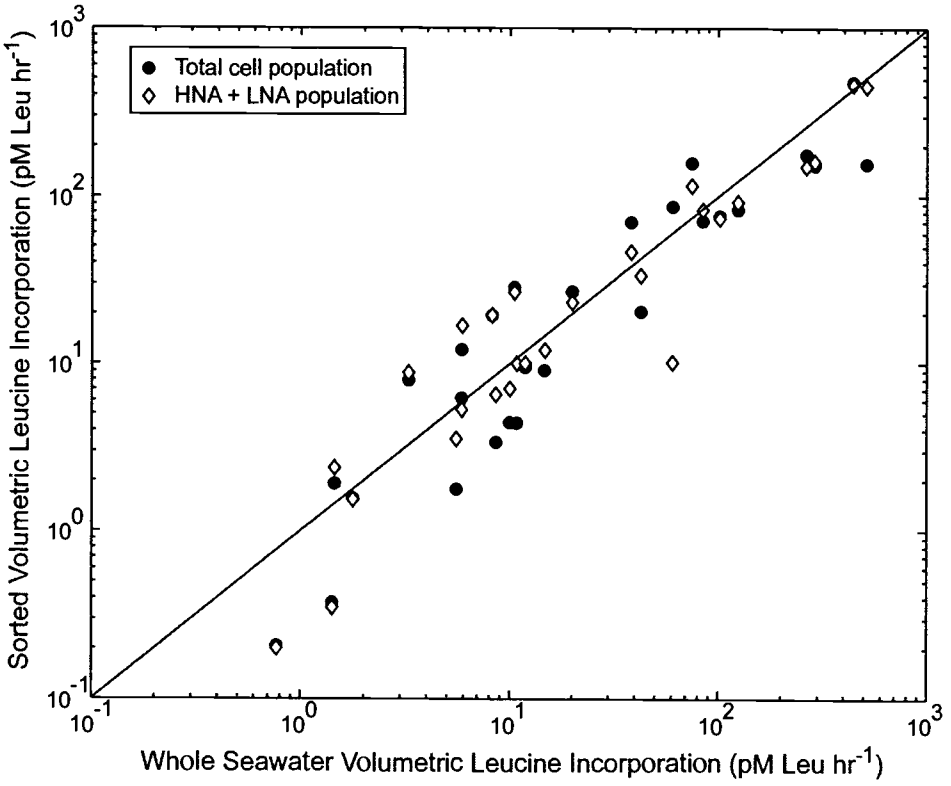

Figure 2-12. Whole seawater volumetric bacterial leucine incorporation rate compared to sorted volumetric leucine incorporation of the sorted total cells, or to the sum of the sorted volumetric leucine incorporation by the HNA cells and LNA cells. The line marks a 1:1 relationship between whole seawater volumetric leucine incorporation rate and the sorted volumetric incorporation rates. Sorted volumetric leucine incorporation is defined as the cell-specific leucine incorporation rate multiplied by the abundance of cells for the group.

The average ratio of sorted volumetric leucine incorporation for the total cells to the whole seawater volumetric leucine incorporation rate was near 1:1 (0.85 to 1.42, 95% confidence interval, Figure 2-12). Since the sorted volumetric leucine incorporation rates for total cells was similar to the whole seawater volumetric leucine incorporation rates, and the sum of sorted volumetric incorporation rates for sorted

HNA and LNA cells generally equaled the sorted volumetric incorporation rates of total cells, the cell sorting process did not seem to bias the data.

Overall activity of the total cell population was due mainly to higher sorted volumetric leucine incorporation rates for HNA cells (Figure 2-13) because of higher HNA cells' cell-specific rates and greater abundances of HNA cells in water samples with higher bacterial leucine incorporation. The proportion of sorted volumetric leucine incorporation due to the LNA cells actually decreased in the samples with highest sorted volumetric leucine incorporation by the total cell population. Additionally, the relative amount of sorted volumetric leucine incorporation due to the CTC-positive cells did not increase in the samples with higher sorted volumetric leucine incorporation rates by the total cell population (Figure 2-13). The percentage of sorted volumetric leucine incorporation attributable to CTC-positive cells in individual samples ranged from 5.2% to 13.2% (95% confidence interval, Table 2-3).

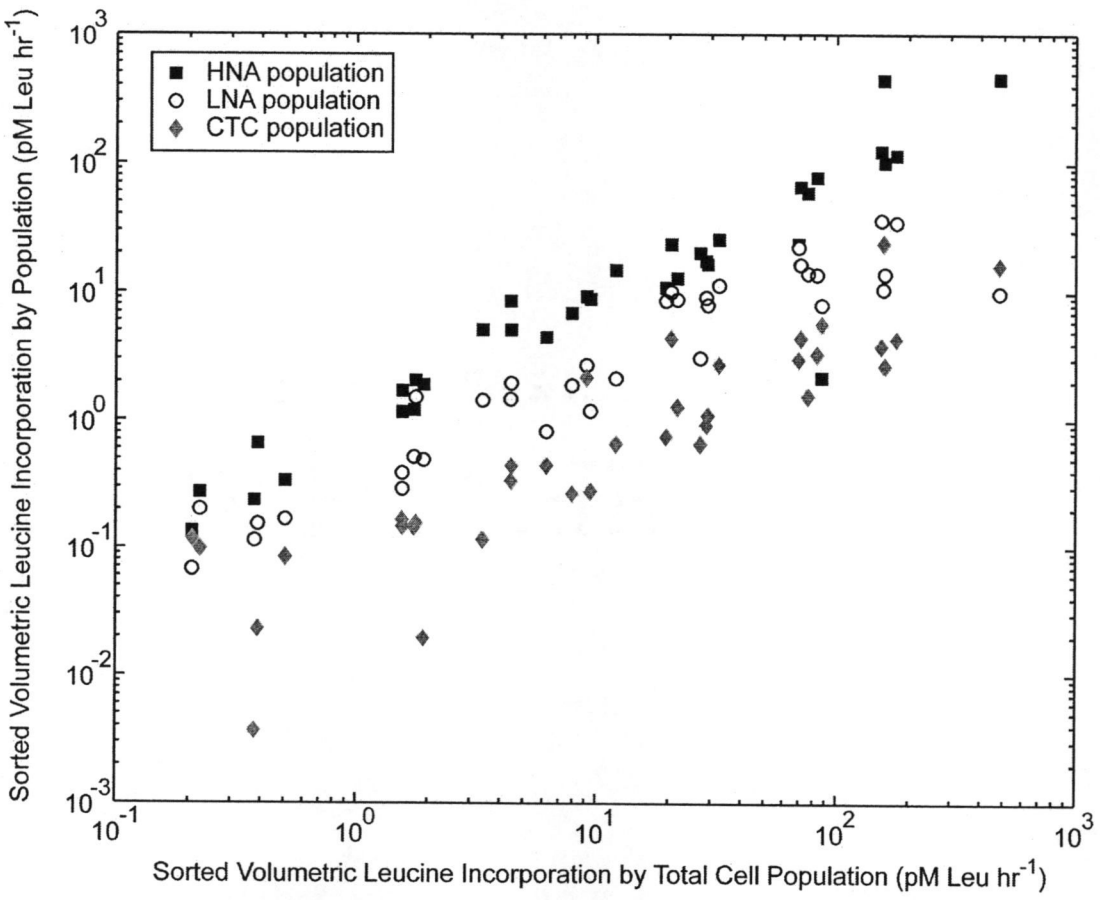

Figure 2-13. Sorted volumetric leucine incorporation rate of the total cells (x-axis) compared to the sorted volumetric leucine incorporation rates by the HNA population, LNA population, and CTC-positive population (y-axis).

Table 2-4. Summary of correlations between environmental parameters and cell-specific leucine incorporation rates for all four sorted populations: total cells, HNA cells, LNA cells, and CTC-positive cells. Spearman rank correlations were calculated for all stations, and for the basin, slope and shelf stations. The partial correlations controlled for sigma-t, and are shown for all sampling stations combined.

	All stations	**Basin**	**Slope**[1]	**Shelf**	**All stations - partial correlations**
Positive	Whole seawater volumetric bacterial leucine incorporation	Whole seawater volumetric bacterial leucine incorporation	Whole seawater volumetric bacterial leucine incorporation	Whole seawater volumetric bacterial leucine incorporation	Whole seawater volumetric bacterial leucine incorporation
	Temperature	Temperature	Temperature	Temperature	Temperature
	Chlorophyll *a*			Chlorophyll *a*	Chlorophyll *a*
Negative	Depth	Depth	Depth	Depth	Depth
	Silicate	Silicate	Silicate	Silicate	
	Phosphate	Phosphate	Phosphate	Phosphate	
	Nitrate	Nitrate	Nitrate	Nitrate	
	Salinity	Salinity	Salinity	Salinity	
No significant correlation		Chlorophyll *a*	Chlorophyll *a*		

[1]One surface sample from the slope station had a cell-specific leucine incorporation rate for the HNA cells that was seven times higher than the rate for LNA cells; including this sample in the analysis caused none of the correlations for the slope station to be significant.

2.4.7 Comparisons to environmental parameters

The cell-specific leucine incorporation rates were significantly positively correlated to whole seawater volumetric leucine incorporation, chlorophyll *a*, and water temperature. The cell-specific leucine incorporation rates were significantly negatively correlated to depth, salinity, sigma-t, and macronutrient concentrations (Spearman rank correlation coefficients, significant at the $p < 0.01$ level, Table 2-4). Cell-specific leucine incorporation rates within the euphotic zone (sampling depths down to 1% of surface PAR levels) were also significantly negatively correlated to macronutrient concentrations (Spearman rank correlation coefficients, significant at the $p < 0.05$ level, Table 2-4). These environmental parameters were all correlated with changes in sigma-t; however, partial correlations calculated while controlling for sigma-t indicated salinity and nutrient concentrations were not significantly correlated to the cell-specific leucine incorporation rates (Table 2-4).

2.4.8 Spatial variability in distribution of cell-specific activity

The variation in overall bacterial activity attributable to each sorted group for the three sampling stations is presented in Table 2-3. According to statistical analysis (Kruskal-Wallis test, $p = 0.042$, followed by a multiple comparison of mean ranks), the proportion of sorted volumetric leucine incorporation by LNA cells was higher at the basin station compared to the shelf station; there were no other between-station differences. More importantly, as noted above, the sorted volumetric leucine incorporation of HNA cells constituted the bulk of sorted volumetric bacterial leucine incorporation at all three sites, and CTC-positive cells were responsible for a relatively small fraction of sorted volumetric leucine incorporation (Table 2-3).

2.5 Discussion

Flow cytometric sorting of radioactively-labeled cells has been used to examine the cell-specific incorporation rate of metabolic precursors concurrently with cell-specific nucleic acid content or the ability to reduce CTC (Servais et al. 1999; Bernard et al. 2000; Lebaron et al. 2001; Zubkov et al. 2001; Servais et al. 2003).

However, these studies did not examine marine systems over as broad a range of trophic states as in our study, nor were environmental data examined with the bacterial assays. In this study, we demonstrated CTC-positive cells have as wide a range of cell-specific leucine incorporation rates as found in the total cell population, and CTC-positive cells were often not exceptionally active with respect to substrate incorporation as found in prior studies (Sherr et al. 1999; Nielsen et al. 2003). HNA cells were consistently responsible for the bulk of volumetric bacterial leucine incorporation. We also found that the leucine incorporation of LNA cells varied with trophic state of the ecosystem, and thus the LNA cells were not simply dead or dying cells as has been reported in previous studies (Li et al. 1995; Jellett et al. 1996; Gasol et al. 1999; Servais et al. 2003).

2.5.1 Leucine incorporation rates in whole seawater compared to rates in HNA or LNA cells

In three of the four cases where the cell-specific leucine incorporation rate for the LNA cells was greater than the rate for HNA cells, the samples were collected at subsurface depths where volumetric bacterial leucine incorporation rates were very low. Since we do not have replicates for each sort, whether there is a significant difference between the HNA and LNA incorporation rates in these samples is not possible to determine. The fourth case, in which the LNA cell-specific leucine incorporation rate was seven times higher than the HNA cell-specific leucine incorporation rate, was a surface sample from the slope station characterized by the warmest and least saline water observed in this data set. This variability in cell-specific leucine incorporation rates raises the question of what causes exceptions to the general trend of higher cell-specific leucine incorporation rates for HNA cells. In the North Sea, HNA and LNA cell assemblages were composed of phylogenetically different groups of bacteria (Zubkov et al. 2001; Zubkov et al. 2002). In our data set, the warm, low salinity water mass with the high cell-specific leucine incorporation rate for the LNA cells may have had a diversity of microorganisms in the HNA and LNA groups different from the other water masses sampled. However, on average, the

surface samples from the slope region had a lower diversity of *Bacteria* present compared to the samples from the pycnocline and deep samples (Chapter 4). The low salinity water may originate from the Columbia River; the river water could be an allochthonous source of organic carbon (Hill and Wheeler 2002), which could be utilized by heterotrophic prokaryotes as a carbon or energy source. Different phylogenetic groups of *Bacteria* have been shown to utilize different types of organic matter (Cottrell and Kirchman 2000), thus the dissolved organic carbon from the Columbia River may only be available to a subset of the in situ bacterioplankton, which were the LNA cells in this sample.

Aside from the exceptions discussed above, the results presented here support previous observations, based on incorporation of ^{3}H-leucine, that the HNA cells are metabolically more active than the LNA cells (Servais et al. 1999; Lebaron et al. 2001; Zubkov et al. 2001; Servais et al. 2003). Examination of the volumetric leucine incorporation rates for each of the sorted groups indicated that the HNA cells were responsible for a larger proportion of the sorted volumetric leucine incorporation than the LNA cells (Table 2-3). At the basin station, the LNA cells had relatively higher cell-specific incorporation rates than at the slope and shelf site, though the values were still less than those obtained for the HNA cells with the exceptions noted above. Due to the higher cell-specific leucine incorporation rate, the LNA assemblage at the basin station was responsible for proportionately more of the volumetric bacterial leucine incorporation than at the two shoreward stations. LNA cells are more abundant in oligotrophic systems (Li et al. 1995; Casotti et al. 2000; Jochem 2001; Vaqué et al. 2001), and can be more active than HNA cells on a cell-specific level, using the incorporation of ^{35}S-methionine as a proxy for activity (Zubkov et al. 2001). Thus, the methionine results from a study conducted in the Celtic Sea and the data presented here using tritiated leucine provide further evidence that LNA cells are not dead or dying cells, and indicate their ecological roles may vary between and within ecosystems at different times. Furthermore, the HNA cell abundance was a better predictor of bacterial leucine incorporation rates than the total heterotrophic cell abundance, or the CTC-positive cell abundance.

2.5.2 CTC as a proxy to identify metabolically active bacterioplankton

One of the problems with the use of CTC has been the detection of weakly-fluorescing CTC-positive cells. Flow cytometry, which is more sensitive than epifluorescence microscopy, can identify a larger number of CTC-positive cells in a sample than can visual observation by epifluorescence microscopy (del Giorgio et al. 1997; Sieracki et al. 1999). However, there are still methodological problems in using a flow cytometer to identify CTC-positive cells since the lower threshold below which cells are not identified as CTC-positive is ambiguous (Figure 2-3) (Gasol and del Giorgio 2000). For selected CTC-stained samples from the Oregon coast, flow cytometer sorts were made of particles in the low CTC-positive fluorescence region, near the origin of the orange fluorescence versus red fluorescence cytogram. This population of particles did have leucine incorporation rates above background (data not shown). However, as this region of the cytogram contains bacterial cells with low or no CTC fluorescence as well as non-cellular debris particles, the leucine incorporation rates for this population of particles would not be specific for low-fluorescing CTC-positive cells.

Based on cell-specific leucine incorporation rates, CTC-positive cells were, on average, more active than the total heterotrophic cell population, and mostly had higher rates of cell-specific activity than the HNA cells. This result supports the hypothesis that CTC-positive cells are highly active cells within a bacterial assemblage (Sherr et al. 1999; Nielsen et al. 2003). However, due to their low abundance, the CTC-positive cells were responsible for a mean of 7% to 14% of volumetric bacterial leucine incorporation (Table 2-3), so they were clearly not driving bacterial community production in this study.

We made two important observations regarding CTC-positive cells in this study. First, the cell-specific leucine incorporation rate of CTC-positive cells had an equivalently large range, over three orders of magnitude (0.9 to 840 x 10^{-21} M leucine $cell^{-1}$ hr^{-1}), as was found for the other groups of cells. The second observation was that, in some samples, the cell-specific leucine incorporation rate of CTC-positive

cells was lower than the total cells' cell-specific incorporation rate. Thus, the CTC-positive cells were incorporating less leucine and, therefore, may have been less metabolically active at those times than the average bacterial cell. However, some of the CTC-positive cells might have been formazan granules released from CTC reducing cells (J. Gasol, personal communication). These granules would not be labeled with tritium but would be counted as cells and so would lower estimates of average leucine incorporation rates. Finally, the relative abundance of CTC-positive cells was not correlated to whole seawater volumetric leucine incorporation. The CTC assay identifies cells that are actively respiring, while leucine incorporation is a proxy for bacterial biomass production, i.e. protein synthesis. Rates of respiration and biosynthesis by marine bacterioplankton may be temporally uncoupled in situations of unbalanced growth, as has been observed in other studies (Bouvier and del Giorgio 2002; Kirchman et al. 2003).

2.5.3 Relationship between variability in rates of leucine incorporation and environmental parameters

The cell-specific rates of leucine incorporation and sorted volumetric leucine incorporation by the various cell groups were both highly correlated to environmental parameters. In the case of chlorophyll *a*, examination of the data on a station-by-station basis revealed correlations were only significant at the shelf station. The samples at the slope and basin station were collected above, in, and below the chlorophyll *a* maxima; however, cell-specific leucine incorporation rates decreased continually with depth leading to a lack of significant correlation with chlorophyll *a* concentrations at the basin and slope stations. Increases in the amount of chlorophyll *a* per cell with depth in small phytoplankton (Olson et al. 1990), and a relative increase in abundance of smaller cells offshore (E.B. Sherr et al. submitted), limits the use of chlorophyll *a* as a proxy for photoautotrophic biomass. Furthermore, bacterial leucine incorporation should correlate more strongly to primary production and not to chlorophyll *a* concentrations (Cole et al. 1988; Ducklow 1999). In our samples, the highest values of cell-specific leucine incorporation occurred at low nitrate

concentrations; however, partial correlations controlling for sigma-t revealed that the cell-specific leucine incorporation rates were not significantly correlated to nutrient concentrations. Therefore changes in the cell-specific leucine incorporation rate were not directly dependent on nutrient concentrations.

There was significant, temporal within-station variability in samples collected during different sampling casts, particularly at the shelf station. This was due to a rather unique and complex hydrology in the nearshore region during the cruise. For example, seasonal survey data from 2002 indicated there was transport of colder, fresher water from the subarctic Pacific into the shelf region off Oregon relative to the previous five years of hydrological observation for the GLOBEC project (Barth 2003; Murphree et al. 2003; Strub and James 2003). During our cruise, evidence of colder, fresher water was seen in the first four casts at the shelf station, compared to the warmer and saltier water observed during the final shelf station cast conducted about two weeks later (data not shown). Wheeler and colleagues (2003) proposed that the increase in primary production in the colder, fresher water was accompanied by an increase in respiration due to the lower than normal oxygen concentrations measured in the bottom water. Yet, in our samples, higher rates of bacterial leucine incorporation were observed in the last cast with the warmer, saltier water. This could be due to variability in the cell-specific leucine incorporation rates caused by environmental variables not measured during this cruise. However, leucine incorporation is not a direct measure of respiration and this could be further evidence of the uncoupling between respiration and biomass production mentioned above.

2.5.4 Distribution of flow cytometrically-defined microorganisms

The distribution of cytometrically-defined microbial groups was more strongly correlated to other biological components of the ecosystem than to the physical and chemical factors. Although top-down effects on the community were not examined during this cruise, the data from the NMS analysis suggest the community was not bottom-up controlled by nutrient limitations since the chemical data had lower correlations with the distribution of cytometrically-defined cells during this cruise.

While this is not unexpected for the heterotrophic community, since they rely on the availability of organic substrates, the photoautotrophic cells also included in the NMS analysis do rely on nutrients for primary production. The nutrient concentrations indicated the phytoplankton had consumed the available nitrate in the surface of all stations except NH127, as has been previously observed off the Oregon coast (Corwith and Wheeler 2002). Under conditions of nitrate limitation, phytoplankton release dissolved organic matter (Wetz and Wheeler 2003) which could serve as a substrate for the heterotrophic community. The lack of nitrate limitation at NH127 may have altered the quality and quantity of dissolved organic matter present in a manner which allowed the LNA cells to become relatively more abundant in the surface waters of NH127. While no data are available on the abundance of different phylogenetic groups within the HNA and LNA assemblages, examination of the phylogenetic diversity indicated that most phylogenetic groups could be present in both the HNA and LNA assemblages (Chapter 4). Therefore, the bacterioplankton may be able to cycle between HNA and LNA assemblages depending on changes in the ecological conditions.

Despite the variability in the physical and biological parameters measured at the shelf stations, the NMS analysis revealed the samples from the shelf stations clustered together. The clustering of the shelf station samples was primarily due to the lower abundances of picoeukaryotes and *Synechococcus* at the shelf stations compared to the slope and basin stations. While the NMS analysis can not determine causes in the observed distribution of the cytometrically-defined populations, lower abundances of small phytoplankton (*Synechococcus* and picoeukaryotes) in the shelf region off the Oregon coast have been previously observed (E. B. Sherr et al. submitted). The high nutrient concentrations may favor larger diatoms, or there may be ions, particularly cadmium, present in the recently upwelled water which inhibit the growth of the smaller phytoplankton in culture conditions (Brand et al. 1986; Payne and Price 1999). Growth of *Synechococcus* may also be inhibited by the lower temperature of the recently upwelled water (Collier and Palenik 2003). Thus, the photoautotrophic cell abundances did vary across the transect, but aside from the samples from NH127

discussed above, the NMS did not reveal large differences in the HNA and LNA cell abundances across the sampling region despite large differences in the environmental parameters.

The abundance of HNA cells relative to the heterotrophic cell abundances increased with depth at NH127, concurrent with the decrease in the relative abundance of LNA cells. This was unexpected given the observed decrease in bacterial leucine incorporation, both cell-specific and volumetric, with depth. However, increases in the proportion of HNA cells with depth has also been observed in the Gulf of Mexico (Jochem 2001) and in Crater Lake (L. Eisner, personal communication). These observations highlight the need to consider the distribution of HNA and LNA cells with caution when attempting to use HNA and LNA abundances as the sole proxy for metabolic activity within a heterotrophic bacterial assemblage. There is millimeter scale heterogeneity in the distribution of cytometrically-defined, heterotrophic cells within samples from Australia (Seymour et al. 2004); furthermore, in 90% of their samples, greater differences were observed within sample sets than were observed between sample sets (Seymour et al. 2004). The distribution of cytometrically-defined cells from the Oregon coast samples may also vary at the same scales examined by Seymour and colleagues (2004), further highlighting the difficulties in assessing cell-specific levels of 'activity' in marine bacterioplankton.

2.5.5 Conclusions

By labeling cells with ^{3}H-leucine and sorting the marine bacterioplankton into different groups based on nucleic acid content or the presence of an active electron transport system, we have provided details on which components of marine bacterioplankton are responsible for variations in overall bacterial activity. Across a wide range of environmental conditions, phytoplankton stocks, and depths, we found that our results support previous results that the HNA cells have higher cell-specific metabolic activities and are responsible for the bulk of the volumetric leucine incorporation rate. However, there were instances where the cell-specific leucine incorporation was higher for the LNA cells and the volumetric leucine incorporation

by the LNA cells was proportionately more of the total leucine incorporation at the offshore station. Furthermore, while the CTC-positive cells did have leucine incorporation rates comparable to the HNA cells' leucine incorporation rates, their low abundances meant they were responsible for only a small fraction of volumetric leucine incorporation.

Acknowledgements We thank R. Condon, J. Fleischbein, J. Jennings, and M. Lichtenberg, the RV *Wecoma*'s captain, crew and marine technicians for assistance at sea, and the other cruise participants for thoughtful discussions during and after the cruise. The comments of three anonymous reviewers greatly improved this paper. This research was funded by NSF OCE-0002236 to B.F.S. and E.B.S.

2.6 Literature cited

Barth, J.A. (2003). Anomalous southward advection during 2002 in the Northern California Current: evidence from lagrangian surface drifters (doi:10.1029/2003GL017511). *Geophysical Research Letters* **30**: 8024.

Bernard, L., C. Courties, P. Servais, M. Troussellier, M. Petit and P. Lebaron (2000). Relationships among bacterial cell size, productivity, and genetic diversity in aquatic environments using cell sorting and flow cytometry. *Microbial Ecology* **40**: 148-158.

Bouvier, T.C. and P.A. del Giorgio (2002). Compositional changes in free-living bacterial communities along a salinity gradient in two temperate estuaries. *Limnology and Oceanography* **47**: 453-470.

Brand, L.E., W.G. Sunda and R.R. Guillard (1986). Reduction of marine phytoplankton reproduction rates by copper and cadmium. *Journal of Experimental Marine Biology and Ecology* **96**: 225-250.

Casotti, R., C. Brunet, B. Aronne and M. Ribera d'Alcala (2000). Mesoscale features of phytoplankton and planktonic bacteria in a coastal area as induced by external water masses. *Marine Ecology Progress Series* **195**: 15-27.

Chavez, F.P., J.T. Pennington, C.G. Castro, J.P. Ryan, R.P. Michisaki, B. Schlining, P. Walz, K.R. Buck, A. McFadyen and C.A. Collins (2002). Biological and chemical consequences of the 1997-1998 El Niño in central California waters. *Progress in Oceanography* **54**: 205-232.

Cole, J.J., S. Findlay and M.L. Pace (1988). Bacterial production in fresh and saltwater ecosystems: a cross-system overview. *Marine Ecology Progress Series* **43**: 1-10.

Collier, J.L. and B. Palenik (2003). Phycoerythrin-containing picoplankton in the Southern California Bight. *Deep-Sea Research* **50**: 2405-2422.

Corwith, H.L. and P.A. Wheeler (2002). El Niño related variations in nutrient and chlorophyll distributions off Oregon. *Progress in Oceanography* **54**: 361-380.

Cottrell, M.T. and D.L. Kirchman (2000). Natural assemblages of marine Proteobacteria and members of the *Cytophaga-Flavobacter* cluster consuming low- and high-molecular-weight dissolved organic matter. *Applied and Environmental Microbiology* **66**: 1692-1697.

Cottrell, M.T. and D.L. Kirchman (2003). Contribution of major bacterial groups to bacterial biomass production (thymidine and leucine incorporation) in the Delaware estuary. *Limnology and Oceanography* **48**: 168-178.

del Giorgio, P.A. and T.C. Bouvier (2002). Linking the physiologic and phylogenetic successions in free-living bacterial communities along an estuarine salinity gradient. *Limnology and Oceanography* **47**: 471-486.

del Giorgio, P.A., Y.T. Prairie and D.F. Bird (1997). Coupling between rates of bacterial production and the number of metabolically active cells in lake bacterioplankton, measured using CTC reduction and flow cytometry. *Microbial Ecology* **34**: 144-154.

Ducklow, H.W. (1999). The bacterial component of the oceanic euphotic zone. *FEMS Microbiology Ecology* **30**: 1-10.

Gasol, J.M. and P.A. del Giorgio (2000). Using flow cytometry for counting natural planktonic bacteria and understanding the structure of planktonic bacterial communities. *Scientia Marina* **64**: 197-224.

Gasol, J.M., U.L. Zweifel, F. Peters, J.A. Fuhrman and Å. Hagström (1999). Significance of size and nucleic acid content in heterogeneity as measured by flow cytometry in natural planktonic bacteria. *Applied and Environmental Microbiology* **65**: 4475-4483.

Gordon, L.I., J. J. C. Jennings, A.A. Ross and J.M. Krest (1994). A suggested protocol for continuous flow automated analysis of seawater nutrients (phosphate, nitrate, nitrite and silicic acid) in the WOCE Hydrographic Program and the Joint Global Ocean Fluxes Study. *WOCE Operations Manual, WOCE Report No. 68/91. Revision 1, 1994.*

Hill, J.K. and P.A. Wheeler (2002). Organic carbon and nitrogen in the northern California current system: comparison of offshore, river plume, and coastally upwelled waters. *Progress in Oceanography* **53**: 369-387.

Huyer, A., R.L. Smith and J. Fleischbein (2002). The coastal ocean off Oregon and northern California during the 1997-8 El Niño. *Progress in Oceanography* **54**: 311-341.

Jellett, J.F., W.K.W. Li, P.M. Dickie, A. Boraie and P.E. Kepkay (1996). Metabolic activity of bacterioplankton communities assessed by flow cytometry and single carbon substrate utilization. *Marine Ecology Progress Series* **136**: 213-225.

Jochem, F.J. (2001). Morphology and DNA content of bacterioplankton in the northern Gulf of Mexico: analysis by epifluorescence microscopy and flow cytometry. *Aquatic Microbial Ecology* **25**: 179-194.

Kara, A.B., P.A. Rochford and H.E. Hurlburt (2000). An optimal definition for ocean mixed layer depth. *Journal of Geophysical Research* **105**: 16,803-16,821.

Karner, M. and J.A. Fuhrman (1997). Determination of active marine bacterioplankton: a comparison of universal 16S rRNA probes, autoradiography, and nucleoid staining. *Applied and Environmental Microbiology* **63**: 1208-1213.

Kirchman, D.L. (1993). Leucine incorporation as a measure of biomass production by heterotrophic bacteria. *Current Methods in Aquatic Microbial Ecology*. P.F. Kemp, B.F. Sherr, E.B. Sherr and J.J. Cole (Eds). New York, Lewis Publishing: 509-512.

Kirchman, D.L., K.A. Hoffman, R. Weaver and D.A. Hutchins (2003). Regulation of growth and energetics of a marine bacterium by nitrogen source and iron availability. *Marine Ecology Progress Series* **250**: 291-296.

Kruskal, J.B. (1964). Multidimensional scaling by optimizing goodness of fit to a nonmetric hypothesis. *Psychometrika* **29**: 1-27.

Lebaron, P., P. Servais, H. Agogué, C. Courties and F. Joux (2001). Does the high nucleic acid content of individual bacterial cells allow us to discriminate between active cells and inactive cells in aquatic systems? *Applied and Environmental Microbiology* **67**: 1775-1782.

Li, W.K.W., J.F. Jellett and P.M. Dickie (1995). DNA distributions in planktonic bacteria stained with TOTO or TO-PRO. *Limnology and Oceanography* **40**: 1485-1495.

Marie, D., F. Partensky, S. Jacquet and D. Vaulot (1997). Enumeration and cell cycle analysis of natural populations of marine picoplankton by flow cytometry using the nucleic acid stain SYBR Green I. *Applied and Environmental Microbiology* **63**: 186-193.

Mather, P.M. (1976). *Computational methods of multivariate analysis in physical geography*. London, J. Wiley & Sons.

Murphree, T., S.J. Bograd, F.B. Schwing and B. Ford (2003). Large scale atmosphere-ocean anomalies in the northeast Pacific during 2002 (doi:10.1029/2003GL017303). *Geophysical Research Letters* **30**: 8026.

Nielsen, J.L., M. Aquino de Muro and P.H. Nielsen (2003). Evaluation of the redox dye 5-cyano-2,3-tolyl-tetrazolium chloride for activity studies by simultaneous use of microautoradiography and fluorescence in situ hybridization. *Applied and Environmental Microbiology* **69**: 641-643.

Olson, R.J., S.W. Chisholm, E.R. Zettler, M.A. Altabet and J.A. Dusenberry (1990). Spatial and temporal distributions of prochlorophyte picoplankton in the North Atlantic Ocean. *Deep-Sea Research* **37**: 1033-1051.

Payne, C.D. and N.M. Price (1999). Effects of cadmium toxicity on growth and elemental composition of marine phytoplankton. *Journal of Phycology* **35**: 293-302.

Peterson, W.T., J.E. Keister and L.R. Feinberg (2002). The effects of the 1997-1999 El Niño/La Niña events on the hydrography and zooplankton off the central Oregon coast. *Progress in Oceanography* **54**: 381-398.

Rodriguez, G.G., D. Phipps, K. Ishiguro and H.F. Ridgway (1992). Use of a fluorescent redox probe for direct visualization of actively respiring bacteria. *Applied and Environmental Microbiology* **58**: 1801-1808.

Servais, P., H. Agogué, C. Courties, F. Joux and P. Lebaron (2001). Are the actively respiring cells (CTC+) those responsible for bacterial production in aquatic environments? *FEMS Microbiology Ecology* **35**: 171-179.

Servais, P., E.O. Casamayor, C. Courties, P. Catala, N. Parthuisot and P. Lebaron (2003). Activity and diversity of bacterial cells with high and low nucleic acid content. *Aquatic Microbial Ecology* **33**: 41-51.

Servais, P., C. Courties, P. Lebaron and M. Troussellier (1999). Coupling bacterial activity measurements with cell sorting by flow cytometry. *Microbial Ecology* **38**: 180-189.

Seymour, J.R., J.G. Mitchell and L. Seuront (2004). Microscale heterogeneity in the activity of coastal bacterioplankton communities. *Aquatic Microbial Ecology* **35**: 1-16.

Sherr, B.F., P. del Giorgio and E.B. Sherr (1999). Estimating abundance and single-cell characteristics of respiring bacteria via the redox dye CTC. *Aquatic Microbial Ecology* **18**: 117-131.

Sherr, E.B., B.F. Sherr and T.J. Cowles (2001). Mesoscale variability in bacterial activity in the Northeast Pacific Ocean off Oregon, USA. *Aquatic Microbial Ecology* **25**: 21-30.

Sieracki, M.E., T.L. Cucci and J. Nicinski (1999). Flow cytometric analysis of 5-cyano-2,3-ditolyl tetrazolium chloride activity of marine bacterioplankton in dilution cultures. *Applied and Environmental Microbiology* **65**: 2409-2417.

Smith, D.C. and F. Azam (1992). A simple, economical method for measuring bacterial protein synthesis rates in sea water using ^{3}H-leucine. *Marine Microbial Food Webs* **6**: 107-114.

Smith, E.M. (1998). Coherence of microbial respiration rate and cell-specific bacterial activity in a coastal planktonic community. *Aquatic Microbial Ecology* **16**: 27-35.

Smith, E.M. and P.A. del Giorgio (2003). Low fractions of active bacteria in natural aquatic communities? *Aquatic Microbial Ecology* **31**: 203-208.

Smith, J.J. and G.A. McFeters (1997). Mechanisms of INT (2-(4-iodophenyl)-3-(4-nitrophenyl)-5-phenyl tetrazolium chloride), and CTC (5-cyano-2,3-ditolyl tetrazolium chloride) reduction in *Escherichia coli* K-12. *Journal of Microbiological Methods* **29**: 161-175.

Strickland, J.D.H. and T.R. Parsons, Eds. (1972). *A Practical Handbook of Seawater Analysis*. Fisheries Research Board of Canada. Ottawa.

Strub, P.T. and C. James (2003). Altimeter estimates of anomalous transports into the northern California Current during 2000–2002 (doi:10.1029/2003GL017513). *Geophysical Research Letters* **30**: 8025.

Vaqué, D., E.O. Casamayor and J.M. Gasol (2001). Dynamics of whole community bacterial production and grazing losses in seawater incubations as related to the changes in the proportions of bacteria with different DNA content. *Aquatic Microbial Ecology* **25**: 163-177.

Wetz, M.S. and P.A. Wheeler (2003). Production and partitioning of organic matter during simulated phytoplankton blooms. *Limnology and Oceanography* **48**: 1808-1817.

Wheeler, P.A., A. Huyer and J. Fleischbein (2003). Cold halocline, increased nutrients and higher chlorophyll off Oregon in 2002 (doi:10.1029/2003GLO17395). *Geophysical Research Letters* **30**: 8021.

Zubkov, M.V., B.M. Fuchs, P.H. Burkill and R. Amann (2001). Comparison of cellular and biomass specific activities of dominant bacterioplankton groups in stratified waters of the Celtic Sea. *Applied and Environmental Microbiology* **67**: 5210-5218.

Zubkov, M.V., B.M. Fuchs, G.A. Tarran, P.H. Burkill and R. Amann (2002). Mesoscale distribution of dominant bacterioplankton groups in the northern North Sea in early summer. *Aquatic Microbial Ecology* **29**: 135-144.

3 Analysis of DNA sequence data and environmental parameters using non-metric multidimensional scaling: A complement to existing methods to analyze DNA sequences

3.1 Abstract

The small size and virtually uniform appearance of prokaryotes has led to the increased use of DNA sequence data for their identification. This paper proposes the use of non-metric multidimensional scaling (NMS) to analyze differences between DNA sequences. The use of NMS in this paper is fundamentally different from other uses of NMS since NMS usually used to compare samples based on differences in the community of organisms present in each sample. In this paper, NMS is used to examine differences between DNA sequences, where each 'sample' in the NMS is a single DNA sequence. The DNA sequences were generated from samples collected off the Oregon coast and each sequence consists of about 500 nucleotides of the V3-V4-V5 variable regions of the 16S rRNA gene. Distance matrices of the DNA sequences were generated using the Jukes and Cantor nucleotide substitution model. These distance matrices were the input data for the NMS. Already available code for NMS was used with additional modifications to allow for Monte Carlo simulations to evaluate the significance of the NMS results. These results are presented concurrently with neighbor joining trees to allow for comparisons between the two methods. The benefit of NMS lies in its ability to consider the DNA sequence data in conjunction with measured environmental parameters. For the Oregon coast data, the DNA sequences clustered into groups such as the *Bacteroidetes* and the *Proteobacteria*. However, the correlations between the DNA sequences and the measured environmental parameters were low, suggesting that the environmental parameters were not being measured on the appropriate scale to explain the differences between the DNA sequences.

3.2 Introduction

DNA sequence data can be used to examine the phylogenetic affiliation of unknown organisms or to compare the diversity of organisms within and between ecosystems. The sequence data can be reduced to lists of organisms from BLAST searches BLAST (basic logic alignment search tool, Altschul et al. 1997), distance matrices, or trees. The trees or distance matrices can also be presented as raw data within the context of a larger project. As the number of DNA sequences increases, examining the sequence data becomes more difficult due to the limitations in the number of sequences that can be understood within the context of a tree. The use of clustered image maps ("heat maps"), which originated with the analysis of the impact of drugs on human cancer lines (Weinstein et al. 1997; Eisen et al. 1998; Scherf et al. 2000), is one method to analyze large numbers of sequences (Lilburn and Garrity 2004). While heat maps do allow for comparison of larger numbers of sequences, they do not allow the differences between sequences to be examined in conjunction with measured environmental parameters.

Ordination is a class of multivariate statistical analyses in which comparisons between samples are reduced from a multidimensional space to fewer dimensions, preferably two or three. The maximum possible number of dimensions in which to examine a set of samples is equal to the number of samples. Therefore, one goal in using ordination is to reduce the number of dimensions needed to explain the differences between samples. One form of ordination, Principal Components Analysis (PCA), has been used to examine the large number of sequences available from the Ribosomal Database Project (RDP-II) (Garrity and Lilburn 2002). The authors' goal was to examine the possibility of using PCA to compare sequences from RDP-II with the taxonomic outline presented in the second edition of *Bergey's Manual of Systematic Bacteriology*. While the authors were able to distinguish between sequences of different taxonomic groups, the use of PCA for this application is questionable due to the assumption of linear relationships between variables inherent within PCA. There is no reason to believe DNA sequence data are linearly related or that DNA sequence data would meet the requirements of multivariate normality. Thus,

while the use of an ordination technique to examine DNA sequence data is an interesting beginning, PCA is perhaps not the best technique to use.

Non-metric, multi-dimensional scaling (NMS, Kruskal 1964; Mather 1976) is a better alternative than PCA to examine the differences within a set of DNA sequences and to present possible correlations with measured environmental variables. Since NMS is a non-parametric method, the data are not expected to be normally distributed, nor is there an assumption of a linear relationship among variables. In community analysis, NMS can be used to examine the similarities (or differences) between samples collected over different temporal and spatial scales (see for example: van Hannen et al. 1999a; Peterson et al. 2002). NMS has been used in the analysis of sequence data to explore the distribution of trees generated during bootstrapping prior to the calculation of a single consensus tree (Amenta and Klingner 2002). However, these uses of NMS unlike the analysis proposed here. In this paper, NMS is used to examine the differences between DNA sequences obtained from samples collected off the Oregon coast. In addition to using NMS to graphically present the differences between the DNA sequences, I used graphical overlays and joint plots to present the correlations between the sequence data and the environmental parameters. This later step allows for examination of the diversity of the DNA sequence data within an ecological context. I do not intend that NMS replace other methods of analyzing DNA sequence data, rather I present NMS to complement existing methods of phylogenetic analysis.

3.3 Methods

3.3.1 Background on NMS

Using NMS to compare DNA sequences is different from other studies where NMS is used to examine ecological differences between samples. To help clarify these differences, the following background information on NMS is summarized from McCune and Grace (2002). I emphasize points where the analysis of DNA sequences that I am presenting here differs from traditional NMS analysis.

When using NMS to analyze community data, data analysis begins with the calculation of a distance matrix on the samples of interest. The distance matrix compares individual samples based on differences (or similarities) between the organisms present in each sample. These differences can be calculated as relationships between sample units (Q-mode analysis (Legendre and Legendre 1988) or 'normal' analysis (McCune and Grace 2002)), or as differences among species (R-mode analysis (Legendre and Legendre 1988), or 'transpose' analysis (McCune and Grace 2002)). The presence or absence of DNA sequences or the relative abundance of DNA sequences can be used as input for traditional NMS (see for example: van Hannen et al. 1999). In this case, the DNA sequences are used to identify the members of the community within each sample. The samples are then compared based on the number of DNA sequences or the presence / absence of the DNA sequences within a sample.

The analysis of DNA sequences I present in this paper is fundamentally different from using NMS to analyze community data in that it can not be classified as Q-mode/R-mode or normal/transpose analysis. In this paper, each 'sample' in the NMS analysis is a single DNA sequence. The differences between the DNA sequences are the unit being analyzed, not differences between the organisms present within a sample.

NMS, both for traditional community analysis and the analysis of DNA sequences I am presenting here, then seeks to graphically explain the ranked distances in a multi-dimensional ordination. In community analysis, the axes in the ordination are determined by differences between samples (Q-mode/normal analysis) or differences between species (R-mode/transpose analysis). In the analysis of DNA sequences, the axes are defined by differences between the DNA sequences. The initial position of the samples (in traditional NMS) or the DNA sequences (as presented here) are either from a given starting position, or random.

After the samples are placed in the ordination, the goodness of fit is determined. Within the ordination, Euclidean distances between samples (sequences in this analysis) are calculated and plotted against the distances in the original distance matrix. A perfect fit between the samples in the ordination space and the samples in

the original distance matrix would be a monotonically increasing line. The amount a sample would have to move to allow for a monotonically increasing line is calculated as 'stress,' where a high stress indicates a poor fit. For the analyses presented here, stress was calculated with 'stress formula one' (as given in: McCune and Grace 2002). The NMS analysis then proceeds to try and reduce the stress by altering the configuration of the samples (in traditional NMS) or sequences (as presented here). The direction of movement for each sample is calculated in order to minimize the stress for each point. These steps are repeated until a preset number of iterations is reached or until the change in stress is below a preset value. In this paper, a change in stress less than 0.0001 allowed the NMS iterations to stop, up to a maximum of 50 iterations.

3.3.2 NMS – determining the number of axes required

The number of axes in an NMS ordination is important since the position of samples on two axes will be altered by the addition of a third axis. Thus, the positions of the samples on the first two axes cannot be considered independently of additional axes added to the ordination results. A Monte Carlo simulation is used to determine whether additional axes significantly improve the NMS. Multiple runs with the real dataset are run and the stress values calculated for data arranged in k=1, 2, ... k dimensions. The data are then randomized and the stress values calculated for the same k=1, 2, ... k dimensions to allow for comparison of the real data with the randomized data. A *p*-value is then calculated as $p = \left(\frac{1+n}{1+\mathrm{N}}\right)$ where n is defined as the number of randomized runs with a final stress less than or equal to the real data's minimum stress; and N is the number of randomized runs. Two criteria based on suggestions by McCune and Grace (2002) were used in the present analysis to decide if the addition of an axis significantly improved the ordination. First, a p-value < 0.05 was used to decide if the addition of an axis significantly improved the ordination compared to the randomized data. Second, a stress reduction greater than 0.05 was required before an additional axis was added to the ordination

3.3.3 DNA sequence data used for the analysis

The sequence data used in this paper were obtained as part of the research presented in Chapter 4. Briefly, water samples collected off the Oregon coast were stained with the nucleic acid stain SYBR Green I and sorted on a flow cytometer based on whether the cells were high nucleic acid or low nucleic acid cells (Marie et al. 1997). Alternatively, the cells were incubated with 5-cyano-2,3-ditolyl tetrazolium chloride (CTC) to identify cells with an active electron transport system and then sorted on a flow cytometer (del Giorgio et al. 1997). The sorted cells were collected on a filter and the DNA extracted from the cells using a modified sucrose lysis method (Giovannoni et al. 1990b). After amplifying the V3-V4-V5 variable regions of the 16S rRNA genes with PCR, denaturing gradient gel electrophoresis (DGGE) was used to separate the PCR-amplified 16S rRNA genes. To obtain the sequences of the individual DGGE bands, the bands were removed from the gels and sequenced by cycle sequencing using fluorescent dideoxy terminators. The sequences were resolved using an ABI 3100 at Oregon State University's Central Services Lab. TraceViewer (CodonCode Corporation) was used to manually check the results of the base calling. The sequences were aligned in ARB (Ludwig et al. 2004), initially using the FastAligner, and then manually checked. The alignment included close representatives that were identified based on data from BLAST (Altschul et al. 1997). Following BLAST searches, the variable regions of the genes were removed to allow subsequent analyses to focus on conserved regions. The Jukes and Cantor (1969) nucleotide substitution model, which assumes equal base frequencies and that all substitutions are equally likely, was used to generate neighbor joining trees in ARB. Distance matrices were constructed with the Jukes and Cantor nucleotide substitution model in PAUP 4.0b10 (Swofford 1998). These distance matrices were used as the input for NMS. Other distance measures presented similar results (Felsenstein 1981; Lanave et al. 1984; Hasegawa et al. 1985; Rodriguez et al. 1990). However, since the purpose of this analysis was not to compare different nucleotide substitution models, the simplest model was chosen for further analysis.

To determine the phylogenetic affiliation of the sequences from the DGGE gels, maximum likelihood trees were constructed in ARB using almost full length 16S rRNA genes. The sequences from the DGGE bands were inserted into the maximum likelihood trees using the parsimony option in ARB. The sequences from the DGGE bands were then divided into the following groups: *Actinobacteria*, *Meiothermus*, *Bacteroidetes*, *Alphaproteobacteria*, *Betaproteobacteria*, *Deltaproteobacteria*, and *Gammaproteobacteria*.

3.3.4 Details on conducting the NMS analysis

The NMS analysis was run on Matlab 6.5 using Mark Steyver's Nonmetric Multidimensional Scaling Toolbox as called by the Fathom toolbox written by David Jones, University of Miami, Department of Marine Biology & Fisheries. Both toolboxes are available at http://www.rsmas.miami.edu/personal/djones. The input for the NMS was the Jukes and Cantor distance matrices calculated based on differences between each pair of DNA sequences. In more traditional uses of NMS, the input for the NMS would be distance matrices calculated based on the number, relative abundance, or presence / absence of organisms within a sample. The NMS analyses were started with random starting positions for 25 runs of real data. Additional Matlab code was written to run the Monte Carlo simulations. For the Monte Carlo simulations, the distance matrix was randomized and the NMS run again, also with a random starting position. After each run, the distance matrix was randomized again. Fifty runs with randomized data were conducted. Once the appropriate number of dimensions was determined from the Monte Carlo simulations, the NMS was rerun with that number of dimensions. The outputs from the NMS were the coordinates for each point in the NMS and the final stress. For the analysis of DNA sequences, each point represented a single DNA sequence. An r^2 was calculated using a Mantel test (Legendre and Legendre 1988; Sokal and Rohlf 1995) to examine the relationship between the two distance matrices: the distances in the original dataset were the Jukes and Cantor distances, while the distances in the ordination were Euclidean distances calculated between each pair of points. Both distance matrices were ranked to avoid

the linear model otherwise inherent in the Mantel test calculation (Dietz 1983). Furthermore, the distances were standardized so the output behaves like a correlation coefficient which ranges from -1 to 1 before being squared. The Mantel test indicates how much of the variation between the DNA sequences is explained by the NMS; larger r^2 values indicate a higher proportion of the differences between DNA sequences is explained by the ordination.

After the NMS analysis was run, joint plots were used to present the correlations between the NMS analysis and the measured environmental parameters. The non-parametric Kendall's coefficient of rank correlations (Kendall's tau, Sokal and Rohlf 1995) was calculated to compare the association between the ordination results and the measured environmental parameters. The length of the joint plot was scaled to the strength of the correlation while the angle of the joint plot was calculated as: $\Theta = \arctan\left(\frac{r_1}{r_2}\right)$ where r_1 is the correlation between the ordination results and the environmental parameters on the first axis and r_2 is the correlation on the second axis (Jongman et al. 1995). Another way of thinking about the joint plots is to consider the angle and relative length of the lines as indicating the direction and relative strength of the relationship between the ordination results and the environmental parameters. The joint plot and r^2 calculations presented here are the same calculations used in traditional uses of NMS.

3.4 Results and Discussion

The results of the Monte Carlo simulations indicated a two-dimensional solution was appropriate for these data, with the scree plot (Figure 3-1) presenting a graphical comparison of the data in Table 3-1. The random stress values were always greater than the real stress values. However, the addition of a third axis did not reduce the stress by more than 0.05, so a two-dimensional solution was appropriate for these data. The NMS was rerun with two dimensions and the stress was 0.19 and $r^2 = 0.88$ in the final NMS run. This was considered a reasonable stress value for environmental data using criteria established by Clarke (Clarke 1993) or Kruskal (1964, as cited in

McCune and Grace (2002)). The results of the two-dimensional ordination are shown in Figure 3-2 and in Figure 3-3. Each point in the ordination is a single DNA sequence. The ordination indicates that there were three clusters of sequences which were closely related and which represent about 60% of the sequences within the ordination. However, there was also a set of sequences which were more divergent from the other sequences; these sequences appear at the periphery of the ordination.

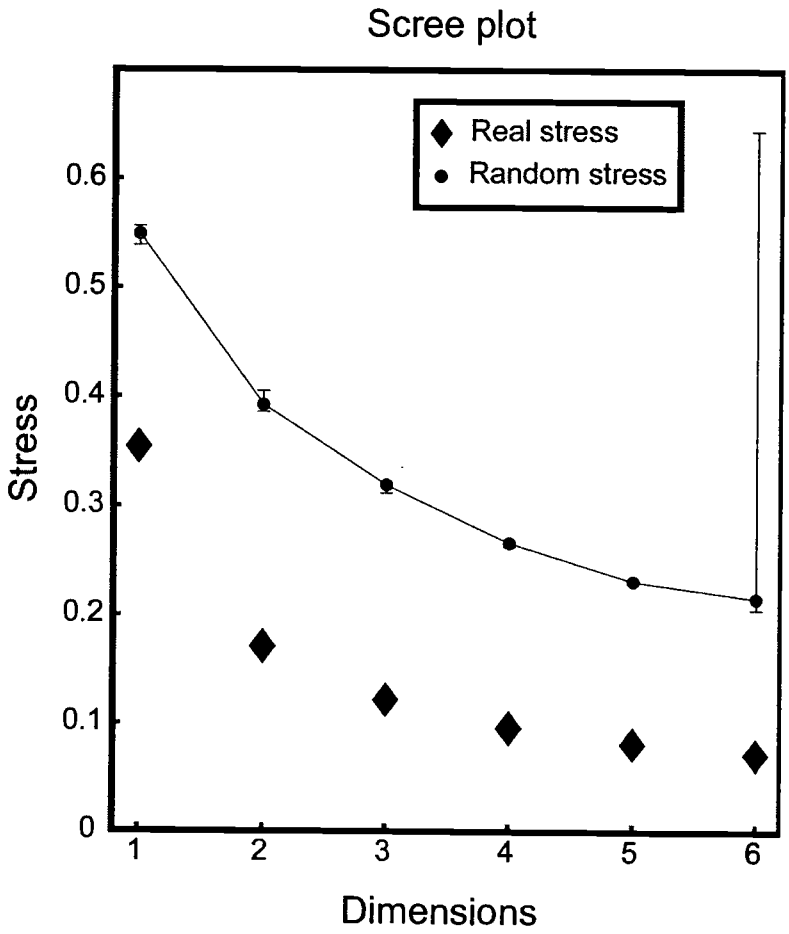

Figure 3-1. Scree plot showing the results of the Monte Carlo simulations used to determine the appropriate number of axes for these data. Up to six dimensions were tested, and the real and random stress values are shown for each dimension, with the minimum and maximum random stress shown as bars above and below the mean random stress.

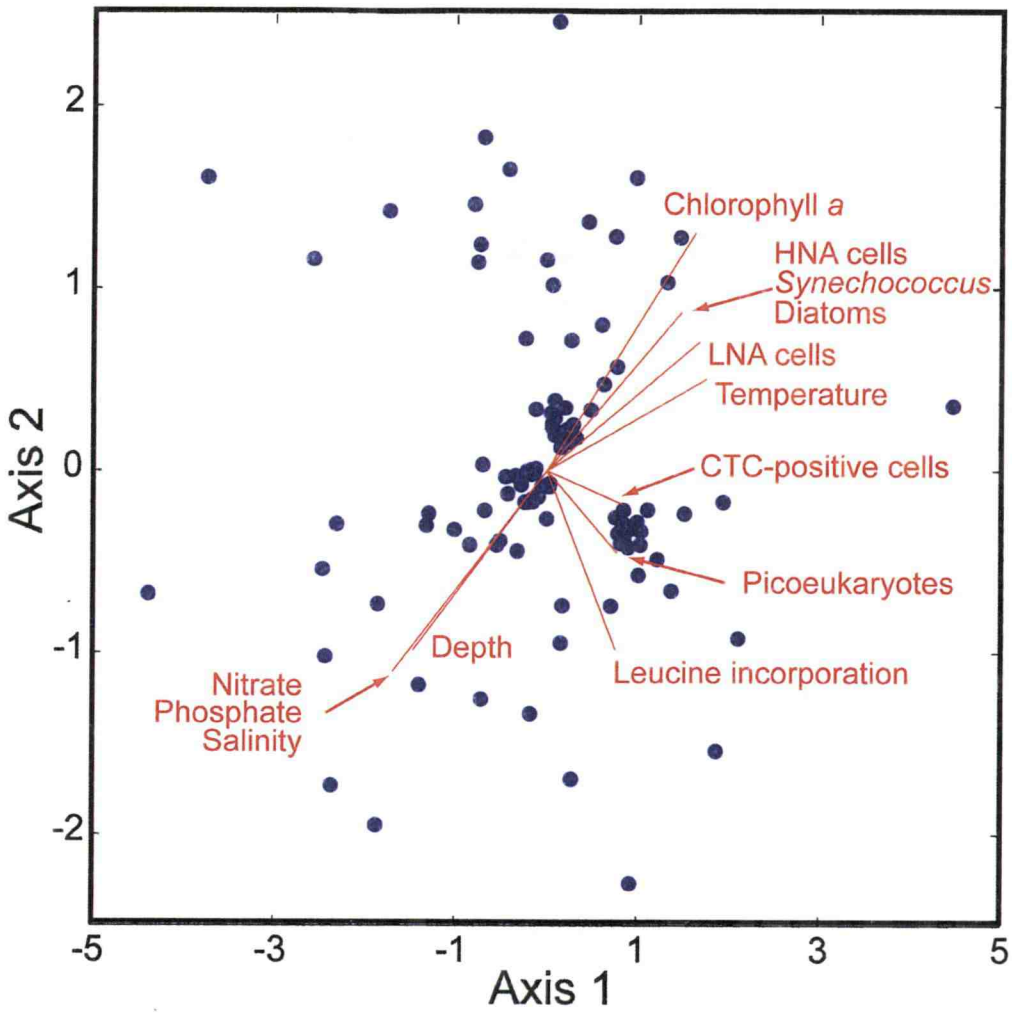

Figure 3-2. Results from the non-metric multidimensional scaling (NMS) of the sequence data obtained from the Oregon coast samples. Overlaid on top of the ordination are the joint plots showing the correlations with the measured environmental parameters.

Table 3-1. Results of the Monte Carlo simulations used to determine the appropriate number of dimensions for the NMS analysis. Six dimensions were tested where 25 runs with real data were compared to 50 runs with randomized data for each dimension. The *p*-values were calculated as indicated in the Methods section and the criteria from McCune and Grace (2002) were used to determine that a two-dimensional solution was appropriate for these data.

	Real data stress	**Randomized data stress**			
Dimensions	**Minimum**	**Minimum**	**Maximum**	**Mean**	***p*-value**
1	0.35	0.54	0.56	0.55	0.02
2	0.17	0.39	0.41	0.39	0.02
3	0.12	0.31	0.32	0.32	0.02
4	0.10	0.26	0.27	0.27	0.02
5	0.08	0.23	0.23	0.23	0.02
6	0.07	0.21	0.65	0.22	0.02

One advantage of using NMS to present differences among DNA sequences is the ability to compare the sequence data in conjunction with measured environmental parameters. These parameters can take the form of joint plots for ordinal variables or plots of categorical data associated with each of the sequences. Following the NMS analysis, correlations between the location of each sample within the ordination and measured environmental parameters can be calculated. These correlations can be presented in tabular form (Table 3-2) or as joint plots overlaid on the ordination (Figure 3-2). These joints plots are shown as red lines in Figure 3-2, the length of the line for each joint plot is an indication of the strength of the correlation between the environmental parameter and the position of the sequences within the ordination. The direction of the line indicates the direction of the correlation. For example, leucine incorporation is negatively correlated with Axis 2, but slightly positively correlated with Axis 1. However, the Kendall correlation coefficients for any of these comparisons were quite low (Table 3-2). Furthermore, inspection of the individual plots of ordination scores against the environmental parameters revealed no other

patterns, such as bimodal or unimodal correlations, which would be obscured by a rank correlation.

Table 3-2. Kendall's tau values comparing the environmental parameters with the ordination for the entire dataset. Inspection of plots of ordination scores against the environmental parameters revealed no other patterns which would be obscured by reliance on Kendall's tau values.

	Axis 1	**Axis 2**
Depth	-0.15	-0.10
Chlorophyll *a*	0.16	0.13
Temperature	0.17	0.05
Salinity	-0.17	-0.11
Nitrate	-0.17	-0.11
Phosphate	-0.17	-0.11
Leucine incorporation	0.08	-0.10
Cell abundances:		
HNA cells	0.15	0.09
LNA cells	0.17	0.07
CTC-positive cells	0.08	-0.02
Synechococcus	0.15	0.09
Diatoms	0.15	0.09
Picoeukaryotes	0.08	-0.04

Another type of environmental data, categorical data, can also be considered along with the NMS results. For categorical data, the samples within the ordination can be color-coded based on pre-defined categories. Within phylogenetic trees usually used to analyze DNA sequences, the sequences from different sampling sites could also be coded. For example, physiological properties of *Synechococcus* and *Prochlorococcus* sequences based on photosynthetic pigments, nutrient utilization patterns, and depth distribution have been noted in conjunction with clustering of sequences obtained from environmental samples and cultured isolates (Moore et al.

1998; Moore and Chisholm 1999; Moore et al. 2002; Rocap et al. 2002; Rocap et al. 2003). However, defining categorical data within trees becomes more complex if there are more than one or two groups, or the categorical codes span several different branches of a given tree. One form of categorical variable possible with these data is the phylogenetic affiliation of the DNA sequences. The phylogenetic affiliation of each sequence is noted with a different symbol in Figure 3-3. Examination of Figure 3-3 indicates the differences between some phylogenetic groups is easily apparent. For example, the *Bacteroidetes* sequences cluster separately from other sequences, with about 10% of the nucleotides varying between the *Bacteroidetes* sequences. However, the *Alphaproteobacteria* span across the ordination, and up to 50% of the nucleotides differ between the sequences.

For comparison, the results of the neighbor joining trees are shown in Figure 3-4. Where possible, the sequences were clustered into groups based on phylogenetic affiliations to ease analysis of the data. The tree and the NMS ordination agreed in the presentation of outliers. In the tree, the group of *Alphaproteobacteria** had long branch lengths. These sequences, marked with an orange oval in Figure 3-3, appeared more distant from the other sequences within the NMS ordination. Furthermore, the single cluster of sequences marked as *Bacteroidetes* in the neighbor joining tree also clustered together in the NMS ordination. Thus, for the *Bacteroidetes* and the *Alphaproteobacteria*, the differences between the DNA sequences were represented in a similar manner in both the NMS and the neighbor joining tree. However, the lack of a separation between the *Betaproteobacteria* and *Gammaproteobacteria* highlights the need to use the NMS analysis in conjunction with other measures, such as calculation of neighbor joining trees.

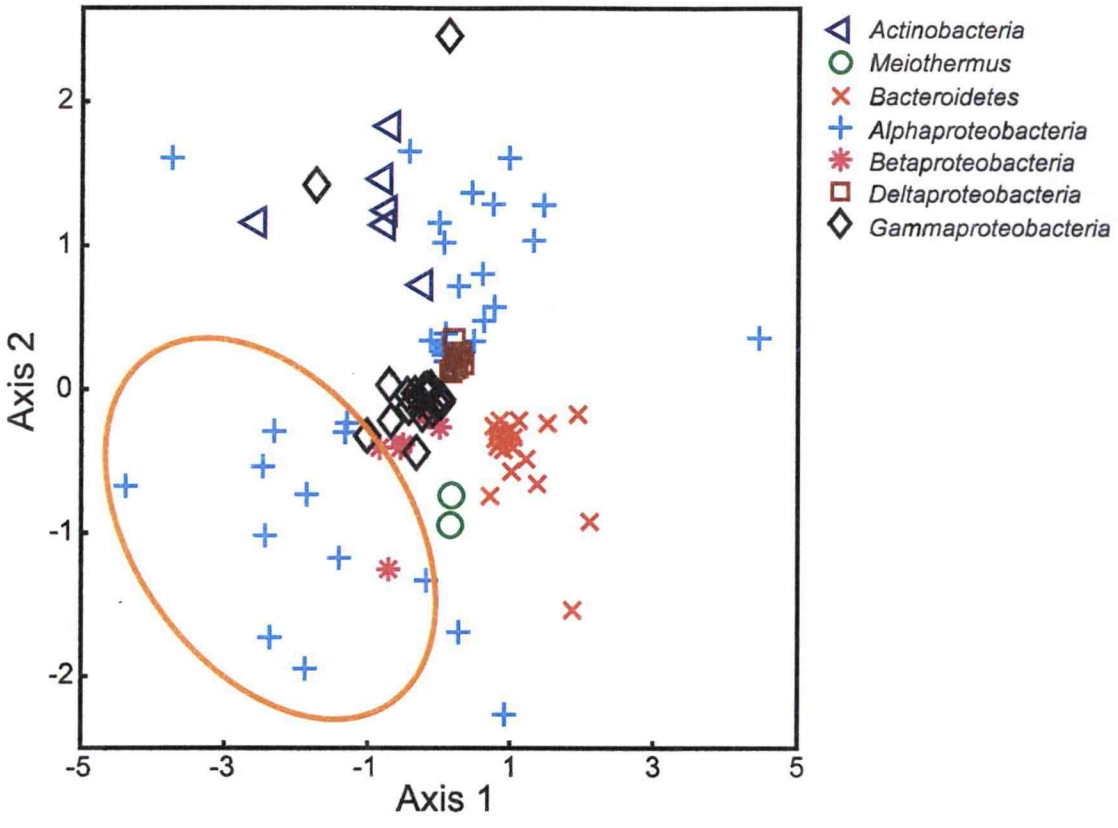

Figure 3-3. The phylogenetic affiliation of the DNA sequences can be plotted on the NMS ordination as categorical variables. The ordination contains the same sequences as in Figure 3-2, only the symbols have changed with the legend indicating the phylogenetic designation for each DNA sequence. The sequences within the orange oval correspond to the *Alphaproteobacteria** sequences in Figure 3-4.

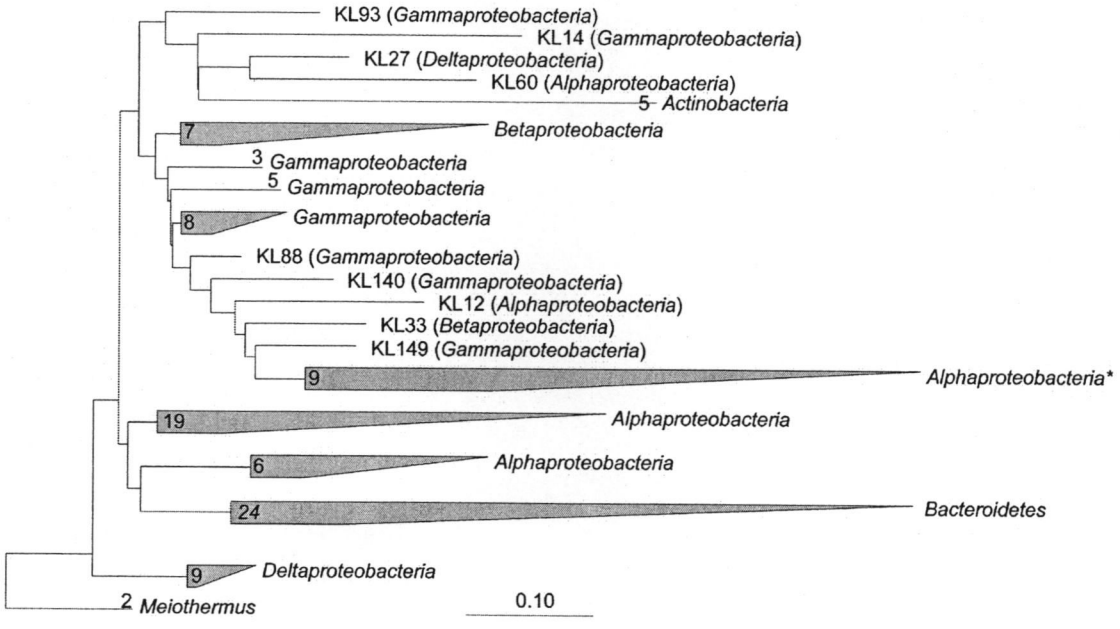

Figure 3-4. Neighbor joining tree constructed from sequence data for the DGGE bands obtained from samples collected off the Oregon coast. To improve the clarity of presentation, the sequences were compressed into groups where possible. The number of sequences within each group are given within the shaded boxes or to the left of the group name. Only sequences used within the NMS analysis were used to generate the tree.

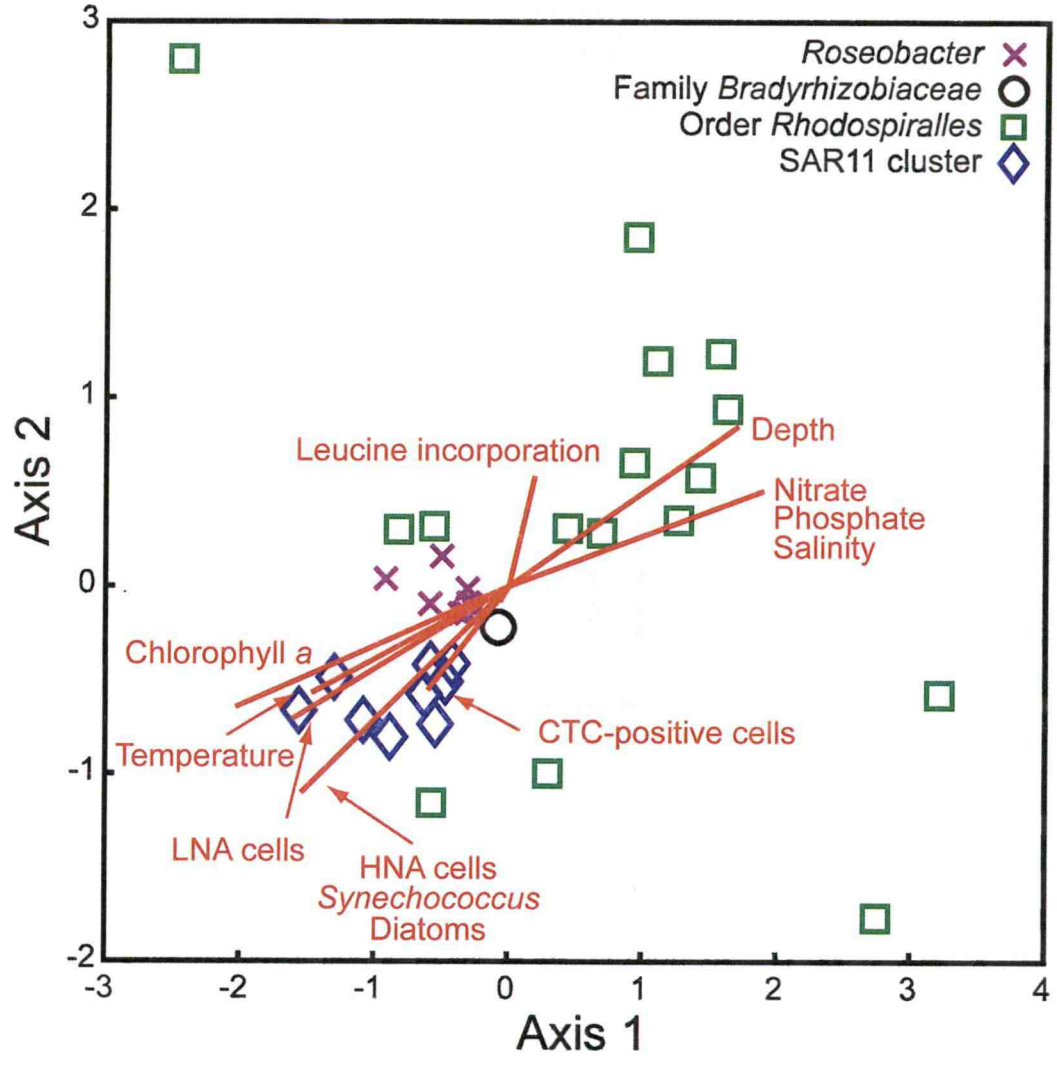

Figure 3-5. Results of the NMS analysis for the *Alphaproteobacteria* with the correlations with the environmental variables overlaid as joint plots. The symbols in the legend correspond to different groups defined within the *Alphaproteobacteria*.

The NMS analysis can also be conducted on the different phylogenetic groups separately. The NMS of the *Alphaproteobacteria* is shown in Figure 3-5 with the correlations with the environmental data overlaid as joint plots. The final stress for this ordination was 0.12 and $r^2 = 0.92$. When only the *Alphaproteobacteria* were analyzed, the correlations with environmental parameters were higher than for the entire set of DGGE sequences (data not shown), although they still did not explain a large

proportion of the differences between the DNA sequences. Thus, even though the analysis considered sequences which were contained within the same class, they were still not closely linked to measured environmental parameters. However, the use of NMS with these data made the variability in the *Alphaproteobacteria* clear by indicating that the more genetically distinct *Alphaproteobacteria* sequences were primarily from the offshore region (Figure 3-6) and were found in samples with high nutrients and salinities.

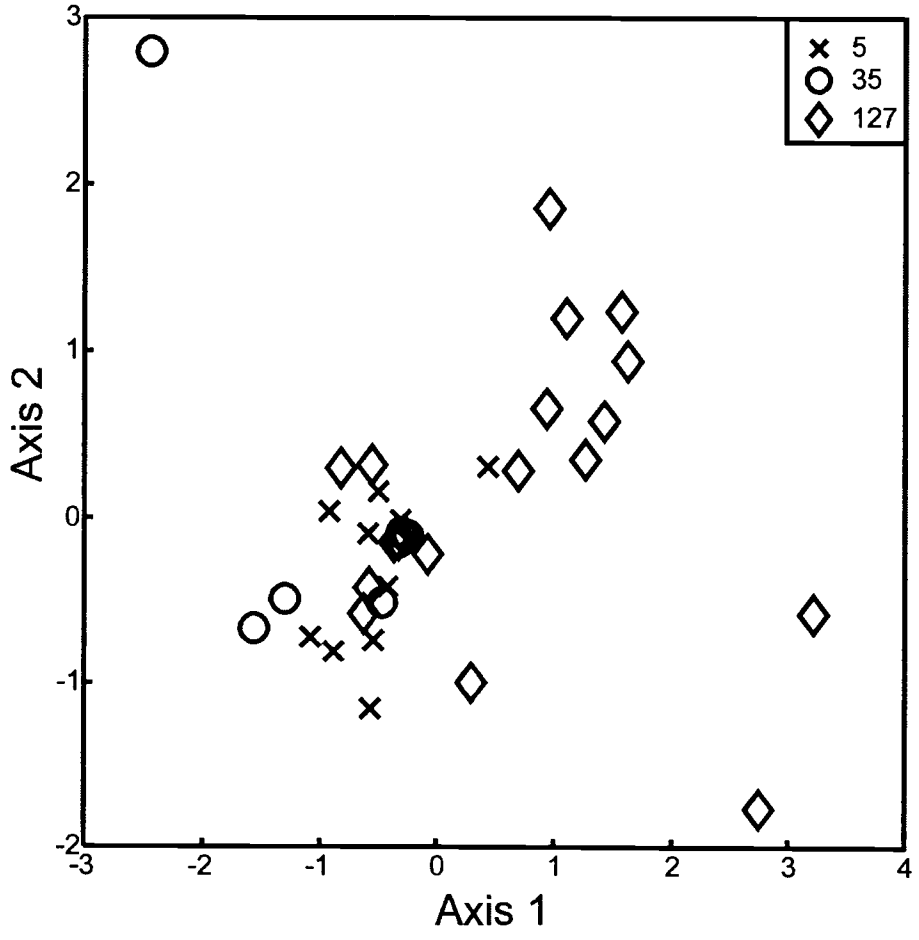

Figure 3-6. NMS ordination of the *Alphaproteobacteria* with the different sampling stations shown as categorical variables. The legend indicates the three different stations given as distances in nautical miles from the Oregon coast.

Although the data from the Oregon coast did not exhibit any strong correlations with the environmental data, plotting the categorical variables with the

ordination results revealed some interesting patterns, particularly with the *Alphaproteobacteria* sequences. Furthermore, the lack of strong correlations between the DNA sequences and the measured environmental parameters suggests that the environmental parameters were not being measured on the appropriate scale to explain the differences between the DNA sequences. This result is not entirely unexpected as DNA sequences change on evolutionary time scales rather than the much shorter ecological time scales which causes variability in the environmental parameters. Use of NMS to analyze DNA sequences from other experiments may reveal stronger correlations between environmental parameters and DNA sequences not observed with this dataset. Since NMS is a non-parametric method, the sequences are not expected to be linearly related, nor are expected to be distributed in a multivariate normal fashion. Thus, the use of NMS to analyze DNA sequence data presents a suitable addition to the suite of tools already available for phylogenetic analysis.

Acknowledgements. The impetus for this project came during Bruce McCune's Community Analysis class. Discussions with Mark Baumgartner, Sam Laney, and Bob Morris were helpful during the development of this idea; however, any faults in the logic and analysis are entirely my own. Support from NSF grants OCE-0002236 and OCE-0240785 to B. and E. Sherr is gratefully acknowledged.

3.5 Literature cited

Altschul, S.F., T.L. Madden, A.A. Schäffer, J. Zhang, Z. Zhang, W. Miller and D.J. Lipman (1997). Gapped BLAST and PSI-BLAST: a new generation of protein database search programs. *Nucleic Acids Research* **25**: 3389-3402.

Amenta, N. and J. Klingner (2002). Case study: visualizing sets of evolutionary trees. *IEEE Information Visualization*: 71-74.

Clarke, K.R. (1993). Non-parametric multivariate analysis of changes in community structure. *Australian Journal of Ecology* **18**: 117-143.

del Giorgio, P.A., Y.T. Prairie and D.F. Bird (1997). Coupling between rates of bacterial production and the number of metabolically active cells in lake bacterioplankton, measured using CTC reduction and flow cytometry. *Microbial Ecology* **34**: 144-154.

Dietz, E.J. (1983). Permutation tests for association between two distance matrices. *Systematic Zoology* **32**: 21-26.

Eisen, M.B., P.T. Spellman, P.O. Brown and D. Botstein (1998). Cluster analysis and display of genome-wide expression patterns. *Proceedings of the National Academy of Sciences, USA* **95**: 14863-14868.

Felsenstein, J. (1981). Evolutionary trees from DNA sequences: A maximum likelihood approach. *Journal of Molecular Evolution* **17**: 368-376.

Garrity, G.M. and T.G. Lilburn (2002). Mapping taxonomic space: an overview of the road map to the second edition of Bergey's Manual of Systematic Bacteriology. *WFCC Newsletter* **35**: 5-15.

Giovannoni, S.J., E.F. DeLong, T.M. Schmidt and N.R. Pace (1990). Tangential flow filtration and preliminary phylogenetic analysis of marine picoplankton. *Applied and Environmental Microbiology* **56**: 2572-2575.

Hasegawa, M., H. Kishino and T. Yano (1985). Dating of the human-ape splitting by a molecular clock of mitochondrial DNA. *Journal of Molecular Evolution* **22**: 160-174.

Jongman, R.H.G., C.J.F. ter Braak and O.F.R. van Tongeren, Eds. (1995). *Data analysis in community and landscape ecology*, Cambridge University Press.

Jukes, T.H. and C.R. Cantor (1969). Evolution of protein molecules. *Mammalian Protein Metabolism*. H.N. Munro (Ed). New York, Academic Press. **3:** 21-132.

Kruskal, J.B. (1964). Multidimensional scaling by optimizing goodness of fit to a nonmetric hypothesis. *Psychometrika* **29**: 1-27.

Lanave, C., G. Preparata, C. Saccone and G. Serio (1984). A new method for calculating evolutionary substitution rates. *Journal of Molecular Evolution* **20**: 86-93.

Legendre, P. and L. Legendre (1988). *Numerical Ecology*. Amsterdam, The Netherlands, Elsevier Science BV.

Lilburn, T.G. and G.M. Garrity (2004). Exploring prokaryotic taxonomy. *International Journal of Systematic and Evolutionary Microbiology* **54**: 7-13.

Ludwig, W., O. Strunk, R. Westram, L. Richter, H. Meier, Yadhukumar, A. Buchner, T. Lai, S. Steppi, G. Jobb, W. Förster, I. Brettske, S. Gerber, A.W. Ginhart, O. Gross, S. Grumann, S. Hermann, R. Jost, A. König, T. Liss, R. Lüßmann, M. May, B. Nonhoff, B. Reichel, R. Strehlow, A. Stamatakis, N. Stuckmann, A. Vilbig, M. Lenke, T. Ludwig, A. Bode and K.-H. Schleifer (2004). ARB: a software environment for sequence data. *Nucleic Acids Research* **32**: 1363-1371.

Marie, D., F. Partensky, S. Jacquet and D. Vaulot (1997). Enumeration and cell cycle analysis of natural populations of marine picoplankton by flow cytometry using the nucleic acid stain SYBR Green I. *Applied and Environmental Microbiology* **63**: 186-193.

Mather, P.M. (1976). *Computational methods of multivariate analysis in physical geography*. London, J. Wiley & Sons.

McCune, B.M. and J.B. Grace (2002). *Analysis of Ecological Communities*. Gleneden Beach, Oregon, MjM Software Design.

Moore, L.R. and S.W. Chisholm (1999). Photophysiology of the marine cyanobacterium *Prochlorococcus*: Ecotypic differences among cultured isolates. *Limnology and Oceanography* **44**: 628-638.

Moore, L.R., A.F. Post, G. Rocap and S.W. Chisholm (2002). Utilization of different nitrogen sources by the marine cyanobacteria *Prochlorococcus* and *Synechococcus*. *Limnology and Oceanography* **47**: 989-996.

Moore, L.R., G. Rocap and S.W. Chisholm (1998). Physiology and molecular phylogeny of coexisting *Prochlorococcus* ecotypes. *Nature* **393**: 464-467.

Peterson, W.T., J.E. Keister and L.R. Feinberg (2002). The effects of the 1997-1999 El Niño/La Niña events on the hydrography and zooplankton off the central Oregon coast. *Progress in Oceanography* **54**: 381-398.

Rocap, G., D.L. Distel, J.B. Waterbury and S.W. Chisholm (2002). Resolution of *Prochlorococcus* and *Synechococcus* ecotypes by using 16S-23S ribosomal DNA internal transcribed spacer sequences. *Applied and Environmental Microbiology* **68**: 1180-1191.

Rocap, G., F.W. Larimer, J. Lamerdin, S. Malfatti, P. Chain, N.A. Ahlgren, A. Arellano, M. Coleman, L. Hauser, W.R. Hess, Z.I. Johnson, M. Land, D. Lindell, A.F. Post, W. Regala, M. Shah, S.L. Shaw, C. Steglich, M.B. Sullivan, C.S. Ting, A. Tolonen, E.A. Webb, E.R. Zinser and S.W. Chisholm (2003). Genome divergence in two *Prochlorococcus* ecotypes reflects oceanic niche differentiation. *Nature* **424**: 1042-1047.

Rodriguez, F., J.F. Oliver, A. Marin and J.R. Medina (1990). The general stochastic model of nucleotide substitutions. *Journal of Theoretical Biology* **142**: 485-501.

Scherf, U., D.T. Ross, M. Waltham, L.H. Smith, J.K. Lee, L. Tanabe, K.W. Kohn, W.C. Reinhold, T.G. Myers, D.T. Andrews, D.A. Scudiero, M.B. Eisen, E.A. Sausville, Y. Pommier, D. Botstein, P.O. Brown and J.N. Weinstein (2000). A gene expression database for the molecular pharmacology of cancer. *Nature Genetics* **24**: 236-244.

Sokal, R.R. and F.J. Rohlf (1995). *Biometry*. New York, W. H. Freeman, New York.

Swofford, D.L. (1998). PAUP*. Phylogenetic Analysis Using Parsimony (*and other methods). Version 4. Sunderland, MA, Sinauer Associates.

van Hannen, E.J., W. Mooij, M.P. van Agterveld, H.J. Gons and H.J. Laanbroek (1999). Detritus-dependent development of the microbial community in an experimental system: qualitative analysis by denaturing gradient gel electrophoresis. *Applied and Environmental Microbiology* **65**: 2478-2484.

Weinstein, J.N., T.G. Myers, P.M. O'Connor, S.H. Friend, A.J. Fornace, Jr., K.W. Kohn, T. Fojo, S.E. Bates, L.V. Rubinstein, N.L. Anderson, J.K. Buolamwini, W.W. van Osdol, A.P. Monks, D.A. Scudiero, E.A. Sausville, D.W. Zaharevitz, B. Bunow, V.N. Viswanadhan, G.S. Johnson, R.E. Wittes and K.D. Paull (1997). An information-intensive approach to the molecular pharmacology of cancer. *Science* **275**: 343-349.

4 Diversity and metabolic status of *Bacteria* in the California Current System off Oregon, U.S.A.

4.1 Abstract

Whether or not the high diversity of marine *Bacteria* is reflected by a similar diversity in metabolically 'active' bacterioplankton is a current focus of study in marine microbial ecology. In this study we addressed the question: do bacterial cells that can be identified as being more or less active segregate into distinct phylogenetic groups, or are the assemblages of more or less active cells characterized by a similar phylogenetic diversity? We sampled bacterioplankton across the California Current System (CCS) off the Oregon coast, from the eutrophic nearshore upwelling zone to oligotrophic waters on the seaward side of the California Current. Relative cell-specific metabolic activity in bacterioplankton cells was identified using flow cytometry in two ways: as relative cell-specific nucleic acid content via staining with SYBR Green I, or as ability to reduce sufficient 5-cyano-2,3-ditolyl tetrazolium chloride (CTC) to be identified as having an active electron transport system. Cells were sorted via flow cytometry into high nucleic acid (HNA), low nucleic acid (LNA), or CTC-positive groups. DNA was extracted from each sorted group, and denaturing gradient gel electrophoresis (DGGE) of the PCR-amplified 16S rRNA gene was used to examine the phylogenetic diversity of *Bacteria*. Sequence data obtained from the DGGE bands indicated that most of the phylogenetic groups identified in this study were present in both the HNA and the LNA assemblages, although not always in the same samples. Furthermore, most of the identified phylotypes were also present in the CTC-positive assemblages of sorted cells. Our results suggest that diverse phylogenetic groups of *Bacteria* in the CCS exhibit a similar range of metabolic activity, and that there is variability in the phylogenetic composition of the more active cells from site to site.

4.2 Introduction

The application of phylogenetic analysis based on 16S rRNA genes has revealed a diverse array of *Bacteria* and *Archaea* are present within marine systems.

However, linking the different phylogenetic groups in marine ecosystems to their ecological and biogeochemical roles in marine ecosystems is difficult. Combining methods used to quantify 'active' cells with molecular analysis has opened new avenues of research into identifying prokaryotic cells within marine systems which are actively involved in global biogeochemical cycles. Identifying a prokaryotic cell as 'active' is not without its own difficulties since there is no clear definition of what constitutes an active cell. There are methods based on cells' ability to incorporate or exclude compounds, methods based on the presence of an active electron transport system, and methods which compare cell-specific nucleic acid or protein contents (for some examples see: del Giorgio et al. 1997; Sherr et al. 1999; Grégori et al. 2001; Zubkov et al. 2002b). For each activity assay, specific subsets of the prokaryotic community may respond differently depending on their metabolic capabilities and status at the time of sampling. This complicates the interpretation of the results from these assays.

Flow cytometric analysis of bacterial cells stained with nucleic acid dyes such as SYBR Green, combined with analysis of cell-specific incorporation rates of radioactively-labeled substrates, have indicated that bacterial cells with higher cell-specific nucleic acid content tend to be the more metabolically active members of the heterotrophic community (Li 1995; Jellett et al. 1996; Marie et al. 1997; Gasol et al. 1999; Gasol and del Giorgio 2000; Lebaron et al. 2001). Phylogenetic evaluation of the different populations of cells sorted based on their nucleic acid content has led to conflicting results about whether the high nucleic acid cells and low nucleic acid cells (HNA and LNA, respectively) contain the same, or different, phylogenetic diversity of prokaryotes. In a study in the North Sea, fluorescence in situ hybridization (FISH) indicated that HNA-high scatter (higher side scatter values in side scatter versus green fluorescence cytograms) cells were primarily *Alphaproteobacteria*, while the HNA-low scatter cells were primarily within the *Cytophaga-Flavobacterium* cluster (Zubkov et al. 2001a; Zubkov et al. 2001b). The LNA cells were all within the SAR86 cluster of the *Gammaproteobacteria*. Conversely, Servais and colleagues (2003) found, using PCR single-strand conformation polymorphism (SSCP), that the HNA

and LNA cell populations sampled in coastal Mediterranean waters were not phylogenetically different.

The use of 5-cyano-2,3-ditolyl tetrazolium chloride (CTC) can identify cells with an active electron transport system (Rodriguez et al. 1992; Smith and McFeters 1997). Sorting cells incubated with a radioactively-labeled metabolic precursor has shown the CTC-positive cells, on average, can incorporate more of the labeled material than the average cell in the total heterotrophic population (Chapter 2, Servais et al. 1999). There are instances when the CTC-positive cells incorporate less than the average heterotrophic cells and, collectively, they are responsible for between 7 (Chapter 2) to 60% (Servais et al. 1999) of the total incorporation. The phylogenetic diversity of CTC-positive cells from coastal Mediterranean seawater indicated most of the DGGE bands in the whole seawater community were also present in the CTC-positive community (Bernard et al. 2000; Bernard et al. 2001). However, the diversity of *Bacteria* within the samples may have been altered by the addition of yeast extract which was added in order to obtain sufficient DNA for further analysis. Sorting of CTC-positive cells from soil microcosms indicated the phylogenetic diversity of the CTC-positive cells, based on length heterogeneity PCR, was a subset of the diversity of the total community (Whiteley et al. 2003). Furthermore, changes in the diversity of the total community in the microcosms was not observed, although the CTC-positive cells did show a shift in phylogenetic diversity over time (Whiteley et al. 2003).

A wide range of environmental conditions and system trophic states are present in the California Current system off the Northwest coast of the United States (Chavez et al. 2002; Huyer et al. 2002; Peterson et al. 2002). This system is therefore an excellent region in which to examine differences in the phylogenetic diversity of 'active' *Bacteria*. In this study, we sorted cells based on cell-specific nucleic acid content and on their ability to reduce CTC, and examined the phylogenetic diversity of *Bacteria* in these sorted assemblages. The results showed that most of the phylogenetic groups of *Bacteria* identified in this study were present in both the HNA and LNA assemblage and had, at times, an active electron transport system (i.e., were able to reduce CTC).

4.3 Materials and Methods

4.3.1 Sample collection

Samples were collected during the spring of 2002 (April 26 to May 20) using General Oceanics 5 L Niskin bottles mounted on a rosette equipped with a SeaBird SBE 911+ CTD, a SeaTech fluorometer, a Biospherical PAR sensor, and a SeaTech 25 cm transmissometer. Three stations in different hydrographic regimes were chosen along the Newport Hydrographic line extending westward from Newport, Oregon; a shelf station 9 km from shore, bottom depth 60 m (NH-5, 44.65°N 124.18°W), a slope station 65 km from shore, bottom depth 450 m (NH-35, 44.65°N 124.88°W), and a basin station above the abyssal plain 249 km from shore, bottom depth 2900 m (NH-127, 44.65°N 127.1°W) (Figure 4-1).

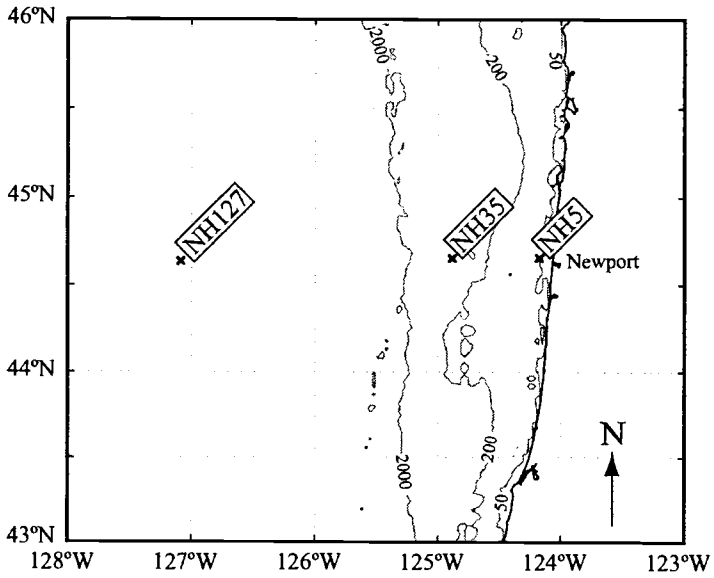

Figure 4-1. Regional map of the sampling area with contour lines indicating the 50 m, 200 m, and 2000 m isobaths. Two casts were conducted at each of the three stations: a shelf station (NH5), a slope station (NH35), and a basin station above the abyssal plain (NH127).

4.3.2 Environmental parameters

Chlorophyll concentration was used as a proxy for phytoplankton biomass. Discrete water samples were filtered through GF/F filters and the filters were kept frozen at -80°C for up to one month before processing. 90% HPLC grade acetone was

added to the filters and allowed to extract overnight at –20°C. Chlorophyll *a* and pheopigment concentrations were determined using a Turner Designs 10-AU fluorometer (Strickland and Parsons 1972). Nutrient samples were collected into 60 ml high-density polyethylene (HDPE) bottles and frozen at sea (-20 °C). The analyses for phosphate, nitrate plus nitrite (N+N), nitrite, and silicic acid (silicate) were performed using a hybrid Technicon AutoAnalyzerII™ and Alpkem RFA300™ system following protocols modified from Gordon et al. (1994). Nitrate concentrations were determined by subtracting nitrite from the N+N value. Results were reported in units of micromoles per liter (μM). The estimated precision for each element is: PO_4 (0.008 μM), N+N (0.15 μM), NO_2 (0.01 μM), silicic acid (0.3 μM).

Incorporation rates of ^{3}H-leucine into whole seawater samples were assayed following the protocol of Smith and Azam (1992). For each water sample, 1.5 ml aliquots were pipetted into four 2-ml plastic microcentrifuge tubes containing ^{3}H-leucine (Perkin Elmer Life Science Products, specific activity 170 Ci mmol^{-1}) to yield 20 nM final concentration. One of the four aliquots served as a killed control, with 5% (final concentration) of trichloroacetic acid (TCA) immediately added to the tube. The aliquots were incubated for one hour in the dark at the in situ water temperature. ^{3}H-leucine labeled samples were then killed with 5% TCA (final concentration) and stored frozen at -20°C. Samples were returned to shore and processed no more than three weeks after the sampling date. Prior experiments with radioactively-labeled samples frozen for up to one month showed no difference in leucine incorporation rates compared to unfrozen samples processed immediately (data not shown). Activity was determined using a Wallac 1141 liquid scintillation counter. The activity of the killed control was subtracted from the values for the three live aliquots.

4.3.3 Labeling cells with an active electron transport system

Immediately following sample collection, water samples were incubated with 5-cyano-2,3-ditolyl tetrazolium chloride (CTC) (Polysciences, Warrington, PA) to identify cells with an active electron transport system. Five ml subsamples were incubated with 2.5 mM CTC (final concentration) for one hour in the dark at 10°C.

Previous studies off the Oregon coast had shown 2.5 mM CTC to be sufficient for detection with a FACSCalibur flow cytometer (Longnecker et al. 2002). Incubations were stopped by the addition of 0.2% w/v paraformaldehyde (final concentration). Samples were kept in the dark at room temperature for 10 min to harden cells, quick-frozen in liquid nitrogen, and then stored at -80°C. Samples were thawed immediately prior to analysis and sorting using a flow cytometer (del Giorgio et al. 1997). The region used to count and sort CTC-positive cells in shown in Figure 4-2A.

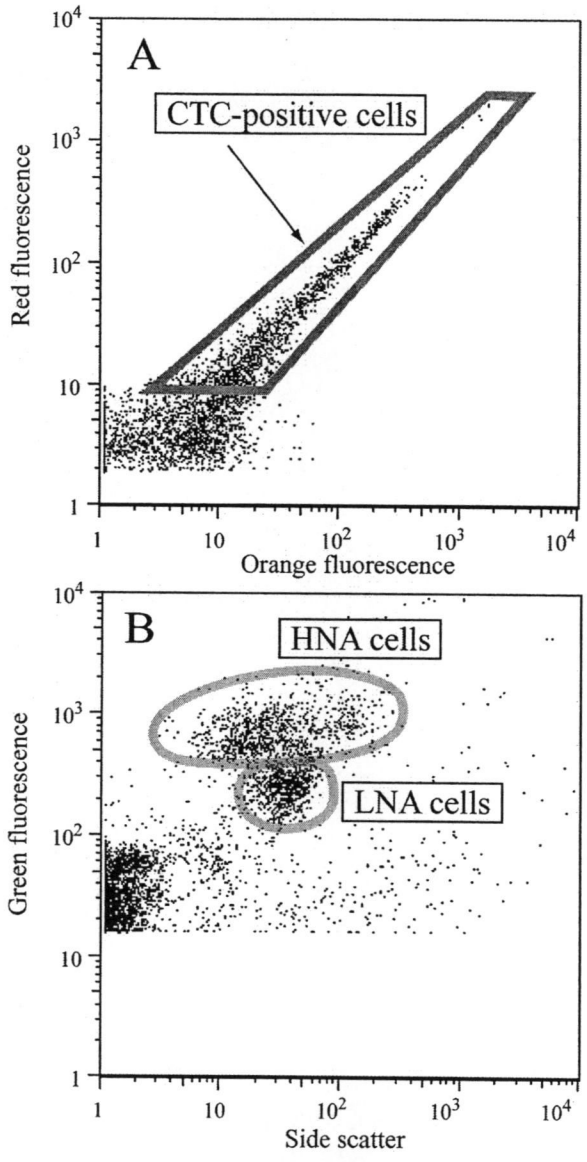

Figure 4-2. Cytograms indicating the sort regions for (A) the CTC-positive cells as defined on cytograms of orange versus red fluorescence and (B) the HNA and LNA regions as defined on the cytograms of side scatter versus green fluorescence.

4.3.4 SYBR-staining of heterotrophic prokaryotes

Water samples in 5 ml aliquots were fixed with 0.2% w/v paraformaldehyde (final concentration), stored in the dark for 10 min at room temperature to harden cells, and quick-frozen in liquid nitrogen. Samples were then stored at -80°C until sample processing on shore. After thawing, subsamples were immediately stained with 1x SYBR Green I (Molecular Probes, Eugene, OR; diluted from the 10,000x stock

solution) following a protocol modified from Marie et al. (1997), although no RNase or potassium citrate was used. Regions were established on the cytograms to define bacterial cells with high nucleic acid content (HNA) and low nucleic content (LNA) (Figure 4-2B); in general these two groups of cells were distinct, as has been observed by others. A known concentration of 1.0 μm green-fluorescent microspheres (Polysciences, Warrington, PA) was added to each sample in order to determine sample volume processed in the flow cytometer, and thus bacterial cell abundance from cytometric counts. The concentration of the working stock of 1.0 μm microspheres was pre-determined using Becton-Dickinson TrueCount Beads (Franklin Lakes, NJ). Logical gating in the Cell Quest software was used to exclude cyanobacteria, based on orange fluorescence, from the abundance counts of heterotrophic prokaryotes.

4.3.5 Sorting cells for molecular analysis

Eighteen different samples were selected from three sampling stations (Table 4-1). For each sample, three sorts were conducted: HNA cells, LNA cells and CTC-positive cells. After including positive controls on the DGGE gels, up to twelve samples were run per gel for a total of six different gels. To minimize bacterial contamination, Milli-Q water was filtered through a 0.1 μm Supor filter and autoclaved prior to use as sheath fluid. Each day, the sheath tank was rinsed once with 100% bleach and four times with filtered, autoclaved Milli-Q water. The sort line was cleaned at the beginning of each day by running 5% bleach for 15 min, followed by filter-sterilized Milli-Q for 20 min. To prevent carryover between samples, the flow cytometer's sort line was also cleaned in between each sample run with a solution of 5% bleach (10 minutes), followed by filter-sterilized, autoclaved Milli–Q (20 minutes). Every day the sort line was tested for the presence of contaminants by sorting only sheath fluid and collecting the outflow from the sort line on a filter; this filter was then treated as a sample. If the negative sort indicated the presence of DNA, the sorts from the entire day were repeated.

After staining with either SYBR Green I or CTC, cells were sorted using the cell concentrator module attached to a Becton-Dickinson (BD; Franklin Lakes, NJ)) FACSCalibur flow cytometer. The existing system was modified to hold a 20 cc syringe with a Swinnex filter holder. The filter holder held a 13 mm 0.2 μm polycarbonate filter and was attached to a vacuum pump. All sorts were conducted on low speed using the single cell option in the BD Cell Quest software in order to minimize sorting of cells outside the region of interest. For the SYBR-stained samples, the samples were stained with a 1x solution of SYBR Green I for 15 minutes. A new aliquot of the sample was placed on the flow cytometer every 15 minutes to prevent alteration in the sort region of interest due to fading of the SYBR stain over time. At least $2x10^4$ cells per sample were sorted for the CTC-positive samples, while at least $5x10^4$ cells were sorted for each region of the SYBR-stained samples. Each sort took between 30 to 90 min to complete.

4.3.6 DNA extractions and PCR conditions

In addition to the sorted samples, DNA was extracted from 3 mL of a whole seawater aliquot of each sample. The following extraction method was chosen after testing several different extraction methods on paraformaldehyde-fixed cells, and was used for both the whole seawater samples and the sorted samples. The DNA extraction method was modified from Giovannoni et al. (1990). Cells were lysed with a lysis buffer (40 mM EDTA, 50 mM Tris, 400 mM NaCl, 0.75 M sucrose, pH=8.0). SDS (final concentration, 0.5%) and proteinase K (final concentration, 500 μg ml^{-1}) was added and the cells were incubated at 42°C overnight. Following incubation, the solutions were extracted once with phenol:chloroform:isoamyl alcohol (25:24:1) and once with chloroform:isoamyl alcohol (24:1). DNA was precipitated with two volumes ice-cold 96% ethanol for six hours at -20° C and then spun at 15,000 x g for 45 minutes at 4° C. After a wash with 70% ethanol, and an additional 30 min centrifugation at 15,000 x g, the DNA was dried, and resuspended in 10 mM Tris (pH=8.0).

Table 4-1. Details on sampling regions and environmental parameters for the 18 samples analyzed in this study. Samples were collected from two separate casts at each sampling station. Three depths were sampled: surface, within the pycnocline, and below the pycnocline. The pycnocline is a region of steep change in water density with depth.

Station / Region	**Sample**	**Depth (m)**	**Salinity**	**Temperature (°C)**	**Phosphate (μM L^{-1})**	**Nitrate (μM L^{-1})**	**Silicate (μM L^{-1})**	**Leucine incorporation (pM Leu hr^{-1})**	**Chlorophyll *a* (μg L^{-1})**
127 / Basin	n24	300	34.0	6.6	2.6	35.4	54.0	0.2	0.3
	n25	110	33.2	8.1	1.6	19.9	21.7	0.5	0.3
	n26	20	32.4	9.3	0.8	5.0	8.6	7.8	0.7
	n37	300	34.0	6.7	2.6	35.9	56.7	0.5	0.3
	n38	120	33.2	7.8	1.7	21.1	23.3	1.8	0.3
	n39	20	32.4	9.3	0.8	5.1	7.8	21.7	0.7
35 / Slope	n85	50	32.3	8.8	0.9	6.1	8.5	6.8	0.7
	n87	20	32.0	9.7	0.5	0.5	6.2	34.1	3.8
	n88	5	29.3	10.9	0.2	0.0	9.3	85.8	0.9
	n103	100	33.2	8.4	1.7	21.2	23.6	1.6	0.3
	n104	30	32.0	9.5	0.4	0.2	5.6	42.7	2.4
	n105	3	29.9	11.0	0.2	0.0	5.8	84.6	0.6

Table 4-1, continued

Station / Region	Sample	Depth (m)	Salinity	Temperature (°C)	Phosphate (µM L^{-1})	Nitrate (µM L^{-1})	Silicate (µM L^{-1})	Leucine incorporation (pM Leu hr^{-1})	Chlorophyll *a* (µg L^{-1})
5 / Shelf	n127	50	33.9	7.6	2.4	32.7	37.5	5.5	0.4
	n128	25	33.6	8.2	2.2	28.7	33.8	5.9	0.4
	n129	6	32.4	8.8	1.4	15.8	23.3	101.8	11.9
	n138	50	33.9	7.8	2.4	31.0	40.8	8.6	0.4
	n139	25	33.5	8.2	2.0	25.5	32.0	10.0	0.5
	n140	5	31.4	9.7	0.4	0.8	3.1	289.7	16.3

The 16S rRNA genes were amplified using PCR with the following reaction conditions: 1X Promega PCR buffer, 200 μM dNTPs, 400 nM of each primer, 2 U of Promega Taq, and 2.5 mM $MgCl_2$. PCR primers were 907RA (Schäfer and Muyzer 2001) and 341F-GC (Muyzer et al. 1993), which has a 40-nucleotide GC-rich section for the DGGE analysis. Conditions for the PCR were an initial denaturation at 94°C for 5 min, 30 cycles of 94°C, 30 s; 48°C, 30 s; 72°C, 90 s; and a final 10 min at 72°C.

4.3.7 Denaturing gradient gel electrophoresis (DGGE)

PCR products of the V3-V4-V5 variable regions (Neefs et al. 1993) were analyzed using denaturing gradient gel electrophoresis (DGGE, Muyzer et al. 1996). Controls were run adjacent to the samples in order to facilitate comparison of the DGGE banding patterns between the different gels. A 6% (w/v) acrylamide/bis-acrylamide gel was prepared in TAE buffer (0.04M Tris, 0.02M glacial acetic acid, 1 mM EDTA). A 30% to 70% urea/formamide denaturing gradient was used where 100% is equal to 40% (vol/vol) formamide and 7 M urea. The gel was run in a CBS Scientific DGGE-2001 system at 60°C at 100 V for 18 h. The acrylamide gel was stained with SYBR Green I for 30 min and then viewed on a UV light box. Gels were imaged with an AlphaImager 2200 Digital Imaging System. Multiple images were collected with different aperture and exposure settings in order to maximize the detection of weak DGGE bands, yet still allow separation of the brighter DGGE bands. Each sample was run on two different DGGE gels to facilitate comparison of the DGGE banding patterns between different samples and different sorts.

The individual bands from the DGGE gel were removed by piercing the gel with a pipet tip and placing it in 20 μL of 10 mM Tris for 10 min at room temperature. Two to five μL of this mixture was used to reamplify the variable regions using conditions as described above except the forward primer lacked the GC-rich section. The PCR products were then purified with the Montage PCR filter kit (Millipore, Billerica, MA) following the manufacturer's instructions.

4.3.8 Sequencing and phylogenetic analysis

The reamplified DGGE bands were sequenced by cycle sequencing using fluorescent dideoxy terminators. The sequences were resolved using an ABI 3100 at Oregon State University's Central Services Lab. Sequences were checked manually using TraceViewer (CodonCode Corporation) and then were aligned in ARB (Ludwig et al. 2004), initially using the FastAligner and then manually checked. The alignment included close representatives that were identified based on data from BLAST (basic logic alignment search tool, Altschul et al. 1997).

4.3.9 Analysis of DGGE banding patterns

The pattern of DGGE bands was reduced into a presence/absence matrix for each of the three sorts. Separate distance matrices for the HNA sorts, LNA sorts and CTC-positive sorts were calculated using the Sorensen distance measure and compared in pairs using a Mantel test (Legendre and Legendre 1988) on ranked distances as suggested by Dietz (1983). The only significant difference between the three matrices was between the LNA DGGE band patterns and the CTC DGGE band patterns ($p = 0.046$, calculated from Monte Carlo randomization of 1000 runs, all other comparisons resulted in $p > 0.05$). Therefore, the matrices were combined for the cluster analysis and nonmetric multidimensional scaling (NMS); the resulting matrix included all the HNA bands, the LNA bands, and the CTC-positive bands. Since our primary interest was heterotrophic cells, we excluded the whole seawater samples from these analyses in order to prevent analysis of geographical patterns related to the photoautotrophic cells. For the cluster analysis, the distance matrix was calculated with the Sorensen distance measure and the group linkage method was flexible beta, with beta set to –0.25.

NMS was also used to examine the differences in the bacterial diversity among the 18 samples examined in this study. Differences between samples were calculated based on either the presence and absence of each group within the sample, or based on the number of DGGE bands obtained within each taxonomic group. The differences were then presented graphically in a multidimensional space, samples which are close

together in the ordination are more similar than samples located further apart. PC-ORD v. 4.19 (MjM Software Design) was used for the NMS (Kruskal 1964; Mather 1976) with the Sorensen distance measure. Eighty runs were done with real data starting with random configurations, and Monte Carlo simulations were conducted with 100 runs of randomized data which were then compared to the output from the real data. The p-values were calculated as the proportion of randomized runs with stress less than or equal to the observed stress. The dimensionality of the data set was assessed by comparison of NMS runs with the real data compared to the Monte Carlo simulations. Additional axes were added if the addition of the axis resulted in a significant improvement over the randomized data (at $p \leq 0.05$) and the reduction in stress was greater than five. The proportion of variation represented by each axis was assessed by calculating the coefficient of determination (r^2) between distances in the ordination space and distance in the original space. One advantage of NMS is the ability to compare differences between samples in conjunction with the environmental variables measured at each station. To do this, joint plots showing the relationship between the environmental data and the ordination scores were overlaid on the NMS plot; the angle and length of the line indicates the direction and strength of the relationship.

A second version of the NMS was run using the sequence data obtained from the DGGE bands. For this analysis, the community data were the number of DGGE bands within each of the different phylogenetic groups defined in Table 4-2. The NMS was run as above, except the relative Sorensen distance measure was used in order to eliminate differences in the absolute number of DGGE bands between the different samples. The results from this NMS focuses on the differences in phylogenetic groups present in each of the samples.

4.4 Results

4.4.1 Hydrographic conditions

The environmental data revealed the lowest salinities and highest temperatures were observed in the surface samples from the slope station, along with the lowest

nitrate and phosphate concentrations (Table 4-1). Leucine incorporation levels were higher in the surface samples of all three stations, and were highest at the shelf station. Chlorophyll *a* concentrations were highest at the surface of the shelf station. However, a mid-depth chlorophyll maxima was present at the slope station.

4.4.2 Sorting cells for molecular analysis

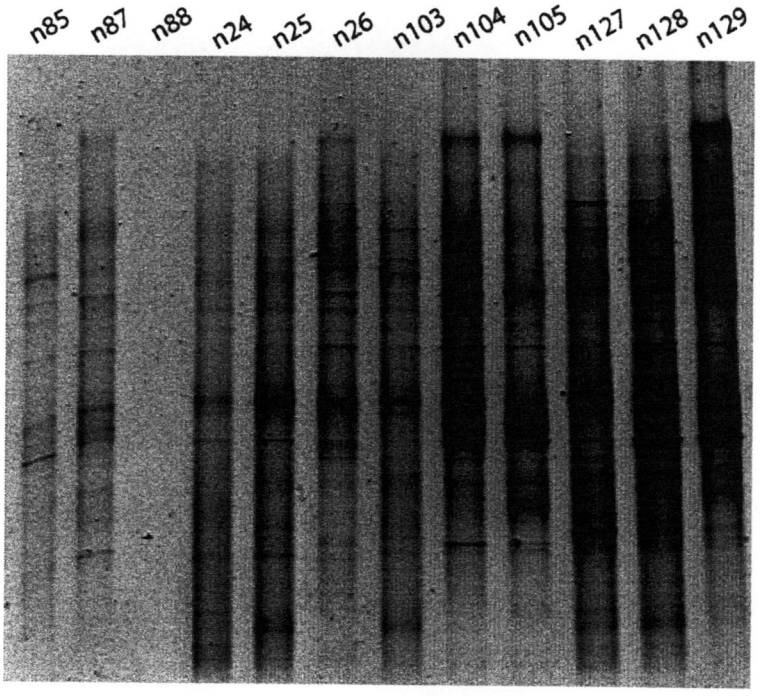

Figure 4-3. Example of one of the six DGGE gels used to compare the samples from the Oregon coast. Each sort was run on two different DGGE gels to facilitate comparison of the DGGE band patterns between samples. The DGGE gel shown is an inverted image of part of the DNA obtained from the HNA sorts. The numbers at the top each lane indicate the sample number from Table 4-1.

DNA was successfully extracted from all the sorts, although very little DNA was obtained from the HNA sort from sample n88 despite two attempts at extracting DNA from the sorted cells. Each PCR-amplified V3-V4-V5 variable region of the bacterial 16S rRNA gene was run on two separate DGGE gels. The first gel grouped the sorts obtained from the same sampling cast, while the second gel grouped the DNA by sort type; an example of the later is shown in Figure 4-3. The presence or absence of the DGGE bands was determined manually by examination of the DGGE

gel images in Photoshop (Adobe Systems Inc). In order to assess the minimum number of sorted cells required for the analysis, different numbers of cells, ranging from $1x10^4$ to $2x10^5$ cells, were sorted from one sample. This DGGE gel revealed that all the DGGE bands could be identified from the different sorts, although the bands were fainter in the sorts with fewer cells.

4.4.3 Comparing the number of DGGE bands obtained from the different sorts

Running all three sorts from a single sample on the same DGGE gel facilitated comparison of the presence or absence of a given band among the three sorts. Bands from different sorts or from the whole seawater sample which migrated to the same point in the DGGE gel were considered as the same DGGE band; however, PCR products from different organisms can migrate to the same location in the DGGE gel (Muyzer and Smalla 1998) which would result in an underestimation of the diversity obtained from these samples. Considering all the DGGE bands, only 7% of the bands were limited to the whole seawater aliquots and were not obtained in any of the sorted assemblages. Since the samples were not prescreened to remove phytoplankton, some of these DGGE bands may be photoautotrophs excluded from the later sorts. However, even with the most stringent sorting criterion, there were DGGE bands which later were identified as phytoplankton or plastids which were removed from subsequent analyses. Examination of all the DGGE bands combined revealed eleven percent of the DGGE bands were observed in both the HNA and the LNA sorted assemblages, while 13% were present in all three assemblages: HNA, LNA and CTC-positive. There was no significant difference between the proportion of DGGE bands observed in both the HNA and CTC-positive assemblage compared to the proportion of DGGE bands observed in both the LNA and CTC-positive assemblage (6.7% and 5.7% of the DGGE bands, respectively, Wilocoxon signed rank test, $p = 0.85$).

Species richness was defined as the number of DGGE bands within a given sort. There were no significant differences in species richness between sampling sites or depths when the total number of bands was considered, nor when all the possible

combinations of bands were considered for the sorts based on nucleic acid combinations or the CTC-positive sorts (Kruskal-Wallis tests). Furthermore, there were no significant correlations between bacterial leucine incorporation and the number of HNA, LNA or HNA + LNA bands (Spearman rank correlations, p-values all > 0.05). However, bacterial leucine incorporation was weakly correlated to the number of CTC bands ($r = 0.49$, $p = 0.039$, Spearman rank correlation).

4.4.4 Analysis of the DGGE banding patterns

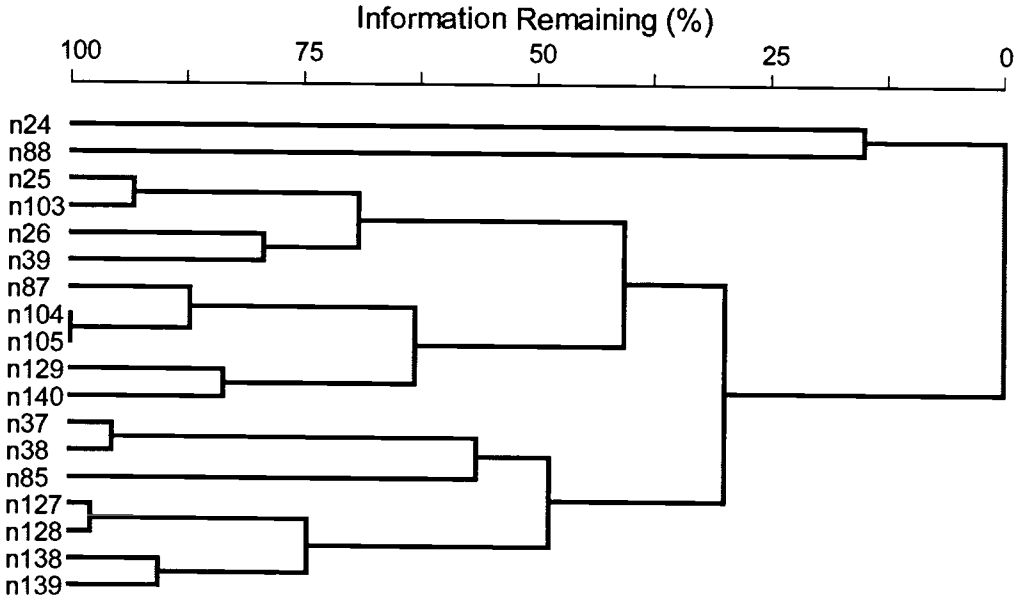

Figure 4-4. Cluster analysis of the Oregon coast samples. The analysis was conducted on the presence/absence matrix of the DGGE band patterns. The sample numbers correspond the numbers in Table 4-1.

Two different methods were used to examine the differences between the samples based on the data from the DGGE gels. A cluster analysis based on the presence / absence of the DGGE bands from the sorted HNA, LNA and CTC-positive assemblages was used to examine which samples were most similar to each other. The results grouped the samples as shown in Figure 4-4. The two surface samples from NH5 (n129 and n140) clustered separately from the other NH5 stations. The two surface samples from the offshore station (n26 and n39) also clustered together to the exclusion of the other offshore samples. However, the remaining samples from the offshore station did not form one single group. The slope station samples were

intermingled with the samples from the shelf and offshore stations. Samples n24 and n88 were separated from the rest of the samples, likely due to the low number of HNA bands identified in both of these samples.

The analysis from the non-metric multidimensional scaling (NMS) for the presence/absence data generated from the DGGE gels resulted in a three-dimensional solution (Figure 4-5). The points within the ordination are the different samples; the distances between the points represent the relative dissimilarity between samples where larger distances represent greater differences between the samples. The final solution was the result of 200 iterations with a final stress of 12.06 and a final instability of 1.6×10^{-3}. The cumulative proportion of variation explained by the final three-dimensional solution was 0.86, with 0.37, 0.07 and 0.41 on Axis 1, Axis 2 and Axis 3, respectively. Although Axis 2 only explained 7% of the variation, a three-dimensional NMS solution was a significant improvement over a two-dimensional solution, therefore three axes were calculated for the final ordination. The separation of the shelf samples from the slope and offshore samples is evident along Axis 2, with the offshore samples primarily clustering at the low end of Axis 3. The slope station samples were intermingled with both the shelf and offshore stations depending on which axes are viewed in the ordination.

Although the NMS was calculated only based on the data from the DGGE gels, the environmental data from the same samples can be considered along with the data from the DGGE gels. Joint plots overlaid on the ordination were used to show the correlations between the environmental data and the ordination scores. None of the environmental parameters showed a high correlation with Axis 1, while Axis 2 defined the split between the abundance of HNA cells relative to the heterotrophic cell abundance and its converse, the relative abundance of LNA cells. The deep samples with high nutrient concentrations were separated along Axis 3 from the surface samples with warmer water, higher bacterial leucine incorporation rates, and higher cell counts.

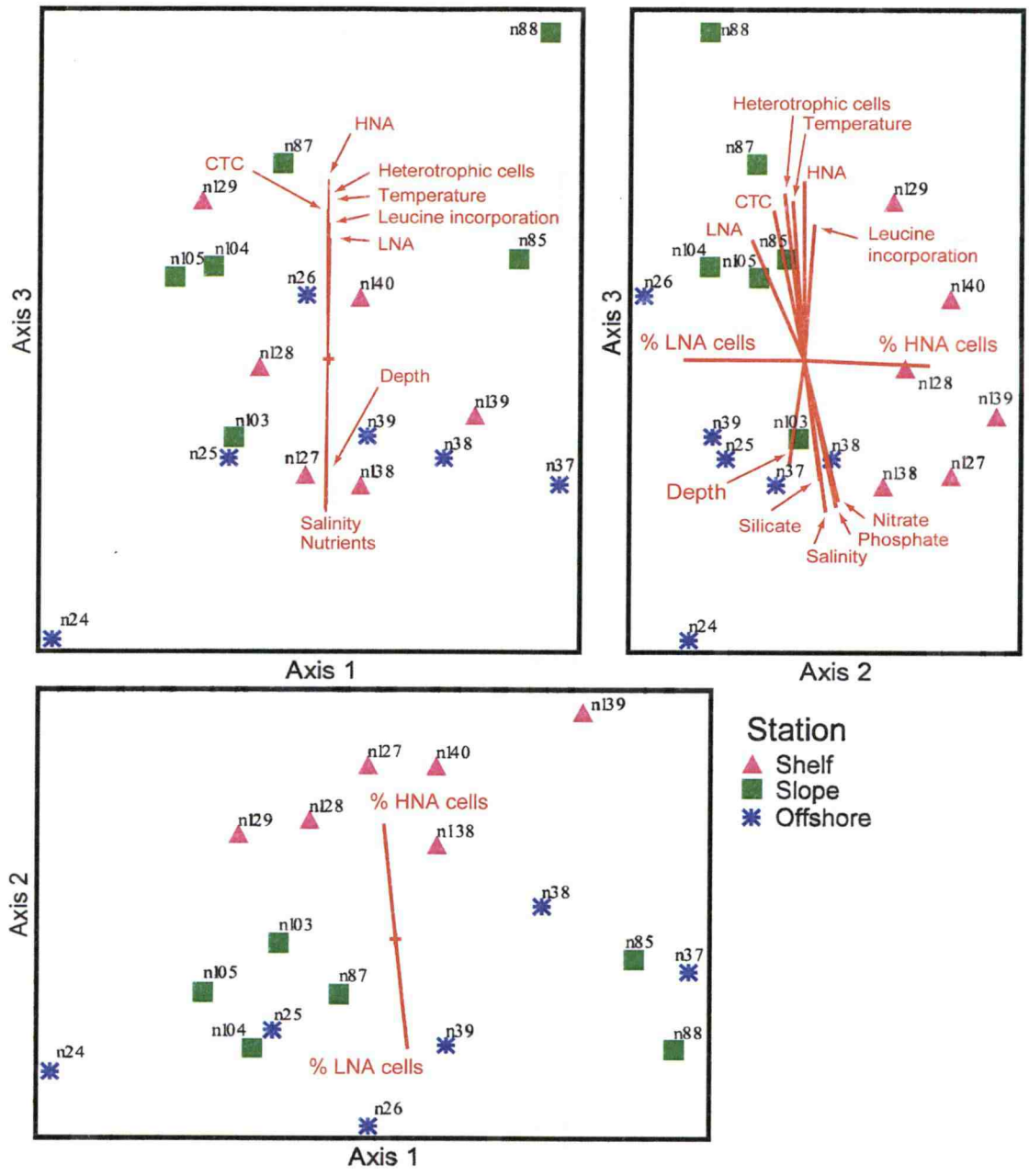

Figure 4-5. The NMS analysis showing the differences between the samples based on the presence / absence data obtained from the DGGE gels. The legend indicates the sampling station, while the numbers correspond to the sample numbers given in Table 4-1. The joint plots highlighting the correlations with environmental data are overlaid in red and labeled for each variable. The nutrients label in Axis 1 vs. Axis 3 refers to nitrate, phosphate, and silicate, which were all overlapping in the joint plots. The percent of HNA and LNA cells is the abundance of HNA or LNA cells divided by the heterotrophic cell abundance in the sample.

Table 4-2. Summary of sequence data obtained from the V3-V4-V5 variable regions of the 16S rRNA gene. The phylogenetic groups were determined by inserting the sequences obtained from the DGGE bands into maximum likelihood trees using the parsimony tool in ARB. The numbers indicate the number of sequences within each group.

			# of sequences		
Phylum	**Class, Order**	**Family, Genus, or environmental cluster**	**NH5**	**NH35**	**NH127**
Acidobacteria				1	1
Actinobacteria		Marine Gram-positives	2	1	3
Deinococcus-Thermus		*Meiothermus*		2	1
Bacteroidetes	*Flavobacteria* Order *Flavobacteriales*	Family *Flavobacteriaceae*, Genus *Polaribacter*	3		
	Sphingobacteria Order *Sphingobacteriales*	Family *Saprospiraceae*		3	1
	Environmental sequences	Delaware cluster 1[1]	3	2	
		Delaware cluster 2[1]	1		
		ZD0203 from the North Sea[2]		3	2
		agg58 Branch 2[3]	4	3	8
		unaffiliated *Cytophaga*	3	1	
Proteobacteria	*Alphaproteobacteria*				
	Order *Rhodospiralles*		5	5	16
	Order *Rickettsiales*	Family *Rhodobacteraceae*, Genus *Roseobacter*	7	6	5
	Environmental sequences	SAR11 cluster[4]	6	5	6
	Order *Rhizobiales*	Family *Bradyrhizobiaceae*, Genus *Afipia*		4	1
		Family *Methylobacteriaceae*	1		

[1] (Kirchman et al. 2003)
[2] (Zubkov et al. 2002a)
[3] (DeLong et al. 1993; O'Sullivan et al. 2004)
[4] (Britschgi and Giovannoni 1990; Giovannoni et al. 1990; Mullins et al. 1995)

Table 4-2, continued

Phylum	Class, Order	Family, Genus, or environmental cluster	NH5	NH35	NH127
Proteobacteria	*Betaproteobacteria*				
	Order *Burkholderiales*	Family *Burkholderiaceae*, Genus *Burkholderia*	2	2	2
		Family *Ralstoniaceae*		5	
		Family *Comamonadaceae*	2	2	1
	Order *Hydrogenophilales*	Family *Hydrogenophilaceae*	3		
	Order *Rhodocyclales*	Family *Rhodocyclaceae*		1	
	Deltaproteobacteria	Marine Group B / SAR324 cluster[5]	2	1	7
	Gammaproteobacteria	Environmental sequences - Bano & Hollibaugh 'Cluster A'[6]	5	1	2
	Order *Alteromonadales*	Family *Alteromonadaceae*, Genus *Marinobacterium*		1	
	Order *Pseudomonadales*	Family *Moraxellaceae*, Genus *Psychrobacter*		1	
		Family *Moraxellaceae*, Genus *Acinetobacter*		2	
		Family *Pseudomonadaceae*, Genus *Pseudomonas*	1		1
	Environmental sequences	SAR86 / OCS5 cluster[7]			1
		Arctic96B-16 cluster[6]	2	1	1
		OM60 cluster[8]	1	1	2
		SAR92 cluster[9]	2	3	
		agg47/KTc1113[10]	8	3	4
unclassified	Candidate division	TM6		2	

[5] (Fuhrman and Davis 1997; Wright et al. 1997)
[6] (Bano and Hollibaugh 2002)
[7] (Fuhrman et al. 1993; Mullins et al. 1995)
[8] (Rappé et al. 1997)
[9] (Britschgi and Giovannoni 1990; Giovannoni et al. 1990; Mullins et al. 1995)
[10] (DeLong et al. 1993; Eilers et al. 2000)

4.4.5 Diversity of sequences obtained from the DGGE bands

More detailed information about the diversity of *Bacteria* within the HNA and LNA assemblages was obtained by removing the DGGE bands from the gels and sequencing the re-amplified V3-V4-V5 regions of the 16S rRNA genes. The diversity of *Bacteria* included sequences within the *Proteobacteria* (including *Alphaproteobacteria*, *Betaproteobacteria*, *Deltaproteobacteria*, and *Gammaproteobacteria*), *Bacteroidetes*, *Acidobacteria*, Marine *Actinobacteria*, *Meiothermus* and the candidate division TM6 (Table 4-2). The phylogenetic identity of each of the sequences was determined initially based on BLAST results; the final determination was based on placement of the sequences into maximum likelihood trees which are contained within the Appendix. The sequences were identified to genera or to the lowest taxonomic division possible to determine unambiguously. Most of the sequences clustered within the *Alphaproteobacteria*, although the *Bacteroidetes* and *Gammaproteobacteria* sequences were also about one-quarter of the sequences obtained from the DGGE bands (Figure 4-6).

There were phylogenetic groups which were unique to a single sampling station. Within the *Gammaproteobacteria*, the SAR86 cluster was only observed once in a sample from the offshore station. Three groups of *Gammaproteobacteria* were only observed at the slope station (*Marinobacterium*, *Acinetobacter*, and *Psychrobacter*). In addition, Family *Ralstoniaceae* within the *Betaproteobacteria* was observed in four DGGE gels, but only in gels with amplified DNA originating from the slope station. Three groups of *Bacteroidetes* sequences were only observed at the shelf station (*Polaribacter*, the environmental sequences grouping with Delaware cluster 2, and the unaffiliated environmental sequences). In addition, the *Methylobacteriaceae* and *Hydrogenophilaceae* were also only observed at the shelf station.

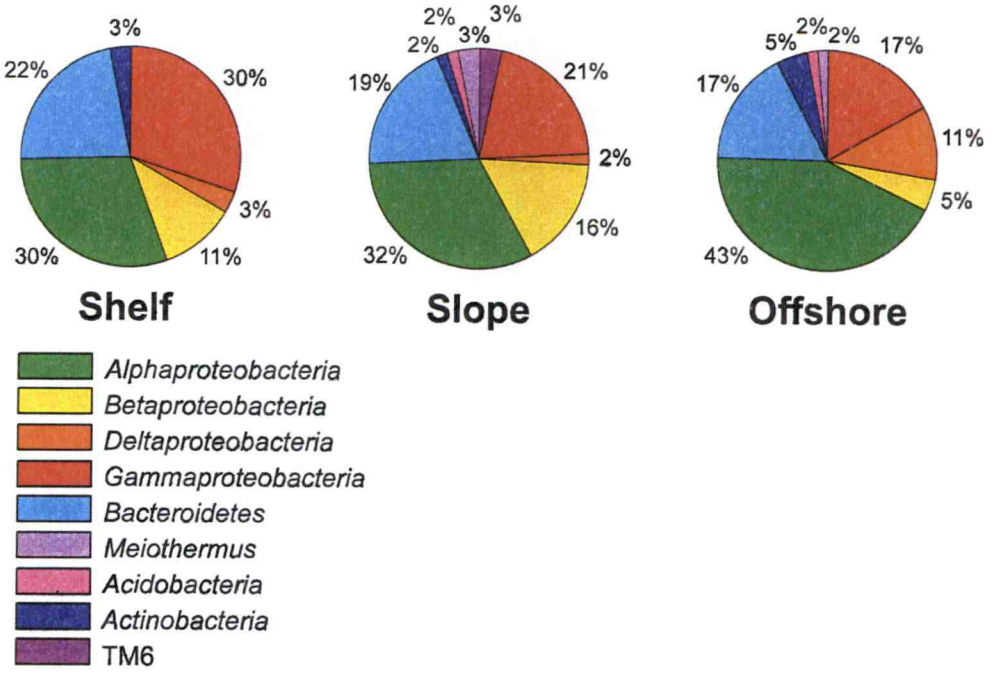

Figure 4-6. Pie graphs highlighting the relative abundance of phylogenetic groups identified for the shelf, slope and offshore regions. The relative abundance of each group was calculated by determining the number of DGGE bands within a given group for each station and divided by the total number of DGGE bands at that station.

The number of DGGE bands representing each of the different phylogenetic groups in Table 4-2 was also analyzed using NMS. For this analysis, the input data were more broadly defined than the presence / absence data used for the NMS presented in Figure 4-5 since each phylogenetic group contained multiple DGGE bands. The results of the three dimensional solution after 400 iterations and a final instability of 0.021 are shown in Figure 4-7. The final stress was 9.76 and the r^2 values were 0.18, 0.27, and 0.31, for Axis 1, Axis 2, and Axis 3 respectively, resulting in a cumulative r^2 of 0.75. For this analysis, the samples showed separation by sampling site more than the ordination based on the presence / absence of all the DGGE bands shown in Figure 4-5. For example, when Axis 3 is plotted against Axis 1 or Axis 2, the samples from the offshore and shelf station cluster together. However, the samples from the slope station form two separate clusters at opposite ends of Axis 3; the two clusters are separating the samples by sampling cast. The two casts from the slope

station were conducted 33 hours apart; the two casts from the offshore station and the two casts from the shelf station were both conducted about 15 hours apart. There were differences between the two slope station casts in some of the measured environmental variables. The autotrophic community, diatoms, *Synechococcus*, and picoeukaryotes, was more abundant during the later sampling cast at the slope station (samples n85, n87, and n88). In addition, the HNA cells were proportionately more of the heterotrophic community at the first slope station sampling cast (samples n103, n104, and n105) compared to the later cast. These patterns do not appear significant for the joint plots since the distribution is bimodal, with lower values for the shelf and offshore stations.

The joint plots representing the correlations with the measured environmental parameters for these samples indicate the predominant pattern is present along Axis 2 and represents the deep samples towards the upper end of the axis with their higher nutrient concentrations and salinities. Conversely, the lower end of Axis 2 contains more of the surface samples with warmer temperatures and higher cell counts. None of the measured environmental parameters were important along Axis 1 or Axis 3.

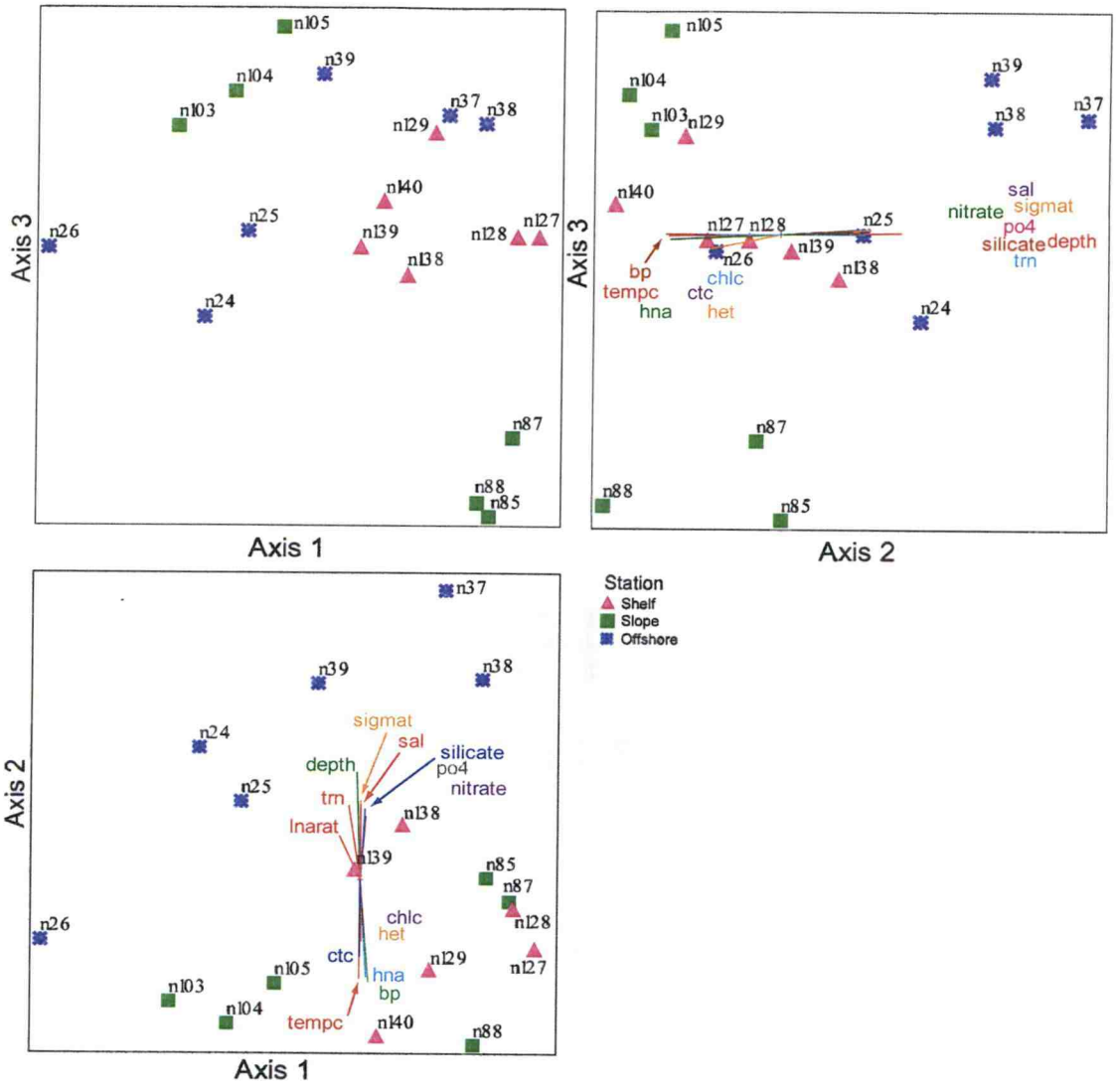

Figure 4-7. Results of the NMS run using the number of DGGE bands identified within the different phylogenetic groups described in Table 4-2. Where the environmental variables were closely lined up, the line color in the joint plot has been color-coded to match the text label for each of the environmental variables. The abbreviations for the environmental variables in the figure are as follows: het (all heterotrophic cells), hna (HNA cells), ctc (CTC cells), lnarat (ratio of LNA cells to heterotrophic cells), tempc (temperature), sigmat (sigma-t), sal (salinity), depth, po4 (phosphate), chlc (chlorophyll *a*), nitrate (nitrate), silicate (silicate), trn (% transmission), and bp (bacterial leucine incorporation).

4.4.6 Sequence data obtained from the HNA, LNA, and CTC-positive DGGE bands

Table 4-3. Summary of phylogenetic groups limited to the HNA or LNA assemblages. Phylogenetic groups were based on the insertion of the sequences from the DGGE bands into maximum likelihood trees. The numbers in parentheses indicate the number of sequences contained within the group.

Groups identified only in the HNA assemblage	
Bacteroidetes	Delaware cluster 2 (1)
	Polaribacter (3)
	environmental sequences - ZD0203 cluster (5)
	unaffiliated (4)
Gammaproteobacteria	environmental sequences - Arctic96B-16 cluster (4)
Groups identified only in the LNA assemblage	
Gammaproteobacteria	*Marinobacterium* (1)
	Pseudomonas (2)
Alphaproteobacteria	*Methylobacteriaceae* (1)
TM6 (2)	
Groups found in either the HNA or LNA assemblage (but not both)	
Betaproteobacteria	*Rhodocyclaceae* (1)
	Comamonadaceae (5)
Gammaproteobacteria	SAR92 cluster (5)

Some of the sequences obtained from the DGGE bands were only observed in a subset of the sorted assemblages. For example, sequences obtained only from the HNA assemblage included *Bacteroidetes* and *Gammaproteobacteria* (Table 4-3). Conversely, *Gammaproteobacteria* clustering with *Marinobacterium* and *Pseudomonas*, the one *Methylobacteriaceae* sequence, and the TM6 sequences were only obtained from the LNA assemblage. There were also sequences obtained from either the HNA or LNA assemblage, but which were not concurrently present in the

HNA and LNA assemblage from the same sample (Table 4-3). The only phylogenetic group absent from the CTC-positive assemblage was the one sequence obtained from the SAR86 cluster within the *Gammaproteobacteria*.

With the data from all the sorts from a single sample contained on one DGGE gel, comparison of the presence of a phylogenetic group in both the CTC-positive assemblage and the HNA or LNA assemblage was possible. The SAR92 cluster within the *Gammaproteobacteria* was observed in the CTC-positive assemblage, but only in conjunction with a band in the LNA sort. There were no instances of SAR92 sequences obtained from both the CTC-positive assemblage and the HNA assemblage. Conversely, the agg46 cluster within the *Gammaproteobacteria* and one of the *Meiothermus* sequences were only observed in the CTC-positive assemblage in conjunction with the HNA assemblage. The SAR11 cluster within the *Alphaproteobacteria* was the only case where, if the band was identified in the CTC-positive assemblage, it was also found in both the HNA and LNA cell assemblages.

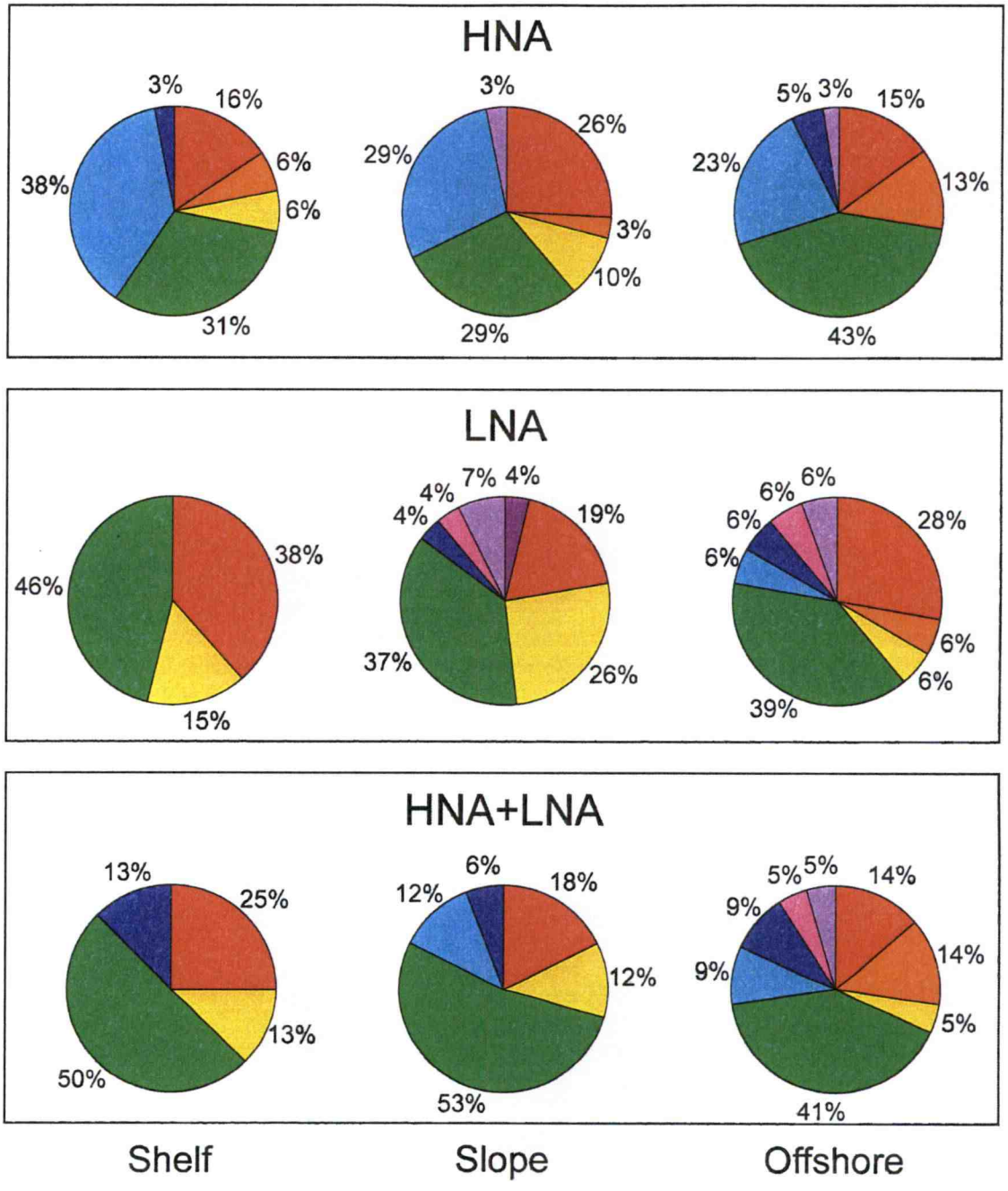

Figure 4-8. Pie graphs detailing the relative abundance of sequences obtained from either the HNA or LNA sorts, or both HNA and LNA sorts in the same sample. The sequences are shown separately for each of the three sampling stations, although sequences representing ≤1% of the community are not shown on the figure. The legend is the same as in Figure 4-6.

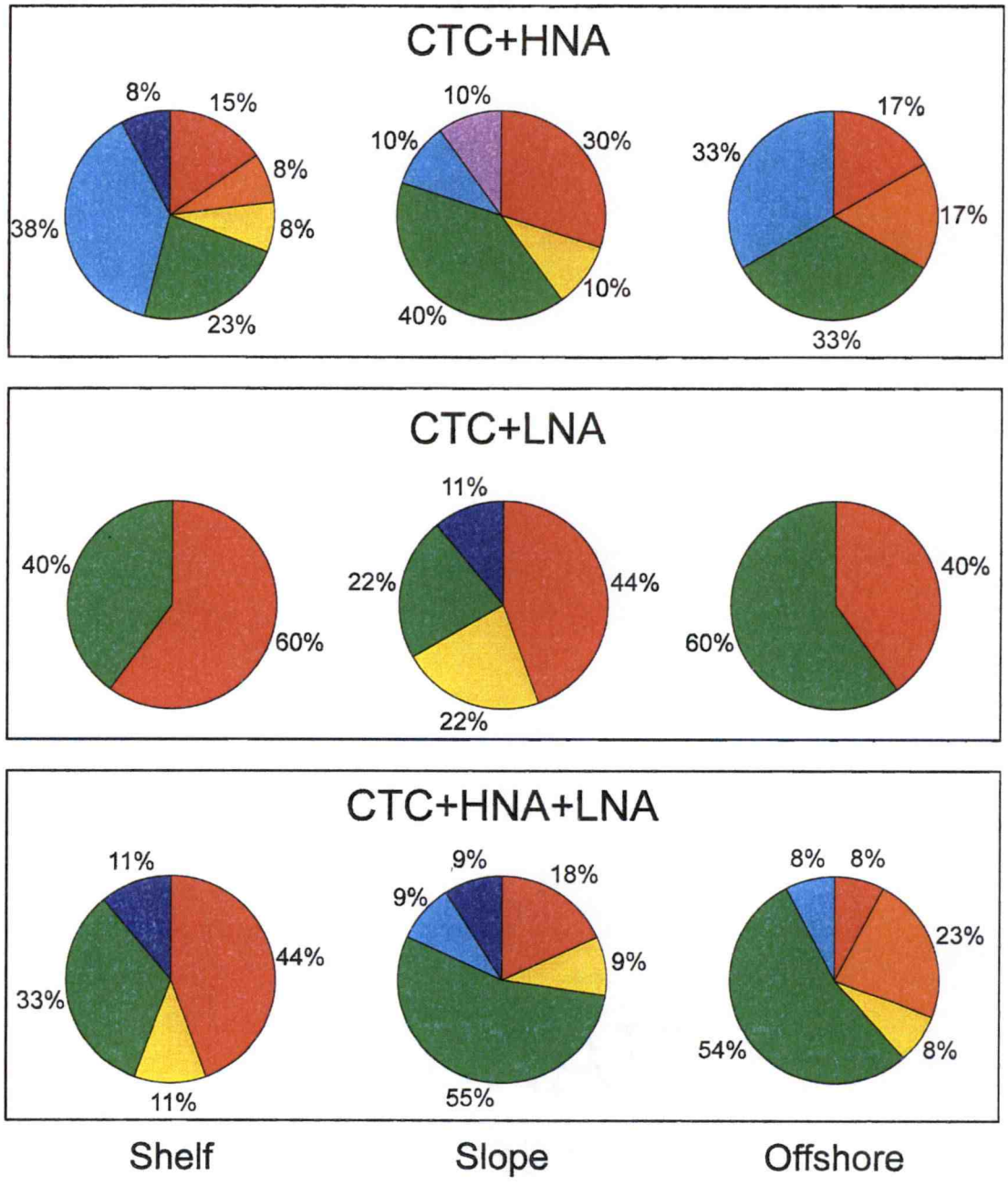

Figure 4-9. Graphs indicating the relative abundance of sequences obtained from both CTC-positive and HNA sorts, CTC-positive and LNA sorts, or the combination of all three sorts. Sequences representing ≤1% of the community at each station are not shown in the figure. The legend is the same as in Figure 4-6.

There were also regional differences in the relative number of sequences obtained in the various sorts, both in those based on nucleic acid content (Figure 4-8), and in the CTC-positive sorts (Figure 4-9). For both Figure 4-8 and Figure 4-9, the presence or absence of a DGGE band in the HNA sort, LNA sort, or CTC-positive sort was compared for the same sample. The *Alphaproteobacteria* dominated the HNA and LNA assemblages and were concurrently present in both assemblages at all three stations (Figure 4-8). The *Gammaproteobacteria* were a large proportion of the LNA assemblage at the shelf and offshore station, while the *Betaproteobacteria* were relatively more abundant in the LNA assemblage at the slope station. The CTC and LNA groups were dominated by *Alphaproteobacteria* and *Gammaproteobacteria*, particularly at the shelf and offshore stations (Figure 4-9).

The distribution of the sequences can also be separated based on deep, pycnocline, or surface sampling depths and looked similar to Figure 4-6. The largest difference was that the *Alphaproteobacteria* were a larger proportion of surface samples at all three stations compared to the percentages shown in Figure 4-6. At the offshore station, there were smaller proportions of *Alphaproteobacteria* in the pycnocline and deep samples, and a smaller proportion of *Deltaproteobacteria* in the surface samples. At the slope station, there were proportionately fewer *Bacteroidetes* in the surface samples. All other differences represented less than 5% change from the proportion of each group shown in Figure 4-6; pie graphs detailing the relative abundance of the different phylogenetic groups with sampling depth are shown in the Appendix.

4.5 Discussion

4.5.1 Flow cytometrically-sorted *Bacteria*: spatial variability examined in conjunction with measured environmental parameters

NMS was used to examine the differences between samples based on the phylogenetic diversity revealed within the HNA, LNA and CTC-positive assemblages, and to further link the observed diversity with the measured environmental parameters. The results of the NMS revealed slightly different patterns depending on

the source of data used for the analysis. The presence/absence matrix did not consider abundance of *Bacteria*, and revealed only subtle differences between the communities present at each of the three sampling stations. Although there was some differentiation between the shelf station and the two stations further from shore, this split occurred along Axis 2 which explained a low proportion of the variation in the data. Examination of the environmental variability indicated Axis 3 was negatively correlated with depth and nutrient concentrations and positively correlated with cell abundances and leucine incorporation. Therefore, both the cluster analysis and the NMS based on presence / absence of the DGGE bands revealed a distinction based on sampling depth between the different samples. However, within the NMS, none of the three sampling depths clustered together to the exclusion of the other sampling regions indicating the distribution of *Bacteria* is a continuum. Furthermore, examination of the different phylogenetic groups with depth did not reveal large differences in the diversity observed in the samples obtained from different regions of the water column. Finally, since none of the environmental parameters were correlated with Axis 1, some other factor which we did not measure, caused the diversity to vary among the different sampling stations. One possibility is that changes in the concentration of dissolved organic matter or its availability to the heterotrophic community caused shifts in the diversity of *Bacteria* observed.

The lack of correlation between species richness, or the number of DGGE bands from each sort, and bacterial leucine incorporation has been previously observed in a series of samples collected along the Rhone River plume in France (Troussellier et al. 2002). There was no correlation between bacterial leucine incorporation and species richness of the HNA or LNA assemblages. However, there was a weak correlation between the species richness of the CTC-positive sorts and bacterial leucine incorporation. This suggests that the species richness of the heterotrophic, bacterial community was not linked to secondary production, although the species richness of the respiring cells was weakly linked to secondary production. Since there were more CTC-positive DGGE bands identified in samples with higher levels of bacterial leucine incorporation, the diversity of CTC-positive cells is greater

than in samples with lower bacterial leucine incorporation rates. Therefore, a more diverse group of cells was involved in respiration, as indicated by their presence in the CTC-positive assemblage, in the more productive ecosystems.

The second NMS analysis relied on the number of sequences obtained from DGGE bands within the 32 different phylogenetic groups defined in Table 4-2. This analysis differs from the first NMS analysis which only considered the presence or absence of each DGGE band. While the presence/absence data showed slight differences between the three hydrographic regimes, larger differences were obvious when the sequences were grouped based on phylogenetic identity. In particular, the shelf and offshore stations clustered together, while the slope station samples were divided into two groups based on sampling cast. The link between two sampling stations that are 240 km apart is difficult to reconcile. The slope station could be different due to the input of fresh water from the Columbia River plume. However, the lower salinities associated with the plume did not extend below the surface samples, and therefore does not adequately explain why the slope stations were so different from the shelf and offshore stations. The phylogenetically different groups present in the two casts from the slope station appear to be correlated to differences in the photoautotrophic community present during each cast since higher abundances of diatoms, *Synechococcus*, and picoeukaryotes were present in the later slope station cast. This suggests that the diversity of the heterotrophic, bacterial community was coupled to changes in the autotrophic community. Examination of the diversity of *Bacteria* associated with phytoplankton blooms studied in a mesocosm (Riemann et al. 2000) and during upwelling (Kerkhof et al. 1999) has revealed changes in the bacterial community composition during different stages of a phytoplankton bloom. Furthermore, detritus from cyanobacterial cultures combined with lake water resulted in a different phylogenetic group of *Bacteria* than when detritus from a green alga was added to the same water sample (van Hannen et al. 1999a). A sample set larger than the two samples presented here will be needed to confirm the presence of specific phylogenetic groups concurrently appearing with increased abundances of picoeukaryotes, diatoms, or *Synechococcus*.

4.5.2 Phylogenetic differences and similarities in the HNA and LNA assemblages

The DGGE band patterns and the sequence data obtained from the individual DGGE bands indicated that most of the bacterial phylogenetic groups identified in this study could be found in both the HNA and LNA cell assemblages, although there were exceptions as noted. Almost one-quarter of all the DGGE bands were present in both the HNA and LNA assemblage. This suggests that at the level of taxonomic resolution employed here, there was not a phylogenetic distinction in Oregon coastal waters at the time of sampling between the two cytometrically-defined groups. These results support conclusions reached during a similar analysis of samples collected in the Mediterranean (Servais et al. 2003). Use of microautoradiography combined with fluorescent in situ hybridization has also revealed that no one phylogenetic group dominates the active proporation of the marine bacterioplankton (Cottrell and Kirchman 2003; Cottrell and Kirchman 2004). Thus, based on multiple studies, it appears that most *Bacteria* are able to exist in both the active and inactive components of the marine bacterioplankton. Furthermore, *Bacteria* were able to switch between the high and low nucleic acid cells depending on the environmental conditions, as has been observed with changes in the proportion of nucleoid-visible cells during log-growth compared to stationary growth (Choi et al. 1996).

The exceptions to the observation that many of the phylogenetic groups could be present in either the HNA or LNA assemblage were interesting. Several different groups within the *Bacteroidetes* were only identified in the HNA sorts. The use of FISH has also confirmed the presence of the *Bacteroidetes*, more specifically the members of the *Cytophaga-Flavobacterium* cluster which bind to the CF319a probe, within the HNA assemblage in the North Sea (Zubkov et al. 2001a; Zubkov et al. 2001b). Studies from the Delaware River estuary have indicated this group is involved in the breakdown of high molecular weight organic matter (Cottrell and Kirchman 2000). Perhaps the metabolic processes used for the consumption of high molecular weight organic matter require the organisms to maintain larger genomes or multiple copies of the genome within their cells. According to the Ribosomal RNA Operon

Copy Number Database (rrndb), members of the phylum *Bacteroidetes* have an average of 4.9 copies of the rRNA operon (Klappenbach et al. 2001). However, the two examples in the rrndb database closest to the sequences from this study, *Cytophaga* and *Rhodothermus*, only have one copy of the rRNA operon. Therefore, any conclusions based on the correlation between operon copy number and a presence limited to the HNA assemblage off the Oregon coast cannot be confirmed. Furthermore, contradictory evidence regarding the growth rates of the *Bacteroidetes* in aquatic systems (as reviewed in Kirchman 2002) indicate they can have higher (Jürgens and Güde 1994) or lower (Fuchs et al. 2000; Šimek et al. 2001) growth rates than other groups. If they have higher growth rates, this may also explain their presence within the HNA assemblage. Given the diversity within the *Bacteroidetes* and the observation that even within this study not all of them were limited to the HNA assemblage, more research is needed to examine whether some *Bacteroidetes* are genetically limited to the HNA assemblage, or whether this was due to the environmental conditions observed during this project.

There were also a smaller number of sequences obtained from the LNA assemblage relative to the HNA assemblage. Since the LNA cells have lower cell-specific DNA content, the lower number of sequences observed in this category could represent our inability to obtain sufficient DNA to detect these cells. Alternatively, the sequences only obtained from the LNA assemblage could represent groups which were not physiologically capable of maintaining higher cell-specific nucleic acid content. Testing this hypothesis is possible using isolates from some of the phylogenetic groups listed in Table 4-2. However, the sequences from the candidate division TM6 have not been obtained in culture and therefore cannot be used to test the hypothesis that some phylogenetic groups cannot switch between the HNA and LNA assemblages.

One interesting absence from the LNA only assemblage were members of the diverse SAR11 group. SAR11 sequences were obtained from both the HNA and LNA components of the heterotrophic community and therefore were not limited to the LNA assemblage. In culture, '*Candidatus*' Pelagibacter ubique is a small organism

with slow growth rates (Rappé et al. 2002), and therefore might be expected to be found exclusively in the LNA assemblage. However, that was not the case in this study. Either the slow growth rates of SAR11 are a manifestation of the culture conditions, or slow growth rates are characteristic of this group and not associated with lower cell-specific nucleic acid content. In the North Atlantic, cells labeled with the SAR11 probe were as big, or bigger than other prokaryotes (Malmstrom et al. 2004), thus the '*Candidatus*' P. ubique culture from the Sargasso Sea may be different than the SAR11 *Bacteria* from the Oregon coast.

There was also an interesting subset of the phylogenetic groups which were observed in either the HNA or LNA assemblages, but were never observed in both assemblages from the same sample. The two groups of *Betaproteobacteria* and the SAR92 cluster within the *Gammaproteobacteria* may be able to switch between the two assemblages, but are not able to maintain an LNA and an HNA assemblage simultaneously. Examination of the environmental parameters did not reveal any clear pattern as to what caused the group to switch from an HNA only to an LNA only assemblage. Finally, there were phylogenetic groups within the *Bacteria* which were not observed in any of the sorted samples which have previously been found off the Oregon coast. In particular, there were no sequences within the *Chloroflexi*-related SAR202 cluster (Morris et al. 2004), or any Marine Group A / SAR406 sequences (Rappé et al. 2000). Since DGGE can only identify microorganisms which comprise at least 1% of the population (Muyzer et al. 1993; Casamayor et al. 2000), these groups may be small proportions of the populations we sampled. Given the missing groups and the known limitations of DGGE, the diversity estimates presented here should be considered minimum diversity estimates.

The diversity of *Bacteria* identified in the different flow cytometrically-defined groups in this study was broader than that obtained from sorted populations originating from samples collected in the North Sea (Zubkov et al. 2001a; Zubkov et al. 2001b). Some of the differences between the North Sea and the Oregon coast data are methodological since the identification of the sorted populations in the North Sea partially relied on fluorescence in situ hybridization using probes targeting broader

phylogenetic groups. However, the *Deltaproteobacteria*, *Actinobacteria*, *Acidobacteria*, *Meiothermus*, and TM6 sequences obtained from the Oregon coast samples were all absent from the subset of sequences obtained from cloned 16S rRNA genes from the North Sea (Zubkov et al. 2001a). These could represent regional or temporal differences in the metabolically 'active' community (Servais et al. 2003). Now that it is possible to obtain DNA from sorted populations, future research can address the causes of temporal and spatial variability in the *Bacteria* present in the HNA or LNA assemblage in more detail, either by examination of the whole community or by focusing on specific phylogenetic groups.

The diversity of *Bacteria* in marine systems can be influenced by top-down processes, i.e. grazing (Jürgens et al. 1999; Suzuki 1999; Šimek et al. 2001; Šimek et al. 2003) or viral lysis (for review see Weinbauer and Rassoulzadegan 2004). Grazing has been shown to act selectively on larger (González et al. 1990; Jürgens and Güde 1994) and more active cells (Sherr et al. 1992; del Giorgio et al. 1996). In microcosms, predators cause decreases in the percent of HNA cells (Gasol et al. 1999), although in field studies, the samples with high grazing rates also had higher proportions of HNA cells (Vaqué et al. 2001). Viral lysis can alter the diversity of the bacterial community either by causing lysis of the heterotrophic cells (Fuhrman and Suttle 1993; Thingstad and Lignell 1997), or by lysis of the autotrophic community (van Hannen et al. 1999b) which can then provide dissolved organic matter to the heterotrophic community. The differences in diversity between the HNA and LNA assemblages may be due to differential effects of grazers or viral lysis on the two assemblages and would be interesting to investigate in the future.

4.5.3 Ability to reduce CTC is wide spread throughout the *Bacteria*

Most of the phylogenetic groups identified in this study were able to reduce CTC as determined by their presence in the CTC-positive cell sorts. The one exception was the SAR86 cluster within the *Gammaproteobacteria* which was not obtained in any CTC-positive sorts. This suggests either the environmental conditions were not

conducive for the SAR86 group to reduce CTC, or that the group is physiologically unable to reduce CTC. Based on BrdU incorporation, SAR86 was a dominant member of the DNA-synthesizing population in the fall in the North Sea when primary production levels were declining (Pernthaler et al. 2002). SAR86 may not have been an ecologically relevant member of the bacterioplankton in the spring when the Oregon coast samples were collected. However, there was only one SAR86 sequence obtained in this study and the SAR86 group remains uncultured; therefore, addressing questions about whether or not the group as a whole is capable of CTC reduction cannot be answered at this time.

The current study used two proxies to identify metabolically 'active' cells: the ability to reduce CTC and cell-specific nucleic acid content. In this study, the CTC-positive cells were not limited to the HNA assemblage. Shifts within the cell to periods of high production, may precede or follow changes in respiratory activity within the cell. Thus, patterns of CTC reduction by bacterial cells may represent a temporal or spatial disconnect between production and respiration since differences in cell-specific nucleic acid content may or may not be correlated to changes in respiration. In an experiment conducted by Pernthaler and colleagues (2001), incubations of two marine isolates showed that one of the strains maintained high ribosome concentrations per cell even after 100 hours in stationary growth. The storage of high titers of nucleic acids may be an adaptation to patchiness since the cell would be better prepared to respond to a change in the environment (Pernthaler et al. 2001). Therefore, the cells which are in the HNA assemblage but are CTC-negative could represent cells maintaining a high cell-specific nucleic acid content in stationary growth, or could be cells about to switch to the CTC-positive assemblage. Additionally, the observation of identical DGGE bands in the LNA and CTC-positive assemblages could represent cells which have functioning electron transport systems, but either do not require high cell-specific nucleic acid content or have shifted towards higher levels of respiration, but not higher levels of production. Grégori et al. (2001) used a combination of propidium iodide (PI) and SYBR to show there was a proportion of the LNA cells which were able to exclude PI, and are therefore

considered 'live' cells. Thus the LNA cells are not all dead, or dying cells, and can respire at levels sufficient to be detected in the CTC-positive assemblage.

4.5.4 Conclusions

The lack of phylogenetic divisions between the HNA and LNA assemblages is consistent with the use of cell-specific nucleic acid content as a proxy for activity. Changing status from HNA to LNA does seem to represent a physiological shift in the general heterotrophic bacterial community and does not appear to be limited to changes in which phylogenetic groups are actually present at a given time and place. Furthermore, while the diversity of cells capable of reducing CTC-positive was broad, the CTC-positive cells were equally likely to be observed with the HNA assemblage as with the LNA assemblage. Thus, the CTC-positive cells may not always represent the most active component of the heterotrophic community.

Acknowledgements We thank Delfina Homen and Maike Lichtenberg for assistance in the lab and the RV *Wecoma*'s captain, crew and marine technicians for assistance at sea. The DNA sequences from the Center for Gene Research and Biotechnology at Oregon State University were outstanding. This research was funded by NSF OCE-0002236 and OCE-0240785 to B.F.S. and E.B.S.

4.6 Literature cited

Altschul, S.F., T.L. Madden, A.A. Schäffer, J. Zhang, Z. Zhang, W. Miller and D.J. Lipman (1997). Gapped BLAST and PSI-BLAST: a new generation of protein database search programs. *Nucleic Acids Research* **25**: 3389-3402.

Bano, N. and J.T. Hollibaugh (2002). Phylogenetic composition of bacterioplankton assemblages from the Arctic Ocean. *Applied and Environmental Microbiology* **68**: 505-518.

Bernard, L., C. Courties, C. Duperray, H. Schäfer, G. Muyzer and P. Lebaron (2001). A new approach to determine the genetic diversity of viable and active bacteria in aquatic ecosystems. *Cytometry* **43**: 314-321.

Bernard, L., H. Schäfer, F. Joux, C. Courties, G. Muyzer and P. Lebaron (2000). Genetic diversity of total, active and culturable marine bacteria in coastal seawater. *Aquatic Microbial Ecology* **23**: 1-11.

Britschgi, T.B. and S.J. Giovannoni (1990). Phylogenetic analysis of a natural marine bacterioplankton population by rRNA gene cloning and sequencing. *Applied and Environmental Microbiology* **57**: 1707-1713.

Casamayor, E.O., H. Schäfer, L. Bañeras, C. Pedrós-Alió and G. Muyzer (2000). Identification of and spatio-temporal differences between microbial assemblages from two neighboring sulfurous lakes: Comparison by microscopy and denaturing gradient gel electrophoresis. *Applied and Environmental Microbiology* **66**: 499-508.

Chavez, F.P., J.T. Pennington, C.G. Castro, J.P. Ryan, R.P. Michisaki, B. Schlining, P. Walz, K.R. Buck, A. McFadyen and C.A. Collins (2002). Biological and chemical consequences of the 1997-1998 El Niño in central California waters. *Progress in Oceanography* **54**: 205-232.

Choi, J.W., E.B. Sherr and B.F. Sherr (1996). Relation between the presence-absence of a visible nucleoid and metabolic activity in bacterioplankton cells. *Limnology and Oceanography* **41**: 1161-1168.

Cottrell, M.T. and D.L. Kirchman (2000). Natural assemblages of marine Proteobacteria and members of the *Cytophaga-Flavobacter* cluster consuming low- and high-molecular-weight dissolved organic matter. *Applied and Environmental Microbiology* **66**: 1692-1697.

Cottrell, M.T. and D.L. Kirchman (2003). Contribution of major bacterial groups to bacterial biomass production (thymidine and leucine incorporation) in the Delaware estuary. *Limnology and Oceanography* **48**: 168-178.

Cottrell, M.T. and D.L. Kirchman (2004). Single-cell analysis of bacterial growth, cell size and community structure in the Delaware estuary. *Aquatic Microbial Ecology* **34**: 139-149.

del Giorgio, P.A., J.M. Gasol, D. Vaqué, P. Mura, S. Agustí and C.M. Duarte (1996). Bacterioplankton community structure: Protists control net production and the proportion of active bacteria in a coastal marine community. *Limnology and Oceanography* **41**: 1169-1179.

del Giorgio, P.A., Y.T. Prairie and D.F. Bird (1997). Coupling between rates of bacterial production and the number of metabolically active cells in lake bacterioplankton, measured using CTC reduction and flow cytometry. *Microbial Ecology* **34**: 144-154.

DeLong, E.F., D.G. Franks and A.L. Alldredge (1993). Phylogenetic diversity of aggregate-attached vs. free-living marine bacterial assemblages. *Limnology and Oceanography* **38**: 924-934.

Dietz, E.J. (1983). Permutation tests for association between two distance matrices. *Systematic Zoology* **32**: 21-26.

Eilers, H., J. Pernthaler, F.O. Glöckner and R. Amann (2000). Culturability and in situ abundance of pelagic bacteria from the North Sea. *Applied and Environmental Microbiology* **66**: 3044-3051.

Fuchs, B.M., M.V. Zubkov, K. Sahm, P.H. Burkill and R. Amann (2000). Changes in community composition during dilution cultures of marine bacterioplankton as assessed by flow cytometric and molecular biological techniques. *Environmental Microbiology* **2**: 191-201.

Fuhrman, J. and C. Suttle (1993). Viruses in marine planktonic systems. *Oceanography* **6**: 51-63.

Fuhrman, J.A. and A.A. Davis (1997). Widespread Archaea and novel Bacteria from the deep sea as shown by 16S rRNA gene sequences. *Marine Ecology Progress Series* **150**: 275-285.

Fuhrman, J.A., K. McCallum and A.A. Davis (1993). Phylogenetic diversity of subsurface marine microbial communities from the Atlantic and Pacific Oceans. *Applied and Environmental Microbiology* **59**: 1294-1302.

Gasol, J.M. and P.A. del Giorgio (2000). Using flow cytometry for counting natural planktonic bacteria and understanding the structure of planktonic bacterial communities. *Scientia Marina* **64**: 197-224.

Gasol, J.M., U.L. Zweifel, F. Peters, J.A. Fuhrman and Å. Hagström (1999). Significance of size and nucleic acid content in heterogeneity as measured by flow cytometry in natural planktonic bacteria. *Applied and Environmental Microbiology* **65**: 4475-4483.

Giovannoni, S.J., T.B. Britschgi, C.L. Moyer and K.G. Field (1990). Genetic diversity in Sargasso Sea bacterioplankton. *Nature* **345**: 60-63.

González, J.M., E.B. Sherr and B.F. Sherr (1990). Size-selective grazing on bacteria by natural assemblages of estuarine flagellates and ciliates. *Applied and Environmental Microbiology*. **56: 3** 583-589.

Gordon, L.I., J. J. C. Jennings, A.A. Ross and J.M. Krest (1994). A suggested protocol for continuous flow automated analysis of seawater nutrients (phosphate, nitrate, nitrite and silicic acid) in the WOCE Hydrographic Program and the Joint Global Ocean Fluxes Study. *WOCE Operations Manual, WOCE Report No. 68/91. Revision 1, 1994.*

Grégori, G., S. Citterio, A. Ghiani, M. Labra, S. Sgorbati, S. Brown and M. Denis (2001). Resolution of viable and membrane-compromised bacteria in freshwater and marine waters based on analytical flow cytometry and nucleic acid double staining. *Applied and Environmental Microbiology* **67**: 4662-4670.

Huyer, A., R.L. Smith and J. Fleischbein (2002). The coastal ocean off Oregon and northern California during the 1997-8 El Niño. *Progress in Oceanography* **54**: 311-341.

Jellett, J.F., W.K.W. Li, P.M. Dickie, A. Boraie and P.E. Kepkay (1996). Metabolic activity of bacterioplankton communities assessed by flow cytometry and single carbon substrate utilization. *Marine Ecology Progress Series* **136**: 213-225.

Jürgens, K. and H. Güde (1994). The potential importance of grazing-resistant bacteria in planktonic systems. *Marine Ecology Progress Series* **112**: 169-188.

Jürgens, K., J. Pernthaler, S. Schalla and R. Amann (1999). Morphological and compositional changes in a planktonic bacterial community in response to enhanced protozoan grazing. *Applied and Environmental Microbiology* **65**: 1241-1250.

Kerkhof, L., M.A. Voytek, R.M. Sherrell, D. Millie and O. Schofield (1999). Variability in bacterial community structure during upwelling in the coastal ocean. *Hydrobiologia* **401**: 139-148.

Kirchman, D.L. (2002). The ecology of *Cytophaga-Flavobacteria* in aquatic environments. *FEMS Microbiology Ecology* **39**: 91-100.

Kirchman, D.L., L. Yu and M.T. Cottrell (2003). Diversity and abundance of uncultured *Cytophaga*-like bacteria in the Delaware Estuary. *Applied and Environmental Microbiology* **69**: 6587-6596.

Klappenbach, J.A., P.R. Saxman, J.R. Cole and T.M. Schmidt (2001). rrndb: the Ribosomal RNA Operon Copy Number Database. *Nucleic Acids Research* **29**: 181-184.

Kruskal, J.B. (1964). Multidimensional scaling by optimizing goodness of fit to a nonmetric hypothesis. *Psychometrika* **29**: 1-27.

Lebaron, P., P. Servais, M. Troussellier, C. Courties, G. Muyzer, L. Bernard, H. Schäfer, R. Pukall, E. Stackebrandt, T. Guindulain and J. Vives-Rego (2001).

Microbial community dynamics in Mediterranean nutrient-enriched seawater mesocosms: changes in abundances, activity and composition. *FEMS Microbiology Ecology* **34**: 255-266.

Legendre, P. and L. Legendre (1988). *Numerical Ecology*. Amsterdam, The Netherlands, Elsevier Science BV.

Li, W.K.W. (1995). Composition of ultraphytoplankton in the central North Atlantic. *Marine Ecology Progress Series* **122**: 1-8.

Longnecker, K., B. Sherr and E. Sherr (2002). Variations in the temporal distribution and diversity of cytometrically-defined marine bacterioplankton in the Oregon upwelling system. *American Society of Limnology and Oceanography Ocean Sciences Meeting*, Honolulu, HI.

Ludwig, W., O. Strunk, R. Westram, L. Richter, H. Meier, Yadhukumar, A. Buchner, T. Lai, S. Steppi, G. Jobb, W. Förster, I. Brettske, S. Gerber, A.W. Ginhart, O. Gross, S. Grumann, S. Hermann, R. Jost, A. König, T. Liss, R. Lüßmann, M. May, B. Nonhoff, B. Reichel, R. Strehlow, A. Stamatakis, N. Stuckmann, A. Vilbig, M. Lenke, T. Ludwig, A. Bode and K.-H. Schleifer (2004). ARB: a software environment for sequence data. *Nucleic Acids Research* **32**: 1363-1371.

Malmstrom, R.R., R.P. Kiene, M.T. Cottrell and D.L. Kirchman (2004). Contribution of the SAR11 bacteria to dissolved organic matter flux in the North Atlantic Ocean. *American Society of Limnology and Oceanography / The Oceanography Society Ocean Research Conference*, Honolulu, HI.

Marie, D., F. Partensky, S. Jacquet and D. Vaulot (1997). Enumeration and cell cycle analysis of natural populations of marine picoplankton by flow cytometry using the nucleic acid stain SYBR Green I. *Applied and Environmental Microbiology* **63**: 186-193.

Mather, P.M. (1976). *Computational methods of multivariate analysis in physical geography*. London, J. Wiley & Sons.

Morris, R.M., M.S. Rappé, E. Urbach, S.A. Connon and S.J. Giovannoni (2004). Prevalence of the *Chloroflexi*-related SAR202 bacterioplankton cluster

throughout the mesopelagic zone and deep ocean. *Applied and Environmental Microbiology* **70**: 2836-2842.

Mullins, T.D., T.B. Britschgi, R.L. Krest and S.J. Giovannoni (1995). Genetic comparisons reveal the same unknown bacterial lineages in Atlantic and Pacific bacterioplankton communities. *Limnology and Oceanography* **40**: 148-158.

Muyzer, G., E.C. de Waal and A.G. Uitterlinden (1993). Profiling of complex microbial populations by denaturing gradient gel electrophoresis analysis of polymerase chain reaction-amplified genes coding for 16S rRNA. *Applied and Environmental Microbiology* **59**: 695-700.

Muyzer, G., S. Hottenträger, A. Teske and C. Wawer (1996). Denaturing gradient gel electrophoresis of PCR-amplified 16S rDNA-A new molecular approach to analyse the genetic diversity of mixed microbial communities. *Molecular Microbial Ecology Manual*. Netherlands, Kluwer Academic Publishers. **3.4.4:** 1-23.

Muyzer, G. and K. Smalla (1998). Application of denaturing gradient gel electrophoresis (DGGE) and temperature gradient gel electrophoresis (TGGE) in microbial ecology. *Antonie van Leeuwenhoek* **73**: 127-141.

Neefs, J.-M., Y. Van De Per, P. De Rijk, S. Chapelle and R. De Wachter (1993). Compilation of small ribosomal subunit RNA structures. *Nucleic Acids Research* **21**: 3025-3049.

O'Sullivan, L.A., K.E. Fuller, E.M. Thomas, C.M. Turley, J.C. Fry and A.J. Weightman (2004). Distribution and culturability of the uncultivated 'AGG58' cluster of the *Bacteroidetes* phylum in aquatic environments. *FEMS Microbiology Ecology* **47**: 359-370.

Pernthaler, A., J. Pernthaler, H. Eilers and R. Amann (2001). Growth patterns of two marine isolates: Adaptations to substrate patchiness. *Applied and Environmental Microbiology* **67**: 4077-4083.

Pernthaler, A., J. Pernthaler, M. Schattenhofer and R. Amann (2002). Identification of DNA-synthesizing bacterial cells in coastal North Sea plankton. *Applied and Environmental Microbiology* **68**: 5728-5736.

Peterson, W.T., J.E. Keister and L.R. Feinberg (2002). The effects of the 1997-1999 El Niño/La Niña events on the hydrography and zooplankton off the central Oregon coast. *Progress in Oceanography* **54**: 381-398.

Rappé, M.S., S.A. Connon, K.L. Vergin and S.J. Giovannoni (2002). Cultivation of the ubiquitous SAR11 marine bacterioplankton clade. *Nature* **418**: 630-633.

Rappé, M.S., P.F. Kemp and S.J. Giovannoni (1997). Phylogenetic diversity of marine coastal picoplankton 16S rRNA genes cloned from the continental shelf off Cape Hatteras, North Carolina. *Limnology and Oceanography* **42**: 811-826.

Rappé, M.S., K. Vergin and S.J. Giovannoni (2000). Phylogenetic comparisons of a coastal bacterioplankton community with its counterparts in open ocean and freshwater systems. *FEMS Microbiology Ecology* **33**: 219-232.

Riemann, L., G.F. Steward and F. Azam (2000). Dynamics of bacterial community composition and activity during a mesocosm diatom bloom. *Applied and Environmental Microbiology* **66**: 578-587.

Rodriguez, G.G., D. Phipps, K. Ishiguro and H.F. Ridgway (1992). Use of a fluorescent redox probe for direct visualization of actively respiring bacteria. *Applied and Environmental Microbiology* **58**: 1801-1808.

Schäfer, H. and G. Muyzer (2001). Denaturing gradient gel electrophoresis in marine microbial ecology. *Methods in Microbiology*. J.H. Paul (Ed). San Diego, Academic Press Ltd. **30:** 425-468.

Servais, P., E.O. Casamayor, C. Courties, P. Catala, N. Parthuisot and P. Lebaron (2003). Activity and diversity of bacterial cells with high and low nucleic acid content. *Aquatic Microbial Ecology* **33**: 41-51.

Servais, P., C. Courties, P. Lebaron and M. Troussellier (1999). Coupling bacterial activity measurements with cell sorting by flow cytometry. *Microbial Ecology* **38**: 180-189.

Sherr, B.F., P. del Giorgio and E.B. Sherr (1999). Estimating abundance and single-cell characteristics of respiring bacteria via the redox dye CTC. *Aquatic Microbial Ecology* **18**: 117-131.

Sherr, B.F., E.B. Sherr and J. McDaniel (1992). Effect of protozoan grazing on the frequency of dividing cells in bacterioplankton assemblages. *Applied and Environmental Microbiology* **58**: 2381-2385.

Šimek, K., K. Hornák, M. Mašín, U. Christaki, J. Nedoma, M.G. Weinbauer and J.R. Dolan (2003). Comparing the effects of resource enrichment and grazing on a bacterioplankton community of a meso-eutrophic reservoir. *Aquatic Microbial Ecology* **31**: 123-135.

Šimek, K., J. Pernthaler, M.G. Weinbauer, K. Hornák, J.R. Dolan, J. Nedoma, M. Mašín and R. Amann (2001). Changes in bacterial community composition and dynamics and viral mortality rates associated with enhanced flagellate grazing in a mesoeutrophic reservoir. *Applied and Environmental Microbiology* **67**: 2723-2733.

Smith, D.C. and F. Azam (1992). A simple, economical method for measuring bacterial protein synthesis rates in sea water using ^{3}H-leucine. *Marine Microbial Food Webs* **6**: 107-114.

Smith, J.J. and G.A. McFeters (1997). Mechanisms of INT (2-(4-iodophenyl)-3-(4-nitrophenyl)-5-phenyl tetrazolium chloride), and CTC (5-cyano-2,3-ditolyl tetrazolium chloride) reduction in *Escherichia coli* K-12. *Journal of Microbiological Methods* **29**: 161-175.

Strickland, J.D.H. and T.R. Parsons, Eds. (1972). *A Practical Handbook of Seawater Analysis*. Fisheries Research Board of Canada. Ottawa.

Suzuki, M.T. (1999). Effect of protistan bacterivory on coastal bacterioplankton diversity. *Aquatic Microbial Ecology* **20**: 261-272.

Thingstad, T.F. and R. Lignell (1997). Theoretical models for the control of bacterial growth rate, abundance, diversity and carbon demand. *Aquatic Microbial Ecology* **13**: 19-27.

Troussellier, M., H. Schäfer, N. Batailler, L. Bernard, C. Courties, P. Lebaron, G. Muyzer, P. Servais and J. Vives-Rego (2002). Bacterial activity and genetic richness along an estuarine gradient (Rhone River plume, France). *Aquatic Microbial Ecology* **28**: 13-24.

van Hannen, E.J., W. Mooij, M.P. van Agterveld, H.J. Gons and H.J. Laanbroek (1999a). Detritus-dependent development of the microbial community in an experimental system: qualitative analysis by denaturing gradient gel electrophoresis. *Applied and Environmental Microbiology* **65**: 2478-2484.

van Hannen, E.J., G. Zwart, M.P. van Agterveld, H.J. Gons, J. Ebert and H.J. Laanbroek (1999b). Changes in bacterial and eukaryotic community structure after mass lysis of filamentous cyanobacteria associated with viruses. *Appl. Environ. Microbiol.* **65**: 795-801.

Vaqué, D., E.O. Casamayor and J.M. Gasol (2001). Dynamics of whole community bacterial production and grazing losses in seawater incubations as related to the changes in the proportions of bacteria with different DNA content. *Aquatic Microbial Ecology* **25**: 163-177.

Weinbauer, M.G. and F. Rassoulzadegan (2004). Are viruses driving microbial diversification and diversity? *Environmental Microbiology* **6**: 1-11.

Whiteley, A.S., R.I. Griffiths and M.J. Bailey (2003). Analysis of the microbial functional diversity within water-stressed soil communities by flow cytometric analysis and CTC+ cell sorting. *Journal of Microbiological Methods* **54**: 257-267.

Wright, T.D., K.L. Vergin, P.W. Boyd and S.J. Giovannoni (1997). A novel δ-subdivision proteobacterial lineage from the lower ocean surface layer. *Applied and Environmental Microbiology* **63**: 1441-1448.

Zubkov, M.V., B.M. Fuchs, S.D. Archer, R.P. Kiene, R. Amann and P.H. Burkill (2001a). Linking the composition of bacterioplankton to rapid turnover of

dissolved dimethylsulphoniopropionate in an algal bloom in the North Sea. *Environmental Microbiology* **3**: 304-311.

Zubkov, M.V., B.M. Fuchs, S.D. Archer, R.P. Kiene, R. Amann and P.H. Burkill (2002a). Rapid turnover of dissolved DMS and DMSP by defined bacterioplankton communities in the stratified euphotic zone of the North Sea. *Deep-Sea Research II* **49**: 3017-3038.

Zubkov, M.V., B.M. Fuchs, P.H. Burkill and R. Amann (2001b). Comparison of cellular and biomass specific activities of dominant bacterioplankton groups in stratified waters of the Celtic Sea. *Applied and Environmental Microbiology* **67**: 5210-5218.

Zubkov, M.V., B.M. Fuchs, G.A. Tarran, P.H. Burkill and R. Amann (2002b). Mesoscale distribution of dominant bacterioplankton groups in the northern North Sea in early summer. *Aquatic Microbial Ecology* **29**: 135-144.

5 Summary

Although the data presented in this dissertation originate from samples collected during a four-week period in the spring of 2002, some interesting observations were made. The data presented in chapter two indicate there was a general decrease in cell-specific leucine incorporation with depth and with increasing distance from shore. While this might suggest a bottom-up control on leucine incorporation, top-down effects were not considered in this project and therefore cannot be eliminated from consideration. Grazing has been shown to act selectively on larger (González et al. 1990; Jürgens and Güde 1994), and more active cells (Sherr et al. 1992; del Giorgio et al. 1996). If grazers are selectively consuming the active cells, at what point, if ever, would the leucine incorporation rate of the HNA cells decrease? Furthermore, will grazing alter the leucine incorporation rate of the LNA cells, even though they are less active than the HNA cells? While there is some evidence the role of grazers in top-down control of bacterial abundance increases in more oligotrophic environments (Gasol et al. 2002), how that would be translated to the cell-specific incorporation rates of the HNA or LNA assemblages remains unknown and would be interesting to consider.

Grazers are also known to change the diversity of *Bacteria* in mesocosms (Jürgens et al. 1999; Suzuki 1999; Šimek et al. 2001; Šimek et al. 2003). As with possible changes in the cell-specific incorporation rate, the role of grazing in potentially changing the diversity of *Bacteria* within the HNA assemblage or LNA assemblage would be a logical question to explore. Predation causes decreases in the percent of HNA cells (Gasol et al. 1999). However, in field studies, the samples with high grazing rates also had higher proportions of HNA cells (Vaqué et al. 2001). Since the HNA cells seem to be the more 'active' component of the bacterioplankton, one hypothesis would be that grazing would have a greater effect on the diversity of HNA cells compared to impacts on the LNA cells' diversity. The hypotheses for grazing could also be examined for viral lysis since viral lysis also alters bacterial diversity (for review see Weinbauer and Rassoulzadegan 2004), either by causing lysis of the

heterotrophic cells (Fuhrman and Suttle 1993; Thingstad and Lignell 1997), or by lysis of the autotrophic community (van Hannen et al. 1999b) which can then provide dissolved organic matter for the heterotrophic community.

The HNA cells were also responsible for more of the total leucine incorporation in all three environments sampled and over the range of sampling depths. However, the LNA cells were responsible for proportionately more leucine incorporation at the offshore station. The values obtained from the sorted populations on the flow cytometer represent average values and, while they allow consideration of average differences, they are still not in fact cell-specific values. One possible line of future research would be to sort radioactively-labeled HNA and LNA cells onto a filter and use FISH to identify the cells which are incorporating the radioactive label. This would be particularly interesting for the LNA cells since their role seems to vary depending on ecosystem and perhaps sampling depth. Preliminary research into this idea indicated that sorting cells and using FISH for identification is not possible with a FACSCalibur flow cytometer. The presence of cell-like particles, which stain with SYBR but do not contain nucleic acids, interfered with the FISH assay. Attempts to clean these particles from the system were unsuccessful, therefore whole seawater samples labeled with ^{3}H-leucine were analyzed. In these samples, *Betaproteobacteria* were more abundant in the population of cells incorporating leucine than in the total population (Longnecker et al. 2004).

One of the questions raised prior to this project was the effectiveness of CTC in assessing the state of metabolic activity within heterotrophic cells. The data presented here indicate that CTC-positive cells tend to incorporate more leucine than the average heterotrophic cell, and that most phylogenetic groups of *Bacteria* were able to reduce CTC based on their presence within the CTC-positive assemblage. The CTC-positive cells could also be less active than the average heterotrophic cell and were responsible for less than 15% of the total leucine incorporation. Consideration of this research, in conjunction with the preliminary results from the other cruise participants, indicates larger problems with the CTC assay. CTC is ostensibly a measure of respiration, yet during this cruise CTC was neither correlated with

respiration rates in whole seawater nor in 0.8 μm filtered seawater. The relative abundance of CTC-positive cells and the mean red fluorescence of the CTC-positive cells was also uncorrelated with respiration rates (P.A del Giorgio, personal communication). Earlier, as yet unpublished, research by another cruise participant has shown that some of the red particles within the CTC-positive region on cytograms are actually CTC granules released from cells (J. Gasol, personal communication). These particles would not be expected to have any associated DNA or ^{3}H-leucine label remaining. Sorting CTC granules and not cells would lower average cell-specific leucine incorporation rates in Chapter two and could result in the absence of some phylogenetic groups from the CTC assemblage in Chapter four. The effectiveness of CTC in marine systems as measure of 'activity' in general, or even respiration, is now questionable.

The observation of a temporal or spatial lag between production and respiration was noted several times in this dissertation. One possibility is that this represents unbalanced growth since different cellular components are produced at different rates. One way to test for balanced growth is to examine the incorporation of leucine concurrently with the incorporation of thymidine. Higher values of leucine incorporation relative to thymidine incorporation indicate the cells are producing biomass, but are not dividing; lower values of leucine incorporation relative to thymidine incorporation indicate the cells are dividing, but not increasing their biomass. Spatial and temporal variability in the Leu:Tdr incorporation ratio has previously been observed in several marine ecosystems (Kirchman and Hoch 1986; Chin-Leo and Benner 1991; Gasol et al. 1998; Sherr et al. 1999a). Cells incubated with radioactive thymidine and leucine could be sorted on the flow cytometer to test hypotheses about whether in situ HNA and LNA cells incorporate thymidine and leucine at the same or different rates.

The diversity of *Bacteria* observed within the HNA and LNA assemblages indicated that most phylogenetic groups could be found in either assemblage. While the HNA cells were generally the more active members of the heterotrophic community, we still do not know what causes specific members of the *Bacteria* to

switch between the HNA and LNA assemblages. In cultures, the majority of cells in exponential phase growth were HNA cells, while the LNA cell numbers increased in late stationary phase (Jellett et al. 1996). There are also cultures which maintain high cell-specific nucleic acid contents, even in stationary growth (Pernthaler et al. 2001). Experiments initiated with only HNA or only LNA cells, and incubated under a range of environmental conditions, could be used to address what causes cells to switch from an HNA only or LNA only population to a mixed community of HNA and LNA cells. This type of experiment would allow more detailed examination of specific hypotheses regarding why cells are able to switch between the HNA and LNA assemblages.

Using non-metric multidimensional scaling to analyze differences between individual DNA sequences revealed the differences were not well explained by the measured environmental data. Changes in DNA sequences occur on much longer time scales than the circulation of water through the deep water conveyer belt, therefore looking at differences in DNA sequences with regard to nutrient concentrations and other environmental parameters is considering data from two very different time scales: evolutionary and ecological. Perhaps a better application of the NMS technique presented in Chapter three would look at the evolution of *Escherichia coli* over many generations (Lenski et al. 2003). This would allow detailed examination of the environmental factors which may cause changes in DNA sequences. The NMS technique did prove useful in the presentation of the categorical variables and the identification of the divergent *Alphaproteobacteria* sequences from the offshore station.

5.1 Summary literature cited

Chin-Leo, G. and R. Benner (1991). Dynamics of bacterioplankton abundance and production in seagrass communities of a hypersaline lagoon. *Marine Ecology Progress Series* **73**: 219-230.

del Giorgio, P.A., J.M. Gasol, D. Vaqué, P. Mura, S. Agustí and C.M. Duarte (1996). Bacterioplankton community structure: Protists control net production and the proportion of active bacteria in a coastal marine community. *Limnology and Oceanography* 41: 1169-1179.

Fuhrman, J. and C. Suttle (1993). Viruses in marine planktonic systems. *Oceanography* **6**: 51-63.

Gasol, J.M., M.D. Doval, J. Pinhassi, J.I. Calderón-Paz, N. Guixa-Boixareu, D. Vaqué and C. Pedrós-Alió (1998). Diel variations in bacterial heterotrophic activity and growth in the northwestern Mediterranean Sea. *Marine Ecology Progress Series*. **164**107-124.

Gasol, J.M., C. Pedrós-Alió and D. Vaqué (2002). Regulation of bacterial assemblages in oligotrophic plankton systems: results from experimental and empirical approaches. *Antonie Van Leeuwenhoek* **81**: 435-452.

Gasol, J.M., U.L. Zweifel, F. Peters, J.A. Fuhrman and Å. Hagström (1999). Significance of size and nucleic acid content in heterogeneity as measured by flow cytometry in natural planktonic bacteria. *Applied and Environmental Microbiology* **65**: 4475-4483.

González, J.M., E.B. Sherr and B.F. Sherr (1990). Size-selective grazing on bacteria by natural assemblages of estuarine flagellates and ciliates. *Applied and Environmental Microbiology*. **56: 3** 583-589.

Jellett, J.F., W.K.W. Li, P.M. Dickie, A. Boraie and P.E. Kepkay (1996). Metabolic activity of bacterioplankton communities assessed by flow cytometry and single carbon substrate utilization. *Marine Ecology Progress Series* **136**: 213-225.

Jürgens, K. and H. Güde (1994). The potential importance of grazing-resistant bacteria in planktonic systems. *Marine Ecology Progress Series* **112**: 169-188.

Jürgens, K., J. Pernthaler, S. Schalla and R. Amann (1999). Morphological and compositional changes in a planktonic bacterial community in response to enhanced protozoan grazing. *Applied and Environmental Microbiology* **65**: 1241-1250.

Kirchman, D.L. and M.P. Hoch (1986). Bacterial production in the Delaware Bay estuary estimated from thymidine and leucine incorporation rates. *Applied and Environmental Microbiology* **45**: 169-178.

Lenski, R.E., C.L. Winkworth and M.A. Riley (2003). Rates of DNA sequence evolution in experimental populations of Escherichia coli during 20,000 generations. *Journal of Molecular Evolution* **56**: 498-508.

Longnecker, K., D.S. Homen, E.B. Sherr and B.F. Sherr (2004). Using MICROFISH to identify biosynthetically active bacterioplankton in the Oregon upwelling system. *American Society of Limnology and Oceanography / The Oceanography Society Ocean Research Conference*, Honolulu, HI.

Pernthaler, A., J. Pernthaler, H. Eilers and R. Amann (2001). Growth patterns of two marine isolates: Adaptations to substrate patchiness. *Applied and Environmental Microbiology* **67**: 4077-4083.

Sherr, B.F., P. del Giorgio and E.B. Sherr (1999). Estimating abundance and single-cell characteristics of respiring bacteria via the redox dye CTC. *Aquatic Microbial Ecology* **18**: 117-131.

Sherr, B.F., E.B. Sherr and J. McDaniel (1992). Effect of protozoan grazing on the frequency of dividing cells in bacterioplankton assemblages. *Applied and Environmental Microbiology* **58**: 2381-2385.

Šimek, K., K. Hornák, M. Mašín, U. Christaki, J. Nedoma, M.G. Weinbauer and J.R. Dolan (2003). Comparing the effects of resource enrichment and grazing on a bacterioplankton community of a meso-eutrophic reservoir. *Aquatic Microbial Ecology* **31**: 123-135.

Šimek, K., J. Pernthaler, M.G. Weinbauer, K. Hornák, J.R. Dolan, J. Nedoma, M. Mašín and R. Amann (2001). Changes in bacterial community composition and dynamics and viral mortality rates associated with enhanced flagellate grazing in a mesoeutrophic reservoir. *Applied and Environmental Microbiology* **67**: 2723-2733.

Suzuki, M.T. (1999). Effect of protistan bacterivory on coastal bacterioplankton diversity. *Aquatic Microbial Ecology* **20**: 261-272.

Thingstad, T.F. and R. Lignell (1997). Theoretical models for the control of bacterial growth rate, abundance, diversity and carbon demand. *Aquatic Microbial Ecology* **13**: 19-27.

van Hannen, E.J., G. Zwart, M.P. van Agterveld, H.J. Gons, J. Ebert and H.J. Laanbroek (1999). Changes in bacterial and eukaryotic community structure after mass lysis of filamentous cyanobacteria associated with viruses. *Appl. Environ. Microbiol.* **65**: 795-801.

Vaqué, D., E.O. Casamayor and J.M. Gasol (2001). Dynamics of whole community bacterial production and grazing losses in seawater incubations as related to the changes in the proportions of bacteria with different DNA content. *Aquatic Microbial Ecology* **25**: 163-177.

Weinbauer, M.G. and F. Rassoulzadegan (2004). Are viruses driving microbial diversification and diversity? *Environmental Microbiology* **6**: 1-11.

6 Dissertation literature cited

Altschul, S.F., T.L. Madden, A.A. Schäffer, J. Zhang, Z. Zhang, W. Miller and D.J. Lipman (1997). Gapped BLAST and PSI-BLAST: a new generation of protein database search programs. *Nucleic Acids Research* **25**: 3389-3402.

Amann, R.I. (1995). Fluorescently labelled, rRNA-targeted oligonucleotide probes in the study of microbial ecology. *Molecular Ecology* **4**: 543-554.

Amann, R.I., L. Krumholz and D.A. Stahl (1990). Fluorescent-oligonucleotide probing of whole cells for determinative, phylogenetic, and environmental studies in microbiology. *Journal of Bacteriology* **172**: 762-770.

Amenta, N. and J. Klingner (2002). Case study: visualizing sets of evolutionary trees. *IEEE Information Visualization*: 71-74.

Amy, P.S. and R.Y. Morita (1983). Starvation-survival patterns of sixteen freshly isolated open-ocean bacteria. *Applied and Environmental Microbiology* **45**: 1109-1115.

Andrade, L., A.M. Gonzalez, F.V. Araujo and R. Paranhos (2003). Flow cytometry assessment of bacterioplankton in tropical marine environments. *Journal of Microbiological Methods* **55**: 841-850.

Bano, N. and J.T. Hollibaugh (2002). Phylogenetic composition of bacterioplankton assemblages from the Arctic Ocean. *Applied and Environmental Microbiology* **68**: 505-518.

Barth, J.A. (2003). Anomalous southward advection during 2002 in the Northern California Current: evidence from lagrangian surface drifters (doi:10.1029/2003GL017511). *Geophysical Research Letters* **30**: 8024.

Beck, P. and R. Huber (1997). Detection of cell viability in cultures of hyperthermophiles. *FEMS Microbiology Letters* **147**: 11-14.

Bernard, L., C. Courties, C. Duperray, H. Schäfer, G. Muyzer and P. Lebaron (2001). A new approach to determine the genetic diversity of viable and active bacteria in aquatic ecosystems. *Cytometry* **43**: 314-321.

Bernard, L., C. Courties, P. Servais, M. Troussellier, M. Petit and P. Lebaron (2000a). Relationships among bacterial cell size, productivity, and genetic diversity in aquatic environments using cell sorting and flow cytometry. *Microbial Ecology* **40**: 148-158.

Bernard, L., H. Schäfer, F. Joux, C. Courties, G. Muyzer and P. Lebaron (2000b). Genetic diversity of total, active and culturable marine bacteria in coastal seawater. *Aquatic Microbial Ecology* **23**: 1-11.

Bouvier, T.C. and P.A. del Giorgio (2002). Compositional changes in free-living bacterial communities along a salinity gradient in two temperate estuaries. *Limnology and Oceanography* **47**: 453-470.

Brand, L.E., W.G. Sunda and R.R. Guillard (1986). Reduction of marine phytoplankton reproduction rates by copper and cadmium. *Journal of Experimental Marine Biology and Ecology* **96**: 225-250.

Britschgi, T.B. and S.J. Giovannoni (1990). Phylogenetic analysis of a natural marine bacterioplankton population by rRNA gene cloning and sequencing. *Applied and Environmental Microbiology* **57**: 1707-1713.

Brussaard, C.P.D., D. Marie, R. Thyrhaug and G. Bratbak (2001). Flow cytometric analysis of phytoplankton viability following viral infection. *Aquatic Microbial Ecology* **26**: 157-166.

Casamayor, E.O., H. Schäfer, L. Bañeras, C. Pedrós-Alió and G. Muyzer (2000). Identification of and spatio-temporal differences between microbial assemblages from two neighboring sulfurous lakes: Comparison by microscopy and denaturing gradient gel electrophoresis. *Applied and Environmental Microbiology* **66**: 499-508.

Casotti, R., C. Brunet, B. Aronne and M. Ribera d'Alcala (2000). Mesoscale features of phytoplankton and planktonic bacteria in a coastal area as induced by external water masses. *Marine Ecology Progress Series* **195**: 15-27.

Chavez, F.P., J.T. Pennington, C.G. Castro, J.P. Ryan, R.P. Michisaki, B. Schlining, P. Walz, K.R. Buck, A. McFadyen and C.A. Collins (2002). Biological and chemical consequences of the 1997-1998 El Niño in central California waters. *Progress in Oceanography* **54**: 205-232.

Chin-Leo, G. and R. Benner (1991). Dynamics of bacterioplankton abundance and production in seagrass communities of a hypersaline lagoon. *Marine Ecology Progress Series* **73**: 219-230.

Choi, J.W., B.F. Sherr and E.B. Sherr (1999). Dead or alive? A large fraction of ETS-inactive marine bacterioplankton cells, as assessed by reduction of CTC, can become ETS-active with incubation and substrate addition. *Aquatic Microbial Ecology* **18**: 105-115.

Choi, J.W., E.B. Sherr and B.F. Sherr (1996). Relation between the presence-absence of a visible nucleoid and metabolic activity in bacterioplankton cells. *Limnology and Oceanography* **41**: 1161-1168.

Clarke, K.R. (1993). Non-parametric multivariate analysis of changes in community structure. *Australian Journal of Ecology* **18**: 117-143.

Cole, J.J., S. Findlay and M.L. Pace (1988). Bacterial production in fresh and saltwater ecosystems: a cross-system overview. *Marine Ecology Progress Series* **43**: 1-10.

Collier, J.L. and B. Palenik (2003). Phycoerythrin-containing picoplankton in the Southern California Bight. *Deep-Sea Research* **50**: 2405-2422.

Corwith, H.L. and P.A. Wheeler (2002). El Niño related variations in nutrient and chlorophyll distributions off Oregon. *Progress in Oceanography* **54**: 361-380.

Cottrell, M.T. and D.L. Kirchman (2000). Natural assemblages of marine Proteobacteria and members of the *Cytophaga-Flavobacter* cluster consuming low- and high-molecular-weight dissolved organic matter. *Applied and Environmental Microbiology* **66**: 1692-1697.

Cottrell, M.T. and D.L. Kirchman (2003). Contribution of major bacterial groups to bacterial biomass production (thymidine and leucine incorporation) in the Delaware estuary. *Limnology and Oceanography* **48**: 168-178.

Cottrell, M.T. and D.L. Kirchman (2004). Single-cell analysis of bacterial growth, cell size and community structure in the Delaware estuary. *Aquatic Microbial Ecology* **34**: 139-149.

Crump, B.C., E.V. Armbrust and J.A. Baross (1999). Phylogenetic analysis of particle-attached and free-living bacterial communities on the Columbia River, its estuary, and the adjacent coastal ocean. *Applied and Environmental Microbiology* **65**: 3192-3204.

del Giorgio, P.A. and T.C. Bouvier (2002). Linking the physiologic and phylogenetic successions in free-living bacterial communities along an estuarine salinity gradient. *Limnology and Oceanography* **47**: 471-486.

del Giorgio, P.A., J.M. Gasol, D. Vaqué, P. Mura, S. Agustí and C.M. Duarte (1996). Bacterioplankton community structure: Protists control net production and the proportion of active bacteria in a coastal marine community. *Limnology and Oceanography* **41**: 1169-1179.

del Giorgio, P.A., Y.T. Prairie and D.F. Bird (1997). Coupling between rates of bacterial production and the number of metabolically active cells in lake bacterioplankton, measured using CTC reduction and flow cytometry. *Microbial Ecology* **34**: 144-154.

DeLong, E.F., D.G. Franks and A.L. Alldredge (1993). Phylogenetic diversity of aggregate-attached vs. free-living marine bacterial assemblages. *Limnology and Oceanography* **38**: 924-934.

DeLong, E.F., G.S. Wickham and N.R. Pace (1989). Phylogenetic stains: ribosomal RNA-based probes for the identification of single cells. *Science* **243**: 1360-1363.

Dietz, E.J. (1983). Permutation tests for association between two distance matrices. *Systematic Zoology* **32**: 21-26.

Ducklow, H.W. (1999). The bacterial component of the oceanic euphotic zone. *FEMS Microbiology Ecology* **30**: 1-10.

Eilers, H., J. Pernthaler, F.O. Glöckner and R. Amann (2000). Culturability and in situ abundance of pelagic bacteria from the North Sea. *Applied and Environmental Microbiology* **66**: 3044-3051.

Eisen, M.B., P.T. Spellman, P.O. Brown and D. Botstein (1998). Cluster analysis and display of genome-wide expression patterns. *Proceedings of the National Academy of Sciences, USA* **95**: 14863-14868.

Evans, C.T., B. Van Mooy, R.G. Keil, C. Greengrove and G. Chin-Leo (2004). Isolation of DNA from actively growing heterotrophic bacteria using 5-bromo-2'-deoxyuridine (BrdU). *American Society of Limnology and Oceanography / The Oceanography Society Ocean Research Conference*, Honolulu, HI.

Felsenstein, J. (1981). Evolutionary trees from DNA sequences: A maximum likelihood approach. *Journal of Molecular Evolution* **17**: 368-376.

Flaten, G.A.F., T. Castberg, T. Tanaka and T.F. Thingstad (2003). Interpretation of nutrient-enrichment bioassays by looking at sub-populations in a marine bacterial community. *Aquatic Microbial Ecology* **33**: 11-18.

Fuchs, B.M., M.V. Zubkov, K. Sahm, P.H. Burkill and R. Amann (2000). Changes in community composition during dilution cultures of marine bacterioplankton as assessed by flow cytometric and molecular biological techniques. *Environmental Microbiology* **2**: 191-201.

Fuhrman, J. and C. Suttle (1993). Viruses in marine planktonic systems. *Oceanography* **6**: 51-63.

Fuhrman, J.A. and A.A. Davis (1997). Widespread Archaea and novel Bacteria from the deep sea as shown by 16S rRNA gene sequences. *Marine Ecology Progress Series* **150**: 275-285.

Fuhrman, J.A., K. McCallum and A.A. Davis (1993). Phylogenetic diversity of subsurface marine microbial communities from the Atlantic and Pacific Oceans. *Applied and Environmental Microbiology* **59**: 1294-1302.

Garrity, G.M. and T.G. Lilburn (2002). Mapping taxonomic space: an overview of the road map to the second edition of Bergey's Manual of Systematic Bacteriology. *WFCC Newsletter* **35**: 5-15.

Gasol, J.M. and P.A. del Giorgio (2000). Using flow cytometry for counting natural planktonic bacteria and understanding the structure of planktonic bacterial communities. *Scientia Marina* **64**: 197-224.

Gasol, J.M., P.A. del Giorgio, R. Massana and C.M. Duarte (1995). Active versus inactive bacteria: size-dependence in a coastal marine plankton community. *Marine Ecology Progress Series* **128**: 91-97.

Gasol, J.M., M.D. Doval, J. Pinhassi, J.I. Calderón-Paz, N. Guixa-Boixareu, D. Vaqué and C. Pedrós-Alió (1998). Diel variations in bacterial heterotrophic activity and growth in the northwestern Mediterranean Sea. *Marine Ecology Progress Series*. **164**107-124.

Gasol, J.M., C. Pedrós-Alió and D. Vaqué (2002). Regulation of bacterial assemblages in oligotrophic plankton systems: results from experimental and empirical approaches. *Antonie Van Leeuwenhoek* **81**: 435-452.

Gasol, J.M., U.L. Zweifel, F. Peters, J.A. Fuhrman and Å. Hagström (1999). Significance of size and nucleic acid content in heterogeneity as measured by flow cytometry in natural planktonic bacteria. *Applied and Environmental Microbiology* **65**: 4475-4483.

Giovannoni, S.J., T.B. Britschgi, C.L. Moyer and K.G. Field (1990a). Genetic diversity in Sargasso Sea bacterioplankton. *Nature* **345**: 60-63.

Giovannoni, S.J., E.F. DeLong, T.M. Schmidt and N.R. Pace (1990b). Tangential flow filtration and preliminary phylogenetic analysis of marine picoplankton. *Applied and Environmental Microbiology* **56**: 2572-2575.

Giovannoni, S.J. and M. Rappé (2000). Evolution, diversity, and molecular ecology of marine prokaryotes. *Microbial Ecology of the Oceans*. D.L. Kirchman (Ed). New York, Wiley-Liss, Inc.: 47-84.

González, J.M., E.B. Sherr and B.F. Sherr (1990). Size-selective grazing on bacteria by natural assemblages of estuarine flagellates and ciliates. *Applied and Environmental Microbiology*. **56: 3** 583-589.

González, J.M., E.B. Sherr and B.F. Sherr (1993). Differential feeding by marine flagellates on growing vs starving, and on motile vs non-motile, bacterial prey. *Marine Ecology Progress Series* **102**: 257-267.

Gordon, L.I., J. J. C. Jennings, A.A. Ross and J.M. Krest (1994). A suggested protocol for continuous flow automated analysis of seawater nutrients (phosphate, nitrate, nitrite and silicic acid) in the WOCE Hydrographic Program and the Joint Global Ocean Fluxes Study. *WOCE Operations Manual, WOCE Report No. 68/91. Revision 1, 1994.*

Grégori, G., S. Citterio, A. Ghiani, M. Labra, S. Sgorbati, S. Brown and M. Denis (2001). Resolution of viable and membrane-compromised bacteria in freshwater and marine waters based on analytical flow cytometry and nucleic acid double staining. *Applied and Environmental Microbiology* **67**: 4662-4670.

Hamasaki, K., R.A. Long and F. Azam (2004). Individual cell growth rates of marine bacteria, measured by bromodeoxyuridine. *Aquatic Microbial Ecology* **35**: 217-227.

Hasegawa, M., H. Kishino and T. Yano (1985). Dating of the human-ape splitting by a molecular clock of mitochondrial DNA. *Journal of Molecular Evolution* **22**: 160-174.

Hill, J.K. and P.A. Wheeler (2002). Organic carbon and nitrogen in the northern California current system: comparison of offshore, river plume, and coastally upwelled waters. *Progress in Oceanography* **53**: 369-387.

Howard-Jones, M.H., V.D. Ballard, A.E. Allen, M.E. Frischer and P.G. Verity (2002). Distribution of bacterial biomass and activity in the marginal ice zone of the central Barents Sea during summer. *Journal of Marine Systems* **38**: 77-91.

Howard-Jones, M.H., M.E. Frischer and P.G. Verity (2001). Determining the physiological status of individual bacterial cells. *Methods in Microbiology*. J.H. Paul (Ed), Academic Press Ltd. **30:** 175-206.

Huyer, A., R.L. Smith and J. Fleischbein (2002). The coastal ocean off Oregon and northern California during the 1997-8 El Niño. *Progress in Oceanography* **54**: 311-341.

Jellett, J.F., W.K.W. Li, P.M. Dickie, A. Boraie and P.E. Kepkay (1996). Metabolic activity of bacterioplankton communities assessed by flow cytometry and single carbon substrate utilization. *Marine Ecology Progress Series* **136**: 213-225.

Jepras, R.I., J. Carter, S.C. Pearson, F.E. Paul and M.J. Wilkinson (1995). Development of a robust flow cytometric assay for determining numbers of viable bacteria. *Applied and Environmental Microbiology* **61**: 2696-2701.

Jochem, F.J. (2001). Morphology and DNA content of bacterioplankton in the northern Gulf of Mexico: analysis by epifluorescence microscopy and flow cytometry. *Aquatic Microbial Ecology* **25**: 179-194.

Jongman, R.H.G., C.J.F. ter Braak and O.F.R. van Tongeren, Eds. (1995). *Data analysis in community and landscape ecology*, Cambridge University Press.

Jukes, T.H. and C.R. Cantor (1969). Evolution of protein molecules. *Mammalian Protein Metabolism*. H.N. Munro (Ed). New York, Academic Press. **3:** 21-132.

Jürgens, K. and H. Güde (1994). The potential importance of grazing-resistant bacteria in planktonic systems. *Marine Ecology Progress Series* **112**: 169-188.

Jürgens, K., J. Pernthaler, S. Schalla and R. Amann (1999). Morphological and compositional changes in a planktonic bacterial community in response to enhanced protozoan grazing. *Applied and Environmental Microbiology* **65**: 1241-1250.

Kara, A.B., P.A. Rochford and H.E. Hurlburt (2000). An optimal definition for ocean mixed layer depth. *Journal of Geophysical Research* **105**: 16,803-16,821.

Karner, M. and J.A. Fuhrman (1997). Determination of active marine bacterioplankton: a comparison of universal 16S rRNA probes, autoradiography, and nucleoid staining. *Applied and Environmental Microbiology* **63**: 1208-1213.

Kemp, P.F., S. Lee and J. LaRoche (1993). Estimating growth rate of slowly growing marine bacteria from RNA content. *Applied and Environmental Microbiology* **59**: 2594-2601.

Kerkhof, L., M.A. Voytek, R.M. Sherrell, D. Millie and O. Schofield (1999). Variability in bacterial community structure during upwelling in the coastal ocean. *Hydrobiologia* **401**: 139-148.

Kerkhof, L. and B.B. Ward (1993). Comparison of nucleic acid hybridization and fluorometry for measurement of the relationship between RNA/DNA ratio and growth rate in a marine bacterium. *Applied and Environmental Microbiology* **59**: 1303-1309.

Kirchman, D.L. (1993). Leucine incorporation as a measure of biomass production by heterotrophic bacteria. *Current Methods in Aquatic Microbial Ecology*. P.F. Kemp, B.F. Sherr, E.B. Sherr and J.J. Cole (Eds). New York, Lewis Publishing: 509-512.

Kirchman, D.L. (2002). The ecology of *Cytophaga-Flavobacteria* in aquatic environments. *FEMS Microbiology Ecology* **39**: 91-100.

Kirchman, D.L. and M.P. Hoch (1986). Bacterial production in the Delaware Bay estuary estimated from thymidine and leucine incorporation rates. *Applied and Environmental Microbiology* **45**: 169-178.

Kirchman, D.L., K.A. Hoffman, R. Weaver and D.A. Hutchins (2003a). Regulation of growth and energetics of a marine bacterium by nitrogen source and iron availability. *Marine Ecology Progress Series* **250**: 291-296.

Kirchman, D.L., L. Yu and M.T. Cottrell (2003b). Diversity and abundance of uncultured *Cytophaga*-like bacteria in the Delaware Estuary. *Applied and Environmental Microbiology* **69**: 6587-6596.

Klappenbach, J.A., P.R. Saxman, J.R. Cole and T.M. Schmidt (2001). rrndb: the Ribosomal RNA Operon Copy Number Database. *Nucleic Acids Research* **29**: 181-184.

Kruskal, J.B. (1964). Multidimensional scaling by optimizing goodness of fit to a nonmetric hypothesis. *Psychometrika* **29**: 1-27.

Lanave, C., G. Preparata, C. Saccone and G. Serio (1984). A new method for calculating evolutionary substitution rates. *Journal of Molecular Evolution* **20**: 86-93.

Lebaron, P., P. Catala and N. Parthuisot (1998). Effectiveness of SYTOX green stain for bacterial viability assessment. *Applied and Environmental Microbiology* **64**: 2697-2700.

Lebaron, P., P. Servais, H. Agogué, C. Courties and F. Joux (2001a). Does the high nucleic acid content of individual bacterial cells allow us to discriminate between active cells and inactive cells in aquatic systems? *Applied and Environmental Microbiology* **67**: 1775-1782.

Lebaron, P., P. Servais, M. Troussellier, C. Courties, G. Muyzer, L. Bernard, H. Schäfer, R. Pukall, E. Stackebrandt, T. Guindulain and J. Vives-Rego (2001b). Microbial community dynamics in Mediterranean nutrient-enriched seawater mesocosms: changes in abundances, activity and composition. *FEMS Microbiology Ecology* **34**: 255-266.

Lee, N., P. Halkjær, K.H. Andreasen, S. Juretschko, J.L. Nielsen, K.-H. Schleifer and M. Wagner (1999). Combination of fluorescent in situ hybridization and microautoradiography—a new tool for structure-function analyses in microbial ecology. *Applied and Environmental Microbiology* **65**: 1289-1297.

Legendre, P. and L. Legendre (1988). *Numerical Ecology*. Amsterdam, The Netherlands, Elsevier Science BV.

Lenski, R.E., C.L. Winkworth and M.A. Riley (2003). Rates of DNA sequence evolution in experimental populations of Escherichia coli during 20,000 generations. *Journal of Molecular Evolution* **56**: 498-508.

Li, W.K.W. (1995). Composition of ultraphytoplankton in the central North Atlantic. *Marine Ecology Progress Series* **122**: 1-8.

Li, W.K.W., J.F. Jellett and P.M. Dickie (1995). DNA distributions in planktonic bacteria stained with TOTO or TO-PRO. *Limnology and Oceanography* **40**: 1485-1495.

Lilburn, T.G. and G.M. Garrity (2004). Exploring prokaryotic taxonomy. *International Journal of Systematic and Evolutionary Microbiology* **54**: 7-13.

Longnecker, K., D.S. Homen, E.B. Sherr and B.F. Sherr (2004). Using MICROFISH to identify biosynthetically active bacterioplankton in the Oregon upwelling system. *American Society of Limnology and Oceanography / The Oceanography Society Ocean Research Conference*, Honolulu, HI.

Longnecker, K., B. Sherr and E. Sherr (2002). Variations in the temporal distribution and diversity of cytometrically-defined marine bacterioplankton in the Oregon upwelling system. *American Society of Limnology and Oceanography Ocean Sciences Meeting*, Honolulu, HI.

López-Amorós, R., S. Castel, J. Comas-Riu and J. Vives-Rego (1997). Assessment of *E. coli* and *Salmonella* viability and starvation by confocal laser microscopy and flow cytometry using rhodamine 123, DiBAC4(3), propidium iodide, and CTC. *Cytometry* **28**: 298-305.

Ludwig, W., O. Strunk, R. Westram, L. Richter, H. Meier, Yadhukumar, A. Buchner, T. Lai, S. Steppi, G. Jobb, W. Förster, I. Brettske, S. Gerber, A.W. Ginhart, O. Gross, S. Grumann, S. Hermann, R. Jost, A. König, T. Liss, R. Lüßmann, M. May, B. Nonhoff, B. Reichel, R. Strehlow, A. Stamatakis, N. Stuckmann, A. Vilbig, M. Lenke, T. Ludwig, A. Bode and K.-H. Schleifer (2004). ARB: a software environment for sequence data. *Nucleic Acids Research* **32**: 1363-1371.

Malmstrom, R.R., R.P. Kiene, M.T. Cottrell and D.L. Kirchman (2004a). Contribution of the SAR11 bacteria to dissolved organic matter flux in the North Atlantic Ocean. *American Society of Limnology and Oceanography / The Oceanography Society Ocean Research Conference*, Honolulu, HI.

Malmstrom, R.R., R.P. Kiene and D.L. Kirchman (2004b). Identification and enumeration of bacteria assimilating dimethylsulfoniopropionate (DMSP) in the North Atlantic and Gulf of Mexico. *Limnology and Oceanography* **49**: 597-606.

Marie, D., F. Partensky, S. Jacquet and D. Vaulot (1997). Enumeration and cell cycle analysis of natural populations of marine picoplankton by flow cytometry using the nucleic acid stain SYBR Green I. *Applied and Environmental Microbiology* **63**: 186-193.

Mather, P.M. (1976). *Computational methods of multivariate analysis in physical geography*. London, J. Wiley & Sons.

McCune, B.M. and J.B. Grace (2002). *Analysis of Ecological Communities*. Gleneden Beach, Oregon, MjM Software Design.

Moore, L.R. and S.W. Chisholm (1999). Photophysiology of the marine cyanobacterium *Prochlorococcus*: Ecotypic differences among cultured isolates. *Limnology and Oceanography* **44**: 628-638.

Moore, L.R., A.F. Post, G. Rocap and S.W. Chisholm (2002). Utilization of different nitrogen sources by the marine cyanobacteria *Prochlorococcus* and *Synechococcus*. *Limnology and Oceanography* **47**: 989-996.

Moore, L.R., G. Rocap and S.W. Chisholm (1998). Physiology and molecular phylogeny of coexisting *Prochlorococcus* ecotypes. *Nature* **393**: 464-467.

Morita, R.Y. (1997). *Bacteria in Oligotrophic Environments*. New York, Chapman and Hall.

Morris, R.M., M.S. Rappé, E. Urbach, S.A. Connon and S.J. Giovannoni (2004). Prevalence of the *Chloroflexi*-related SAR202 bacterioplankton cluster throughout the mesopelagic zone and deep ocean. *Applied and Environmental Microbiology* **70**: 2836-2842.

Mullins, T.D., T.B. Britschgi, R.L. Krest and S.J. Giovannoni (1995). Genetic comparisons reveal the same unknown bacterial lineages in Atlantic and Pacific bacterioplankton communities. *Limnology and Oceanography* **40**: 148-158.

Murphree, T., S.J. Bograd, F.B. Schwing and B. Ford (2003). Large scale atmosphere-ocean anomalies in the northeast Pacific during 2002 (doi:10.1029/2003GL017303). *Geophysical Research Letters* **30**: 8026.

Muyzer, G., E.C. de Waal and A.G. Uitterlinden (1993). Profiling of complex microbial populations by denaturing gradient gel electrophoresis analysis of polymerase chain reaction-amplified genes coding for 16S rRNA. *Applied and Environmental Microbiology* **59**: 695-700.

Muyzer, G., S. Hottenträger, A. Teske and C. Wawer (1996). Denaturing gradient gel electrophoresis of PCR-amplified 16S rDNA-A new molecular approach to analyse the genetic diversity of mixed microbial communities. *Molecular Microbial Ecology Manual*. Netherlands, Kluwer Academic Publishers. **3.4.4:** 1-23.

Muyzer, G. and K. Smalla (1998). Application of denaturing gradient gel electrophoresis (DGGE) and temperature gradient gel electrophoresis (TGGE) in microbial ecology. *Antonie van Leeuwenhoek* **73**: 127-141.

Neefs, J.-M., Y. Van De Per, P. De Rijk, S. Chapelle and R. De Wachter (1993). Compilation of small ribosomal subunit RNA structures. *Nucleic Acids Research* **21**: 3025-3049.

Nielsen, J.L., M. Aquino de Muro and P.H. Nielsen (2003). Evaluation of the redox dye 5-cyano-2,3-tolyl-tetrazolium chloride for activity studies by simultaneous use of microautoradiography and fluorescence in situ hybridization. *Applied and Environmental Microbiology* **69**: 641-643.

Novo, D., N.G. Perlmutter, R.H. Hunt and H.M. Shapiro (1999). Accurate flow cytometric membrane potential measurement in bacteria using diethyloxacarbocyanine and a ratiometric technique. *Cytometry* **35**: 55-63.

Oda, Y., S.-J. Slagman, W.G. Meijer, L.J. Forney and J.C. Gottschall (2000). Influence of growth rate and starvation on fluorescent in situ hybridization of *Rhodopseudomonas palustris*. *FEMS Microbiology Ecology* **32**: 205-213.

Olsen, G.J., D.L. Lane, S.J. Giovannoni, N.R. Pace and D.R. Stahl (1986). Microbial ecology and evolution: A ribosomal RNA approach. *Annual Review of Microbiology* **40**: 337-366.

Olson, R.J., S.W. Chisholm, E.R. Zettler, M.A. Altabet and J.A. Dusenberry (1990). Spatial and temporal distributions of prochlorophyte picoplankton in the North Atlantic Ocean. *Deep-Sea Research* **37**: 1033-1051.

O'Sullivan, L.A., K.E. Fuller, E.M. Thomas, C.M. Turley, J.C. Fry and A.J. Weightman (2004). Distribution and culturability of the uncultivated 'AGG58' cluster of the *Bacteroidetes* phylum in aquatic environments. *FEMS Microbiology Ecology* **47**: 359-370.

Ouverney, C.C. and J.A. Fuhrman (1999). Combined microautoradiography-16S rRNA probe technique for determination of radioisotope uptake by specific microbial cell types in situ. *Applied and Environmental Microbiology* **65**: 1746-1752.

Ouverney, C.C. and J.A. Fuhrman (2000). Marine planktonic *Archaea* take up amino acids. *Applied and Environmental Microbiology* **66**: 4829-4833.

Palenik, B., B. Brahamsha, F.W. Larimer, M. Land, L. Hauser, P. Chain, J. Lamerdin, W. Regala, E.E. Allen, J. McCarren, I. Paulsen, A. Dufresne, F. Partensky, E.A. Webb and J. Waterbury (2003). The genome of a motile marine *Synechococcus*. *Nature* **424**: 1037-1042.

Payne, C.D. and N.M. Price (1999). Effects of cadmium toxicity on growth and elemental composition of marine phytoplankton. *Journal of Phycology* **35**: 293-302.

Pernthaler, A., J. Pernthaler, H. Eilers and R. Amann (2001). Growth patterns of two marine isolates: Adaptations to substrate patchiness. *Applied and Environmental Microbiology* **67**: 4077-4083.

Pernthaler, A., J. Pernthaler, M. Schattenhofer and R. Amann (2002). Identification of DNA-synthesizing bacterial cells in coastal North Sea plankton. *Applied and Environmental Microbiology* **68**: 5728-5736.

Peterson, W.T., J.E. Keister and L.R. Feinberg (2002). The effects of the 1997-1999 El Niño/La Niña events on the hydrography and zooplankton off the central Oregon coast. *Progress in Oceanography* **54**: 381-398.

Poulsen, L.K., G. Ballard and D.A. Stahl (1993). Use of rRNA fluorescence in situ hybridization for measuring the activity of single cells in young and established biofilms. *Applied and Environmental Microbiology* **59**: 1354-1360.

Rappé, M.S., S.A. Connon, K.L. Vergin and S.J. Giovannoni (2002). Cultivation of the ubiquitous SAR11 marine bacterioplankton clade. *Nature* **418**: 630-633.

Rappé, M.S., P.F. Kemp and S.J. Giovannoni (1997). Phylogenetic diversity of marine coastal picoplankton 16S rRNA genes cloned from the continental shelf off Cape Hatteras, North Carolina. *Limnology and Oceanography* **42**: 811-826.

Rappé, M.S., K. Vergin and S.J. Giovannoni (2000). Phylogenetic comparisons of a coastal bacterioplankton community with its counterparts in open ocean and freshwater systems. *FEMS Microbiology Ecology* **33**: 219-232.

Riemann, L., G.F. Steward and F. Azam (2000). Dynamics of bacterial community composition and activity during a mesocosm diatom bloom. *Applied and Environmental Microbiology* **66**: 578-587.

Rocap, G., D.L. Distel, J.B. Waterbury and S.W. Chisholm (2002). Resolution of *Prochlorococcus* and *Synechococcus* ecotypes by using 16S-23S ribosomal DNA internal transcribed spacer sequences. *Applied and Environmental Microbiology* **68**: 1180-1191.

Rocap, G., F.W. Larimer, J. Lamerdin, S. Malfatti, P. Chain, N.A. Ahlgren, A. Arellano, M. Coleman, L. Hauser, W.R. Hess, Z.I. Johnson, M. Land, D. Lindell, A.F. Post, W. Regala, M. Shah, S.L. Shaw, C. Steglich, M.B. Sullivan, C.S. Ting, A. Tolonen, E.A. Webb, E.R. Zinser and S.W. Chisholm (2003). Genome divergence in two *Prochlorococcus* ecotypes reflects oceanic niche differentiation. *Nature* **424**: 1042-1047.

Rodriguez, F., J.F. Oliver, A. Marin and J.R. Medina (1990). The general stochastic model of nucleotide substitutions. *Journal of Theoretical Biology* **142**: 485-501.

Rodriguez, G.G., D. Phipps, K. Ishiguro and H.F. Ridgway (1992). Use of a fluorescent redox probe for direct visualization of actively respiring bacteria. *Applied and Environmental Microbiology* **58**: 1801-1808.

Roth, B.L., M. Poot, S.T. Yue and P.J. Millard (1997). Bacterial viability and antibiotic susceptibility testing with SYTOX green nucleic acid stain. *Applied and Environmental Microbiology* **63**: 2421-2431.

Schäfer, H. and G. Muyzer (2001). Denaturing gradient gel electrophoresis in marine microbial ecology. *Methods in Microbiology*. J.H. Paul (Ed). San Diego, Academic Press Ltd. **30:** 425-468.

Scherf, U., D.T. Ross, M. Waltham, L.H. Smith, J.K. Lee, L. Tanabe, K.W. Kohn, W.C. Reinhold, T.G. Myers, D.T. Andrews, D.A. Scudiero, M.B. Eisen, E.A. Sausville, Y. Pommier, D. Botstein, P.O. Brown and J.N. Weinstein (2000). A gene expression database for the molecular pharmacology of cancer. *Nature Genetics* **24**: 236-244.

Servais, P., H. Agogué, C. Courties, F. Joux and P. Lebaron (2001). Are the actively respiring cells (CTC+) those responsible for bacterial production in aquatic environments? *FEMS Microbiology Ecology* **35**: 171-179.

Servais, P., E.O. Casamayor, C. Courties, P. Catala, N. Parthuisot and P. Lebaron (2003). Activity and diversity of bacterial cells with high and low nucleic acid content. *Aquatic Microbial Ecology* **33**: 41-51.

Servais, P., C. Courties, P. Lebaron and M. Troussellier (1999). Coupling bacterial activity measurements with cell sorting by flow cytometry. *Microbial Ecology* **38**: 180-189.

Seymour, J.R., J.G. Mitchell and L. Seuront (2004). Microscale heterogeneity in the activity of coastal bacterioplankton communities. *Aquatic Microbial Ecology* **35**: 1-16.

Sherr, B.F., P. del Giorgio and E.B. Sherr (1999a). Estimating abundance and single-cell characteristics of respiring bacteria via the redox dye CTC. *Aquatic Microbial Ecology* **18**: 117-131.

Sherr, B.F., E.B. Sherr and J. McDaniel (1992). Effect of protozoan grazing on the frequency of dividing cells in bacterioplankton assemblages. *Applied and Environmental Microbiology* **58**: 2381-2385.

Sherr, E.B., B.F. Sherr and T.J. Cowles (2001). Mesoscale variability in bacterial activity in the Northeast Pacific Ocean off Oregon, USA. *Aquatic Microbial Ecology* **25**: 21-30.

Sherr, E.B., B.F. Sherr and C.T. Sigmon (1999b). Activity of marine bacteria under incubated and *in situ* conditions. *Aquatic Microbial Ecology* **20**: 213-223.

Sieracki, M.E., T.L. Cucci and J. Nicinski (1999). Flow cytometric analysis of 5-cyano-2,3-ditolyl tetrazolium chloride activity of marine bacterioplankton in dilution cultures. *Applied and Environmental Microbiology* **65**: 2409-2417.

Šimek, K., K. Hornák, M. Mašín, U. Christaki, J. Nedoma, M.G. Weinbauer and J.R. Dolan (2003). Comparing the effects of resource enrichment and grazing on a bacterioplankton community of a meso-eutrophic reservoir. *Aquatic Microbial Ecology* **31**: 123-135.

Šimek, K., J. Pernthaler, M.G. Weinbauer, K. Hornák, J.R. Dolan, J. Nedoma, M. Mašín and R. Amann (2001). Changes in bacterial community composition and dynamics and viral mortality rates associated with enhanced flagellate grazing in a mesoeutrophic reservoir. *Applied and Environmental Microbiology* **67**: 2723-2733.

Smith, D.C. and F. Azam (1992). A simple, economical method for measuring bacterial protein synthesis rates in sea water using ^{3}H-leucine. *Marine Microbial Food Webs* **6**: 107-114.

Smith, E.M. (1998). Coherence of microbial respiration rate and cell-specific bacterial activity in a coastal planktonic community. *Aquatic Microbial Ecology* **16**: 27-35.

Smith, E.M. and P.A. del Giorgio (2003). Low fractions of active bacteria in natural aquatic communities? *Aquatic Microbial Ecology* **31**: 203-208.

Smith, J.J. and G.A. McFeters (1997). Mechanisms of INT (2-(4-iodophenyl)-3-(4-nitrophenyl)-5-phenyl tetrazolium chloride), and CTC (5-cyano-2,3-ditolyl tetrazolium chloride) reduction in *Escherichia coli* K-12. *Journal of Microbiological Methods* **29**: 161-175.

Sokal, R.R. and F.J. Rohlf (1995). *Biometry*. New York, W. H. Freeman, New York.

Søndergaard, M. and M. Danielsen (2001). Active bacteria (CTC+) in temperate lakes: temporal and cross-system variations. *Journal of Plankton Research* **23**: 1195-1206.

Strickland, J.D.H. and T.R. Parsons, Eds. (1972). *A Practical Handbook of Seawater Analysis*. Fisheries Research Board of Canada. Ottawa.

Strub, P.T. and C. James (2003). Altimeter estimates of anomalous transports into the northern California Current during 2000–2002 (doi:10.1029/2003GL017513). *Geophysical Research Letters* **30**: 8025.

Suller, M.T.E. and D. Lloyd (1999). Fluorescence monitoring of antibiotic-induced bacterial damage using flow cytometry. *Cytometry* **35**: 235-241.

Suzuki, M.T. (1999). Effect of protistan bacterivory on coastal bacterioplankton diversity. *Aquatic Microbial Ecology* **20**: 261-272.

Swofford, D.L. (1998). PAUP*. Phylogenetic Analysis Using Parsimony (*and other methods). Version 4. Sunderland, MA, Sinauer Associates.

Thingstad, T.F. and R. Lignell (1997). Theoretical models for the control of bacterial growth rate, abundance, diversity and carbon demand. *Aquatic Microbial Ecology* **13**: 19-27.

Troussellier, M., H. Schäfer, N. Batailler, L. Bernard, C. Courties, P. Lebaron, G. Muyzer, P. Servais and J. Vives-Rego (2002). Bacterial activity and genetic richness along an estuarine gradient (Rhone River plume, France). *Aquatic Microbial Ecology* **28**: 13-24.

Ullrich, S., B. Karrasch and H.-G. Hoppe (1999). Is the CTC dye technique an adequate approach for estimating active bacterial cells? *Aquatic Microbial Ecology* **17**: 207-209.

Ullrich, S., B. Karrasch, H.-G. Hoppe, K. Jeskulke and M. Mehrens (1996). Toxic effects on bacterial metabolism of the redox dye 5-cyano-2,3-ditolyl tetrazolium chloride. *Applied and Environmental Microbiology* **62**: 4587-4593.

Urbach, E., K.L. Vergin and S.J. Giovannoni (1999). Immunochemical detection and isolation of DNA from metabolically active bacteria. *Applied and Environmental Microbiology* **65**: 1207-1213.

van Hannen, E.J., W. Mooij, M.P. van Agterveld, H.J. Gons and H.J. Laanbroek (1999a). Detritus-dependent development of the microbial community in an experimental system: qualitative analysis by denaturing gradient gel electrophoresis. *Applied and Environmental Microbiology* **65**: 2478-2484.

van Hannen, E.J., G. Zwart, M.P. van Agterveld, H.J. Gons, J. Ebert and H.J. Laanbroek (1999b). Changes in bacterial and eukaryotic community structure after mass lysis of filamentous cyanobacteria associated with viruses. *Appl. Environ. Microbiol.* **65**: 795-801.

Vaqué, D., E.O. Casamayor and J.M. Gasol (2001). Dynamics of whole community bacterial production and grazing losses in seawater incubations as related to the changes in the proportions of bacteria with different DNA content. *Aquatic Microbial Ecology* **25**: 163-177.

Veldhuis, M.J.W., G.W. Kraay and K.R. Timmermans (2001). Cell death in phytoplankton: correlation between changes in membrane permeability, photosynthetic activity, pigmentation and growth. *European Journal of Phycology* **36**: 167-177.

Venter, J.C., K. Remington, J.F. Heidelberg, A.L. Halpern, D. Rusch, J.A. Eisen, D. Wu, I. Paulsen, K.E. Nelson, W. Nelson, D.E. Fouts, S. Levy, A.H. Knap, M.W. Lomas, K. Nealson, O. White, J. Peterson, J. Hoffman, R. Parsons, H. Baden-Tillson, C. Pfannkoch, Y.-H. Rogers and H.O. Smith (2004). Environmental genome shotgun sequencing of the Sargasso Sea. *Science* **304**: 66-74.

Weinbauer, M.G. and F. Rassoulzadegan (2004). Are viruses driving microbial diversification and diversity? *Environmental Microbiology* **6**: 1-11.

Weinstein, J.N., T.G. Myers, P.M. O'Connor, S.H. Friend, A.J. Fornace, Jr., K.W. Kohn, T. Fojo, S.E. Bates, L.V. Rubinstein, N.L. Anderson, J.K. Buolamwini, W.W. van Osdol, A.P. Monks, D.A. Scudiero, E.A. Sausville, D.W. Zaharevitz, B. Bunow, V.N. Viswanadhan, G.S. Johnson, R.E. Wittes and

K.D. Paull (1997). An information-intensive approach to the molecular pharmacology of cancer. *Science* **275**: 343-349.

Wetz, M.S. and P.A. Wheeler (2003). Production and partitioning of organic matter during simulated phytoplankton blooms. *Limnology and Oceanography* **48**: 1808-1817.

Wetz, M.S. and P.A. Wheeler (2004). Response of bacteria to simulated upwelling phytoplankton blooms. *Marine Ecology Progress Series* **272**: 49-57.

Wheeler, P.A., A. Huyer and J. Fleischbein (2003). Cold halocline, increased nutrients and higher chlorophyll off Oregon in 2002 (doi:10.1029/2003GLO17395). *Geophysical Research Letters* **30**: 8021.

Whiteley, A.S., R.I. Griffiths and M.J. Bailey (2003). Analysis of the microbial functional diversity within water-stressed soil communities by flow cytometric analysis and CTC+ cell sorting. *Journal of Microbiological Methods* **54**: 257-267.

Williams, S.C., Y. Hong, D.C.A. Danavall, M.H. Howard-Jones, D. Gibson, M.E. Frischer and P.G. Verity (1998). Distinguishing between living and nonliving bacteria: evaluation of the vital stain propidium iodide and its combined use with molecular probes in aquatic samples. *Journal of Microbiological Methods* **32**: 225-236.

Wright, T.D., K.L. Vergin, P.W. Boyd and S.J. Giovannoni (1997). A novel δ-subdivision proteobacterial lineage from the lower ocean surface layer. *Applied and Environmental Microbiology* **63**: 1441-1448.

Yamaguchi, N. and M. Nasu (1997). Flow cytometric analysis of bacterial respiratory and enzymatic activity in the natural aquatic environment. *Journal of Applied Microbiology* **83**: 43-52.

ZoBell, C.E. (1946). *Marine Microbiology*. Waltham, MA, Chronica Botanica.

Zubkov, M.V., B.M. Fuchs, S.D. Archer, R.P. Kiene, R. Amann and P.H. Burkill (2001a). Linking the composition of bacterioplankton to rapid turnover of

dissolved dimethylsulphoniopropionate in an algal bloom in the North Sea. *Environmental Microbiology* **3**: 304-311.

Zubkov, M.V., B.M. Fuchs, S.D. Archer, R.P. Kiene, R. Amann and P.H. Burkill (2002a). Rapid turnover of dissolved DMS and DMSP by defined bacterioplankton communities in the stratified euphotic zone of the North Sea. *Deep-Sea Research II* **49**: 3017-3038.

Zubkov, M.V., B.M. Fuchs, P.H. Burkill and R. Amann (2001b). Comparison of cellular and biomass specific activities of dominant bacterioplankton groups in stratified waters of the Celtic Sea. *Applied and Environmental Microbiology* **67**: 5210-5218.

Zubkov, M.V., B.M. Fuchs, G.A. Tarran, P.H. Burkill and R. Amann (2002b). Mesoscale distribution of dominant bacterioplankton groups in the northern North Sea in early summer. *Aquatic Microbial Ecology* **29**: 135-144.

7 Appendix

7.1 Calibrations and method details

7.1.1 Chlorophyll regression

Chlorophyll concentrations were obtained from the raw fluorescence values from the SeaTech fluorometer. Discrete samples collected during the cruise were processed as discussed in Chapter 2. The chlorophyll *a* values from the discrete samples were plotted against raw fluorescence (Figure 7-1). Two different calibrations were necessary since the sensitivity of the SeaTech fluorometer was lowered after cast 114 due to the high chlorophyll values observed in shore at the end of the cruise. Model I linear regressions, which assume little error in the raw fluorescence, were used to calculate the appropriate variables. For the data from the first part of the cruise, a quadratic equation was a significant improvement over a linear equation (*F*-test to compare the fit of the higher model compared to the lower model (Zar 1999), $p<<0.0005$). The samples from the later part of the cruise were best fitted with a linear equation. The dotted lines in Figure 7-1 indicate the fitted values. The parameters from the lines were then used to convert the raw fluorescence data into chlorophyll concentrations for all the CTD casts.

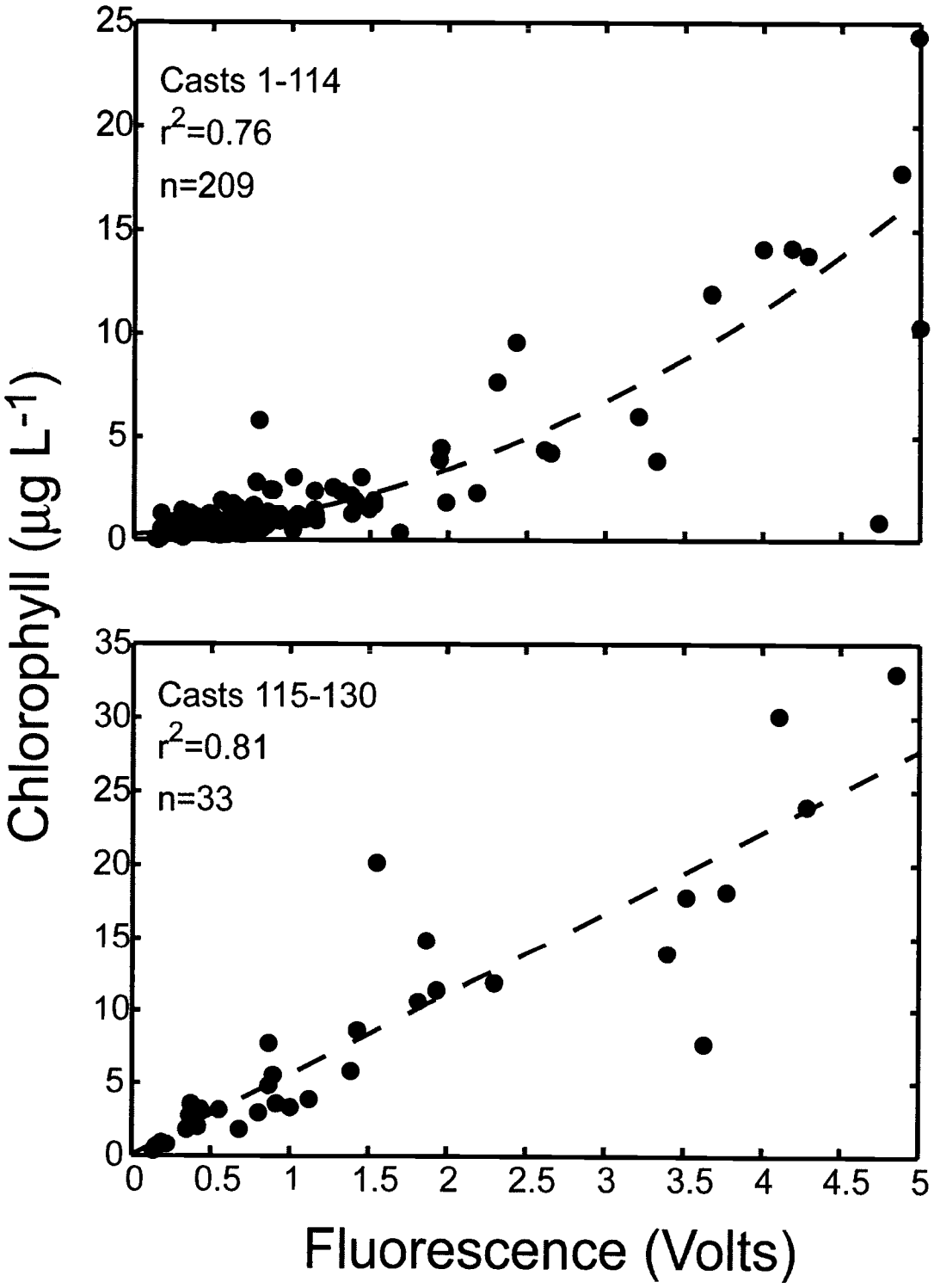

Figure 7-1.Raw fluorescence from the SeaTech fluorometer plotted against the chlorophyll values obtained from the discrete chlorophyll samples. Two different calibrations were done since the sensitivity of the fluorometer was changed after cast 114.

7.1.2 Defining regions on the cytograms from the flow cytometer

The regions on the cytograms defining the HNA and LNA cells are shown in Chapters 2 and 4, as are the regions for the CTC-positive cells. CTC-positive cells were defined with a combination of the cytograms of orange fluorescence (FL2) versus red fluorescence (FL3). However, the lower limits were defined on cytograms of side scatter versus orange fluorescence (Figure 7-2) and then gated out on cytograms of orange fluorescence versus red fluorescence.

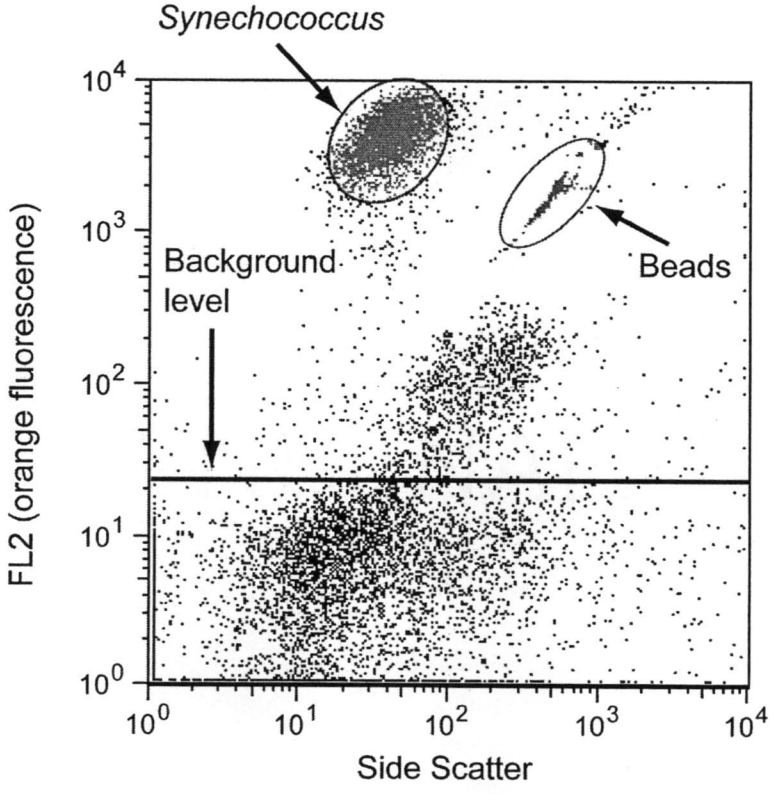

Figure 7-2. Example of cytogram of side scatter versus FL2 used to define the noise region for the CTC-positive cells. The points below the background level line indicated were logically gated out of the CTC-positive cell counts. *Synechococcus* was also observed as a separate population in the cytograms.

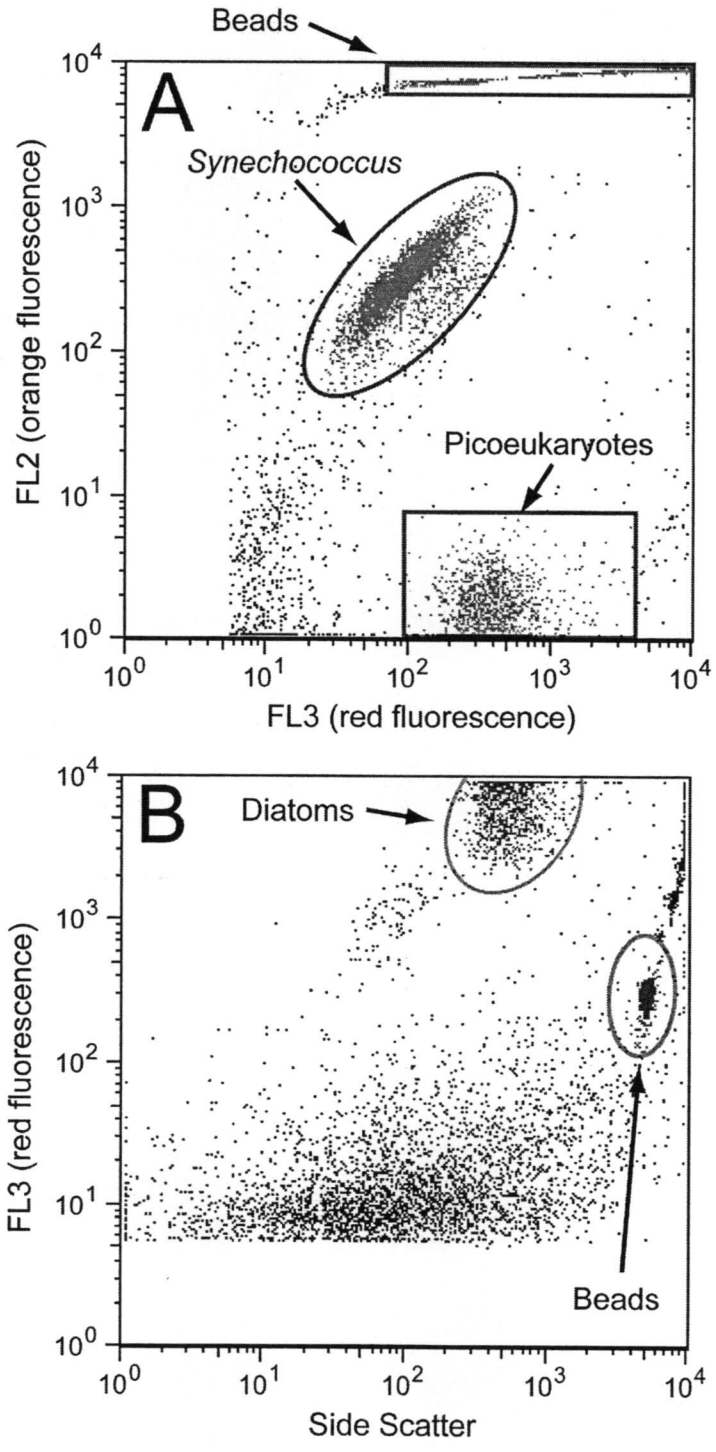

Figure 7-3. (A) shows the cytogram of FL3 versus FL2 used to define picoeukaryotes and *Synechococcus* while (B) shows a cytogram of side scatter versus FL3 from a different sample used to define diatoms.

Three different groups of phytoplankton were defined using the flow cytometer: diatoms, picoeukaryotes, and *Synechococcus*. *Prochlorococcus* cells were not observed in any of the samples. Cytograms of FL3 (red) fluorescence versus FL2 (orange) fluorescence were used to count *Synechococcus* and picoeukaryotes (Figure 7-3A), while cytograms of side scatter versus FL3 fluorescence were used to count diatoms (Figure 7-3B).

7.2 Data collected

7.2.1 Sample log

The information regarding the discrete samples is given in Table 7-1. The table indicates the location for each sampling cast, the date and time of the cast, and the numbers used to label each of the discrete samples. Discrete samples were taken for nutrients, chlorophyll (used for both chlorophyll *a* and pheopigments), flow cytometer counts (FCM, used to count heterotrophic and autotrophic cells), CTC samples, and bacterial leucine incorporation samples (BP in the table). Data for these samples are available on request.

CTD data for all the casts are also available and include the following parameters: pressure, temperature, salinity, potential temperature, sigma-t, specific volume anomaly, dynamic height, fluorescence (in volts), percent transmission, oxygen, meters above the bottom, and photosynthetically available radiation (PAR).

Table 7-1. Summary of discrete sample data collected during the spring 2002 sampling cruise on the R/V *Wecoma*. Samples were collected from a total of 130 casts. The numbers in the discrete sample columns indicate the sample number to reference in order to obtain the raw data.

				GMT		Discrete samples				
Cast	**Station**	**Lat (°N)**	**Long (°W)**	**Date**	**Time**	**Nutrients**	**Chlorophyll**	**FCM**	**CTC**	**BP**
1	NH5	44 39.145	124 10.575	04/26/02	2012	1-2	1-2	1-2		
2	NH10	44 39.003	124 17.664	04/26/02	2114	3-5	3-5	3-5		
3	NH15	44 39.007	124 24.671	04/26/02	2209	6-7	6-7	6-7		
4	NH25	44 39.097	124 38.984	04/26/02	2328	8-9	8-9	8-9		
5	NH35	44 39.086	124 53.016	04/27/02	0103	10-11	10-11	10-11		
6	NH45	44 39.055	125 06.924	04/27/02	0245	12-13	12-13	12-13		
7	NH65	44 39.069	125 35.922	04/27/02	0529	14-15	14-15	14-15		
8	NH127	44 39.097	127 06.025	04/27/02	1710	16-17	16-19	16-18		1-16,51-98,151-198,311-358
9	NH127	44 39.086	127 06.023	04/27/02	2025		20-21	20-21		
10	NH127	44 39.102	127 05.979	04/27/02	2133	22-26	22	22-26	22-26	18-29
11	NH127	44 39.100	127 06.012	04/27/02	2316		27			
12	NH127	44 39.089	127 05.996	04/28/02	0134		28			
13	NH127	44 38.076	127 05.092	04/28/02	1230	29-33	29-33	29-33		31-50

Cast	Station	Lat (°N)	Long (°W)	Date	Time	Nutrients	Chlorophyll	FCM	CTC	BP
14	NH127	44 39.097	127 06.009	04/28/02	1510	34-39	38-39	34-39	34-39	
15	NH127	44 39.108	127 06.005	04/28/02	2004		40			
16	NH127	44 39.088	127 06.010	04/28/02	2220	42	42,44,46	41-47		99-126
17	NH127	44 39.131	127 05.999	04/29/02	0330			48-53		127-150
18	NH127	44 39.098	127 05.986	04/29/02	1620	54	54	54		
19	NH127	44 39.081	127 05.992	04/29/02	1924	55-59,61-65	59,63,65	55-59,61-65	55-59	219-254
20	NH127	44 39.075	127 05.965	04/29/02	2227		67			
21	NH127	44 39.104	127 05.992	04/30/02	0342		76	68-76		255-290
22	NH127	44 39.065	127 05.986	04/30/02	1235	78,80	78-82	78-82		291-310
23	NH35	44 39.104	124 52.991	05/01/02	0120	83	83	83		359-362
24	NH35	44 39.099	124 53.005	05/01/02	0310	84-88	84-88	84-88		363-383
25	NH35	44 39.106	124 53.007	05/01/02	1410	89	89	89		
26	NH35	44 39.113	124 52.978	05/01/02	1603	90	90	90		
27	NH35	44 39.094	124 53.002	05/01/02	1906	91	91	91		
28	NH35	44 39.099	124 53.003	05/01/02	2020	92-95	92-96	92-95	92-94	383-398
29	NH35	44 39.096	124 53.011	05/02/02	0206	97	97	97		
30	NH35	44 39.076	124 53.033	05/02/02	0333	98-101	98-102	98-101		399-414
31	NH35	44 38.562	124 53.008	05/02/02	1230	103-108	103-108	103-108	103-105	435-454,455-458

Cast	Station	Lat (N)	Long (W)	Date	Time	Nutrients	Chlorophyll	FCM	CTC	BP
32	NH35	44 39.099	124 52.986	05/02/02	1409					
33	NH10	44 39.078	124 17.726	05/02/02	1757					
34	NH5	44 39.081	124 10.607	05/02/02	1900	109-110	109-110	109-110		459-474,511-558,595-642,687-734
35	NH5	44 39.105	124 10.598	05/02/02	2041	111-113	111-113	111-113	111-113	475-486
36	NH5	44 39.105	124 10.599	05/02/02	2216	114	114	114		
37	NH5	44 39.092	124 10.609	05/03/02	0330	115-117	115-117	115-117	115-117	487-498
38	NH5	44 39.102	124 10.574	05/03/02	1535	118	118-119	118		
39	NH5	44 39.071	124 10.632	05/03/02	1921	120-122	120-122	120-122		499-510
40	NH5	44 39.086	124 10.614	05/03/02	2300	123	123	123		
41	NH5	44 39.085	124 10.532	05/04/02	0330	124-126	124-126	124-126		559-570
42	NH5	44 39.077	124 10.619	05/04/02	1235	127-129	127-133	127-129	127-129	571-582
43	NH5	44 39.080	124 10.578	05/04/02	1459	134	134	134		
44	NH5	44 39.064	124 10.618	05/04/02	1930	135-137	135-137	135-137	135-137	667-686
45	NH5	44 39.116	124 10.586	05/05/02	0330	138-140	138-140	138-140	138-140	643-654
46	NH5	44 39.091	124 10.514	05/05/02	0800	141-143	143	141-143	141-143	655-666
47	NH5	44 39.072	124 10.586	05/06/02	2115	144-145	144-145	144-145		
48	NH10	44 39.040	124 17.713	05/06/02	2205	146-147	146-147	146-147		

Cast	Station	Lat (N)	Long (W)	Date	Time	Nutrients	Chlorophyll	FCM	CTC	BP
49	NH15	44 39.097	124 24.730	05/06/02	2255	148-149	148-149	148-149		
50	NH25	44 39.061	124 38.986	05/07/02	0008	150-151	150-151	150-151		
51	NH35	44 39.091	124 53.018	05/07/02	0128	152-153	152-153	152-153		
52	NH127	44 39.087	127 05.916	05/07/02	1221	154-156	154-159	154-159		735-758
53	NH127	44 39.094	127 06.003	05/07/02	1628	160	160	160	160	
54	NH127	44 39.110	127 05.992	05/07/02	1930	161	161	161	161	
55	NH127	44 39.100	127 06.00	05/07/02	2303	162		162		
56	NH127	44 39.095	127 05.978	05/08/02	0329	163-167	164-167	163-167		795-810
57	NH127	44 39.099	127 05.991	05/08/02	1600	168	168	168	168	
58	NH127	44 39.094	127 05.992	05/08/02	1757	169	169	169	169	
59	NH127	44 39.082	127 05.992	05/08/02	1923	170-174	174	170-174	170-174	899-910
60	NH127	44 39.102	127 05.993	05/09/02	0344	175-179	177-179	175-179	175-179	931-950
61	NH127	44 39.087	127 05.990	05/09/02	1223	180-182	180-182	180-182		967-978
62	NH127	44 39.084	127 05.979	05/09/02	1559	183	183	183		
63	NH127	44 39.091	127 05.991	05/09/02	1802	184	184	184		
64	NH127	44 39.100	127 06.002	05/09/02	1927	185-187	187	185-187	185-187	1011-1022
65	NH127	44 39.107	127 06.006	05/10/02	0341	188-190	188-190	188-190		1079-1090
66	NH85	44 39.102	126 03.044	05/10/02	1224	191-193	191-193	191-193	191-193	1143-1154
67	NH85	44 39.086	126 02.993	05/10/02	1556	194	194	194	914	

Cast	Station	Lat (N)	Long (W)	Date	Time	Nutrients	Chlorophyll	FCM	CTC	BP
68	NH85	44 39.100	126 03.001	05/10/02	1802	195	195	195	195	
69	NH85	44 39.104	126 03.020	05/10/02	1930	196-198	196-198	196-198	196-198	1297-1308
70	NH85	44 39.097	126 03.027	05/10/02	2323	199		199		
71	NH85	44 39.096	126 02.932	05/11/02	0216	200	200	200		
72	NH85	44 39.082	126 03.000	05/11/02	0340	201-206	204-206	201-206	201-206	1417-1428
73	NH85	44 39.068	126 03.013	05/11/02	0528	207		207		
74	NH65	44 39.083	125 35.972	05/11/02	1218	208-211	208-211	208-211	208-211	1429-1440
75	NH65	44 39.096	125 36.002	05/11/02	1918	212-216	212-215	212-216		1449-1460,1513-1520
76	NH65	44 39.093	125 35.996	05/11/02	2030	218		218		
77	NH65	44 39.061	125 35.993	05/11/02	2159	219		219		
78	NH65	44 39.083	125 35.999	05/12/02	0101	220		220		
79	NH65	44 39.095	125 36.015	05/12/02	0345	221-228	224-228	221-228		1725-1744
80/81[1]	NH55	44 39.076	125 21.898	05/12/02	1217	229-231	229-231	229-231		1885-1896
82	NH55	44 39.087	125 22.022	05/12/02	1558	232	232	232	232	
83	NH55	44 39.044	125 22.005	05/12/02	1658	233	233	233	233	
84	NH55	44 39.102	125 22.006	05/12/02	1928	234-236	234-236	234-236		1913-1924
85	NH55	44 39.107	125 21.977	05/13/02	0343	237-244	241-244	237-244		1945-1972

Cast	Station	Lat (N)	Long (W)	Date	Time	Nutrients	Chlorophyll	FCM	CTC	BP
86	NH45	44 39.100	125 06.995	05/13/02	1219	245-246	245-246	245-246	245-246	2095-2106
87	NH45	44 39.109	125 07.040	05/13/02	1602	248	248	248	248	
88	NH45	44 39.097	125 06.997	05/13/02	1700	249	249	249	249	
89	NH45	44 39.102	125 07.013	05/13/02	1930	250-252	250-252	250-252		2139-2150
90	NH45	44 39.105	125 06.964	05/13/02	2022	253	253	253		
91	NH45	44 39.091	125 06.952	05/13/02	2154	254		254		
92	NH45	44 39.086	125 06.991	05/14/02	0116	255		255		
93	NH45	44 39.100	125 07.007	05/14/02	0345	256-260	257,259-260	256-260		2171-2190
94	NH35	44 39.139	124 53.063	05/14/02	1215	261-263	261-263	261-263	261-263	2207-2218
95	NH35	44 39.106	124 53.003	05/14/02	1557	264	264	264	264	
96	NH35	44 39.097	124 52.997	05/14/02	1700	265	265	265	265	
97	NH35	44 39.087	124 53.004	05/14/02	1930	266-268	266-270	266-268		2271-2282
98	NH35	44 39.078	124 53.025	05/15/02	0342	271-275	273-275	271-275		2283-2294
99	NH35	44 39.083	124 52.993	05/15/02	1220	276-278	276-278	276-278	276-278	2311-2322
100	NH35	44 39.091	124 52.992	05/15/02	1558			279-281		
101	NH35	44 39.096	124 53.014	05/15/02	1929	282-287	282-289	282-287	282-284	2367-2370,2481-2508
102	NH35	44 39.099	124 52.989	05/16/02	0345	290-292	290-292	290-292		2497-2508

Cast	Station	Lat (N)	Long (W)	Date	Time	Nutrients	Chlorophyll	FCM	CTC	BP
103	NH25	44 39.099	124 38.968	05/16/02	1219	293-295	293-295	293-295		2529-2540
104	NH25	44 39.077	124 38.975	05/16/02	1555	296	296	296	296	
105	NH25	44 39.103	124 38.997	05/16/02	1700	297	297	297	297	
106	NH25	44 39.098	124 39.002	05/16/02	1930	298-301	298-303	298-301		2585-2608
107	NH25	44 39.096	124 39.046	05/16/02	2330			304-307		
108	NH25	44 39.096	124 39.008	05/17/02	0343	308-311	308-311	308-311		2609-2624
109	NH15	44 39.083	124 24.747	05/17/02	1217	312-314	312-314	312-314	312-314	2677-2688
110	NH15	44 39.092	124 24.706	05/17/02	1558	315-316	315-316	315-316	315-316	
111	NH15	44 39.097	124 24.711	05/17/02	1655	317	317	317	317	
112	NH15	44 39.107	124 24.695	05/17/02	1930	318-322	318-324	318-322		2749-2768
113	NH15	44 39.088	124 24.639	05/17/02	2331		327	325-328		
114	NH15	44 39.086	124 24.704	05/18/02	0014	329	329	329		
115	NH15	44 39.095	124 24.697	05/18/02	0345	332-335	332-335	330-335		2797-2816
116	NH10	44 39.174	124 17.651	05/18/02	1219	336-338	336-338	336-338	336-338	2841-2852
117	NH10	44 39.107	124 17.712	05/18/02	1603	339	339	339	339	
118	NH10	44 39.097	124 17.725	05/18/02	1710	340	340	340	340	
119	NH10	44 39.086	124 17.694	05/18/02	1930	341-344	341-346	341-344		2940-2952
120	NH10	44 39.174	124 17.694	05/18/02	2334		348-350	347-350		
121	NH10	44 39.098	124 17.207	05/19/02	0021	351	351	351		

Cast	Station	Lat (N)	Long (W)	Date	Time	Nutrients	Chlorophyll	FCM	CTC	BP
122	NH10	44 39.116	124 17.698	05/19/02	0345	352-356	352-356	352-356		2953-2972
123/124[1]	NH5	44 39.279	124 10.512	05/19/02	1235	357-359	357-359	357-359		3017-3028
125	NH5	44 39.092	124 10.605	05/19/02	1558	360	360	360	360	
126	NH5	44 39.099	124 10.598	05/19/02	1700	361	361	361		
127	NH5	44 39.093	124 10.572	05/19/02	1930	362-365	362-367	362-365	362-364	3089-3112
128	NH5	44 39.033	124 10.602	05/20/02	0345	368-371	368-371	368-371	368-371	3113-3128
129	NH10	44 39.106	124 17.703	05/20/02	1600			372-275		
130	NH10	44 39.105	124 17.705	05/20/02	1726			376-379		

[1]Casts 81 and 124 were conducted immediately after casts 80 and 123 respectively. The surface niskins for both casts had not been fired prior to removing the rosette from the water, therefore the rosette was placed back into the water before any of the other niskins had been opened. The casts were grouped together since the samples from the second cast are considered as part of the initial cast.

7.2.2 Raw data for the sorted ^{3}H-leucine labeled cells

The raw data for the SYBR-stained samples discussed in Chapter 2 are given in Table 7-2. The table shows the disintegrations per minute (DPM) for the four different sort groups (total cells, HNA cells, LNA cells, and CTC-positive cells). In addition, the values for the control region are given as background values in the table. For the instances when multiple sorts were conducted, the value in the table is the mean of the multiple sorts. The raw data for the CTC-positive sorts are given in Table 7-3. As for the SYBR-stained samples, the data are given as DPM for the CTC-positive region and for the background cells. For both the SYBR-stained samples and CTC-positive samples, the number of cells sorted is also given. "FCM" refers to the sample number, which is also listed in Table 7-1. Note that different number of cells were sorted for the noise region in the CTC-positive samples. Therefore, the noise was normalized to the noise per particle and then multiplied by the number of particles sorted for the sample region.

Table 7-2. Raw data for Chapter 2 for the SYBR-stained cells sorted on the flow cytometer. Samples were incubated with ^{3}H-leucine immediately following sample collection and kept frozen until sample processing back on shore. FCM refers to the sample number.

	RawDPM				Cells sorted			
FCM	Total cells	HighNA	LowNA	background	Total cells	HighNA	LowNA	background
037	118.47	135.18	96.02	30.29	1.00E+05	1.00E+05	1.00E+05	1.00E+05
038	215.65	254.13	156.59	26.41	1.00E+05	1.00E+05	1.00E+05	1.00E+05
039	723.64	987.26	588.86	47.37	1.00E+05	1.00E+05	1.00E+05	1.00E+05
055	88.88	94.4	78.34	37.91	1.00E+05	1.00E+05	1.00E+05	1.00E+05
056	72.15	116.09	118.54	32.66	1.00E+05	1.00E+05	1.00E+05	1.00E+05
057	75.56	148.82	82.39	29.55	1.00E+05	1.00E+05	1.00E+05	1.00E+05
058	161.55	222.72	95.57	29.7	1.00E+05	1.00E+05	1.00E+05	1.00E+05
059	329.95	413.18	283.24	35.33	1.00E+05	1.00E+05	1.00E+05	1.00E+05
092	379.15	689.52	188.62	38.12	1.00E+05	1.00E+05	1.00E+05	1.00E+05
093	1869.58	1497.93	1271.6	94.85	1.00E+05	1.00E+05	1.00E+05	1.00E+05
094	4904.61	5270.87	1410.21	146.8	1.00E+05	1.00E+05	1.00E+05	1.00E+05
103	204.8	295.69	140.55	35.57	1.00E+05	1.00E+05	1.00E+05	1.00E+05
104	518.75	1042.56	577.98	63.46	1.00E+05	1.00E+05	1.00E+05	1.00E+05
105	2926.07	4400.37	1947.79	60.71	1.00E+05	1.00E+05	1.00E+05	1.00E+05
127	171.41	255.88	438.81	37.12	1.00E+05	1.00E+05	1.00E+05	1.00E+05

Table 7-2, continued

FCM	RawDPM Total cells	HighNA	LowNA	background	Cells sorted Total cells	HighNA	LowNA	background
128	391.66	413.49	200.49	34.13	1.00E+05	1.00E+05	1.00E+05	1.00E+05
129	2429.99	2525.53	1908.36	130.3	1.00E+05	1.00E+05	1.00E+05	1.00E+05
135	351.35	778.33	627.45	37.79	1.00E+05	1.00E+05	1.00E+05	1.00E+05
136	560.17	874.06	434.39	44.55	1.00E+05	1.00E+05	1.00E+05	1.00E+05
137	2896.14	3741.71	1881.95	146.53	1.00E+05	1.00E+05	1.00E+05	1.00E+05
138	303.06	621.93	395.69	40.58	1.00E+05	1.00E+05	1.00E+05	1.00E+05
139	351.78	603.51	383.26	74.91	1.00E+05	1.00E+05	1.00E+05	1.00E+05
140	6710.71	8218.13	5223.89	312.62	1.00E+05	1.00E+05	1.00E+05	1.00E+05
141	470.49	668.62	205.68	59.94	1.00E+05	1.00E+05	1.00E+05	1.00E+05
142	467.03	709.79	403.82	51.5	1.00E+05	1.00E+05	1.00E+05	1.00E+05
143	4950.68	5217.5	2758.2	232.42	1.00E+05	1.00E+05	1.00E+05	1.00E+05
185	118.4	112.21	120.05	60.81	1.00E+05	1.00E+05	1.00E+05	1.00E+05
186	260.4	347.87	242.86	34.97	1.00E+05	1.00E+05	1.00E+05	5.44E+04
187	807.42	1072.55	554.77	48.45	1.00E+05	1.00E+05	1.00E+05	9.00E+04
282	1046.39	1159.73	699.52	108.93	1.00E+05	1.00E+05	1.00E+05	1.00E+05
283	1088.99	1485.26	1061.72	89.05	1.00E+05	1.00E+05	1.00E+05	1.00E+05
284	3286.69	200.37	1458.14	95.23	1.00E+05	1.00E+05	1.00E+05	1.00E+05
362	1572.35	1630.2	690.32	71.64	1.00E+05	1.00E+05	1.00E+05	1.00E+05
363	3029.26	9273.9	1747.59	300.07	1.00E+05	1.00E+05	1.00E+05	1.00E+05
364	13755.41	14519.97	3370.65	324.42	1.00E+05	1.00E+05	1.00E+05	1.00E+05

Table 7-3. Raw data for the CTC-positive cells labeled with ^{3}H-leucine and sorted as discussed in Chapter 2.

	DPM		Cells sorted	
FCM	**CTC-positive**	**NoiseCTC**	**CTC-positive**	**NoiseCTC**
037	122.04	96.2	2.00E+04	2.00E+04
038	111.25	63.44	2.00E+04	2.00E+04
039	1539.8	324.21	1.00E+05	1.00E+05
055	525.15	277.48	1.00E+05	1.00E+05
056	407.05	216.36	1.00E+05	1.00E+05
057	403.69	356.67	1.00E+05	1.00E+05
058	491.91	239.04	1.00E+05	1.00E+05
059	1039.7	293.97	1.00E+05	1.00E+05
092	140.76	69.77	2.00E+04	2.00E+04
093	480.98	129.81	2.00E+04	2.00E+04
094	640	121.34	2.00E+04	2.00E+04
103	154.94	78.56	5.00E+04	5.00E+04
104	540.43	94.55	2.00E+04	2.00E+04
105	673.88	95.17	2.00E+04	2.00E+04
127	88.76	42.47	2.00E+04	2.00E+04
128	167.9	45.65	2.00E+04	2.00E+04
129	278.44	46	2.00E+04	2.00E+04
135	180.4	45.9	2.00E+04	2.00E+04
136	215.54	50.54	2.00E+04	2.00E+04
137	669.62	64.87	2.00E+04	2.00E+04
138	93.72	43.43	2.00E+04	2.00E+04
139	226.84	44.92	2.00E+04	2.00E+04
140	954.03	126.27	2.00E+04	2.00E+04
141	112.5	44.7	2.00E+04	2.00E+04
142	323.72	50.02	1.00E+04	3.00E+04
143	364.24	212.72	1.00E+04	3.00E+04

Table 7-3, continued

	DPM		Cells sorted	
FCM	**Level2**	**NoiseCTC**	**Level2**	**NoiseCTC**
185	176.9	142.05	1.00E+05	1.00E+05
186	321.34	195.25	1.00E+05	1.00E+05
187	951.33	210.93	3.69E+04	1.00E+05
282	255.67	97.76	1.00E+04	2.00E+04
283	487.87	79.18	1.00E+04	2.00E+04
284	712.96	61.24	5.00E+03	1.00E+04
362	677.95	49.91	2.00E+04	2.00E+04
363	4226.5	205.6	2.00E+04	2.00E+04
364	6330.5	358.32	2.00E+04	1.00E+05

7.2.3 DGGE data and diversity of sequences obtained from the DGGE bands

The phylogenetic affiliation of each sequence obtained from a DGGE band was initially determined by BLAST searches. Following the BLAST searches, maximum likelihood trees were calculated using almost full length 16S rRNA genes closely related to the DGGE sequences. Additional 16S rRNA gene sequences were added to the maximum likelihood trees to make trees with sequences representing different Classes and Orders within the tree. Once a maximum likelihood tree was established in ARB, the DGGE sequences were added to the trees using the parsimony option in ARB. A mask of conserved regions was used to define which regions of the almost full-length sequence were considered in insertion of the sequences from the DGGE bands. The maximum likelihood trees are given here in the Appendix and the results summarized in Chapter 4. Note that some of the DGGE bands were sequenced more than once to confirm their phylogenetic identity. Therefore, the number of sequences in the trees presented in the Appendix is greater than the number of sequences presented in Chapter 4 where all duplicate sequences have been removed.

Table 7-4. Key to the labels in the maximum likelihood trees used to define the phylogenetic group for each sequence obtained from the DGGE bands. The table lists the family, genus, or environmental cluster listed in Table 4-2 and the corresponding label used in the trees shown on the following pages.

Family, Genus, or environmental cluster	**Label in tree**
Family *Flavobacteriaceae*, Genus *Polaribacter*	*Bacteroidetes* 3
Family *Saprospiraceae*	*Bacteroidetes* 10
Delaware cluster 1	*Bacteroidetes* 1
Delaware cluster 2	*Bacteroidetes* 2
ZD0203 from the North Sea	*Bacteroidetes* 5
agg58 Branch 2	*Bacteroidetes* 7
unaffiliated *Cytophaga*	*Bacteroidetes* 6
Order *Rhodospiralles*	*Alphaproteobacteria* 6
Family *Rhodobacteraceae*, Genus *Roseobacter*	*Alphaproteobacteria* 1
SAR11 cluster	*Alphaproteobacteria* 7
Family *Bradyrhizobiaceae*, Genus *Afipia*	*Alphaproteobacteria* 5
Family *Methylobacteriaceae*	*Alphaproteobacteria* 8
Family *Burkholderiaceae*, Genus *Burkholderia*	*Betaproteobacteria* 3
Family *Ralstoniaceae*	*Betaproteobacteria* 4
Family *Comamonadaceae*	*Betaproteobacteria* 2
Family *Hydrogenophilaceae*	*Betaproteobacteria* 5
Family *Rhodocyclaceae*	*Betaproteobacteria* 1
Bano & Hollibaugh 'Cluster A'	*Gammaproteobacteria* 1
Family *Alteromonadaceae*, Genus *Marinobacterium*	*Gammaproteobacteria* 12
Family *Moraxellaceae*, Genus *Psychrobacter*	*Gammaproteobacteria* 3
Family *Moraxellaceae*, Genus *Acinetobacter*	*Gammaproteobacteria* 9
Family *Pseudomonadaceae*, Genus *Pseudomonas*	*Gammaproteobacteria* 7
SAR86 / OCS5 cluster	*Gammaproteobacteria* 2
Arctic96B-16 cluster	*Gammaproteobacteria* 4
OM60	*Gammaproteobacteria* 5
SAR92	*Gammaproteobacteria* 6
agg47/KTc1113	*Gammaproteobacteria* 8

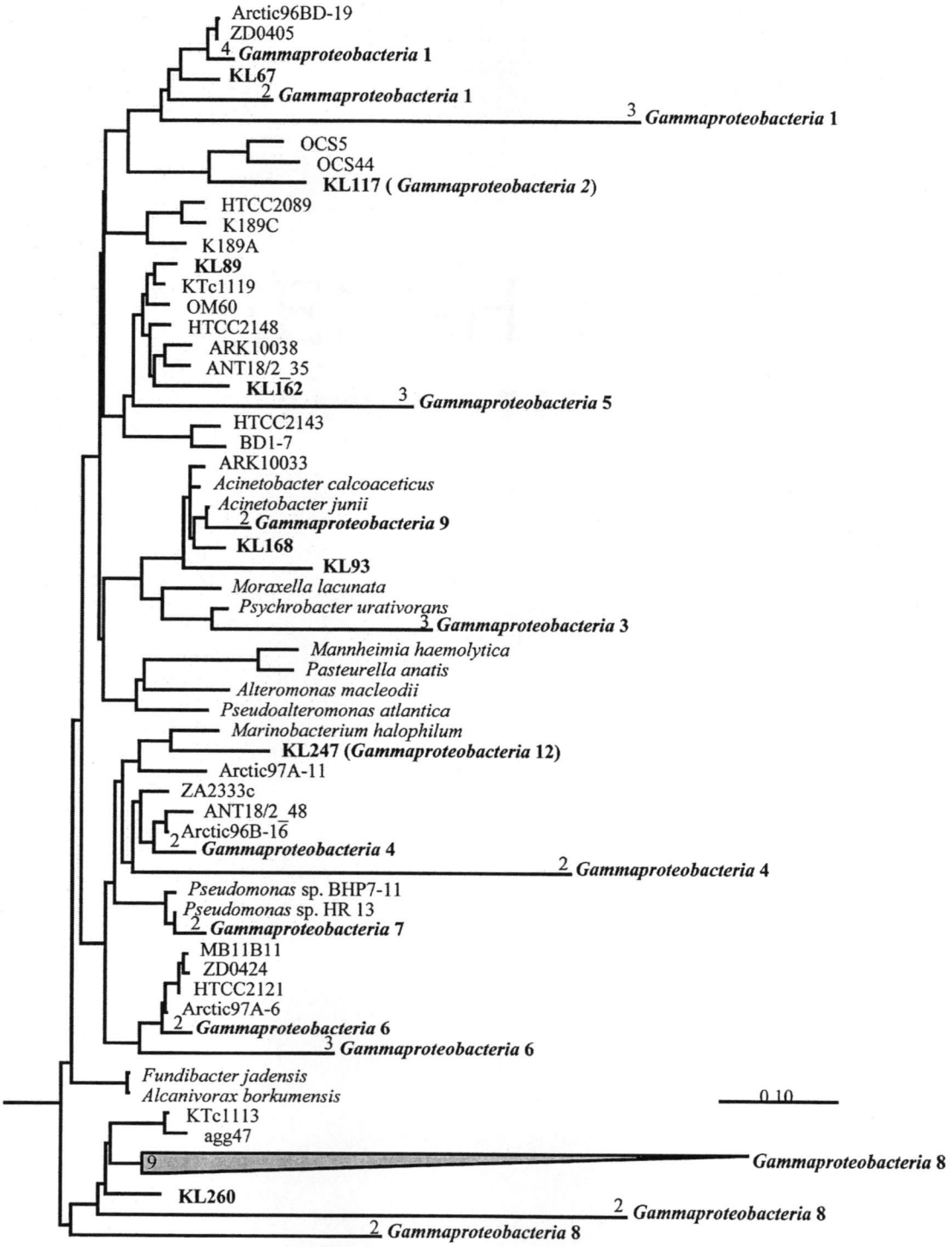

Figure 7-4 Maximum likelihood tree of the *Gammaproteobacteria* with the DGGE bands obtained from samples collected off the Oregon coast. The DGGE bands from this study are shown in bold type. The sequences have been grouped within the figure where possible to ease the viewing of the figure. The outgroup was five sequences from members of the *Alphaproteobacteria*.

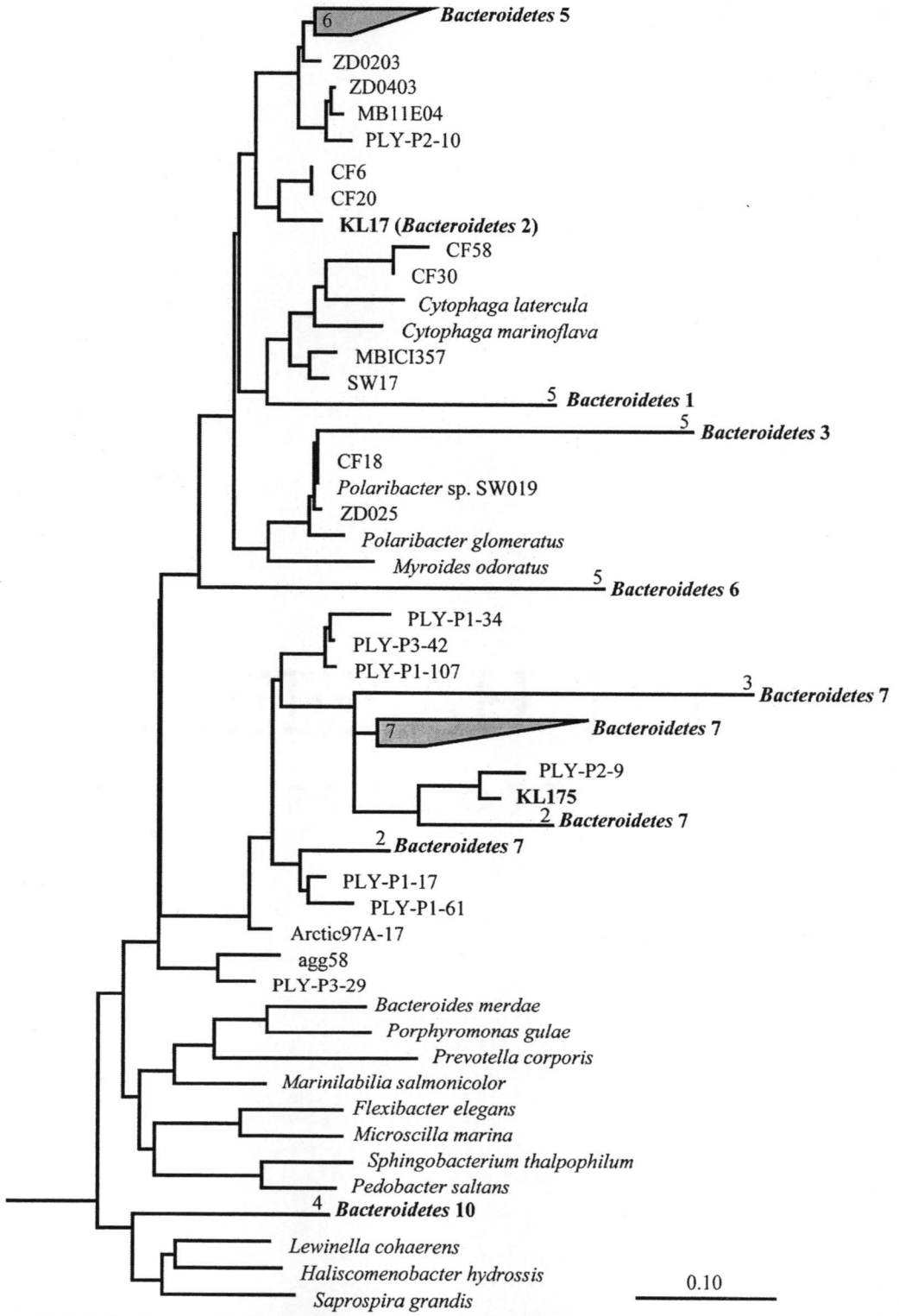

Figure 7-5. Maximum likelihood tree of the sequences obtained from the DGGE bands and representatives from the phylum *Bacteroidetes*, although all of the sequences from this project cluster within the classes *Flavobacteria* and *Sphingobacteria*. The outgroup contained two sequences from the cyanobacteria.

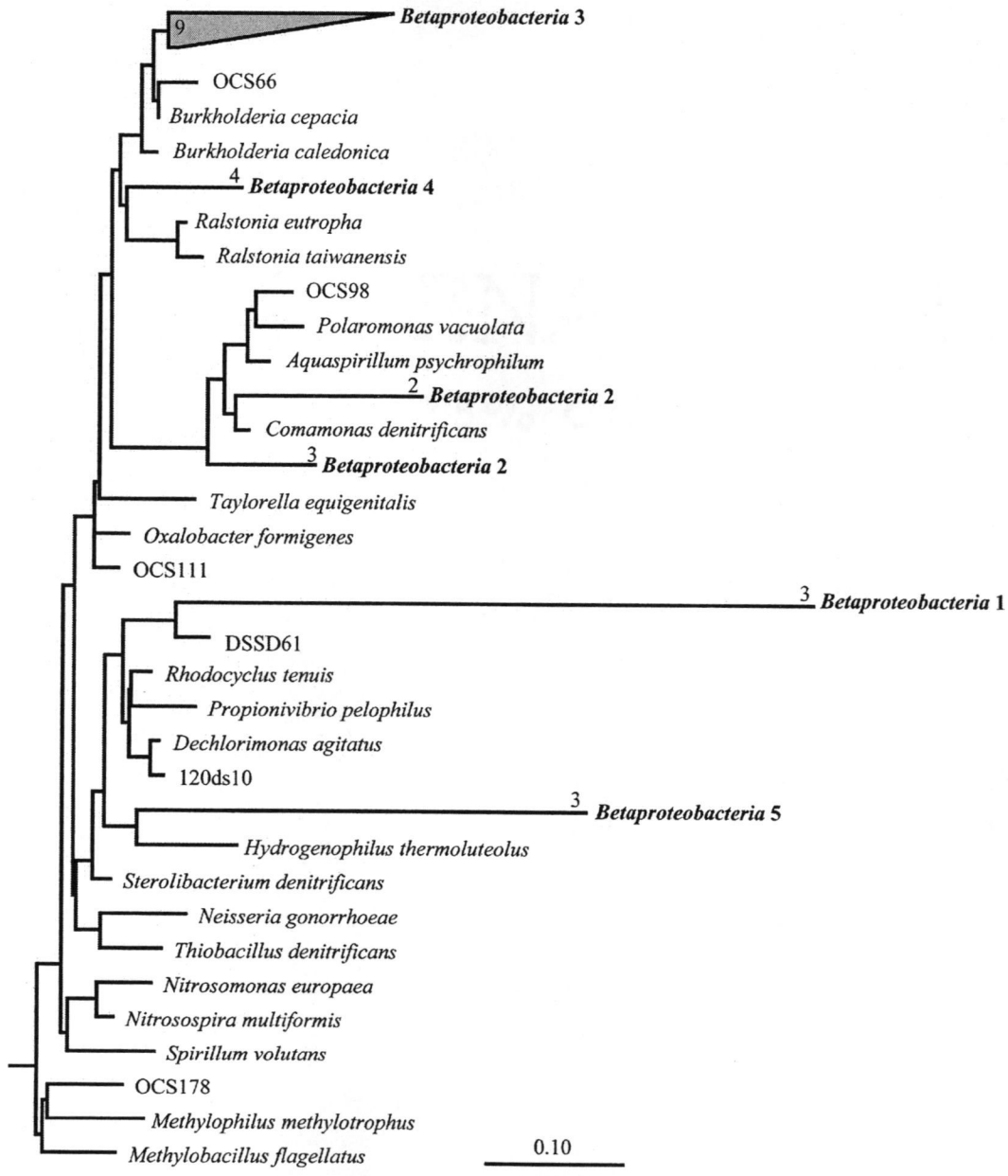

Figure 7-6 Maximum likelihood tree of the *Betaproteobacteria* and representatives from different orders within the *Betaproteobacteria* and the sequences obtained from the DGGE bands. Three sequences from the *Alphaproteobacteria* and *Gammaproteobacteria* were used as the outgroup.

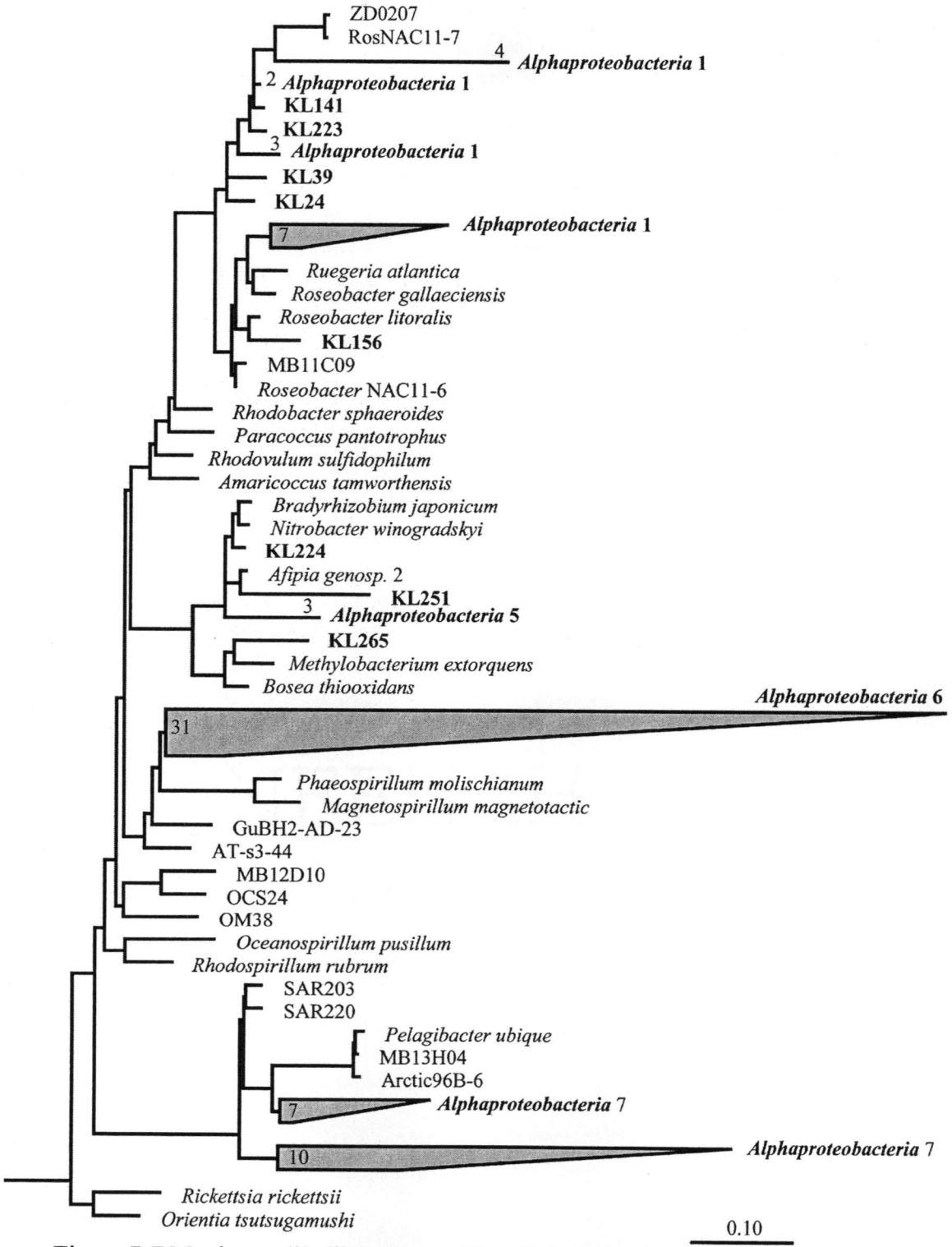

Figure 7-7 Maximum likelihood tree of the *Alphaproteobacteria* with the sequences obtained from the DGGE bands and representatives of different orders within the *Alphaproteobacteria*. Five sequences from the *Betaproteobacteria* were used as the outgroup.

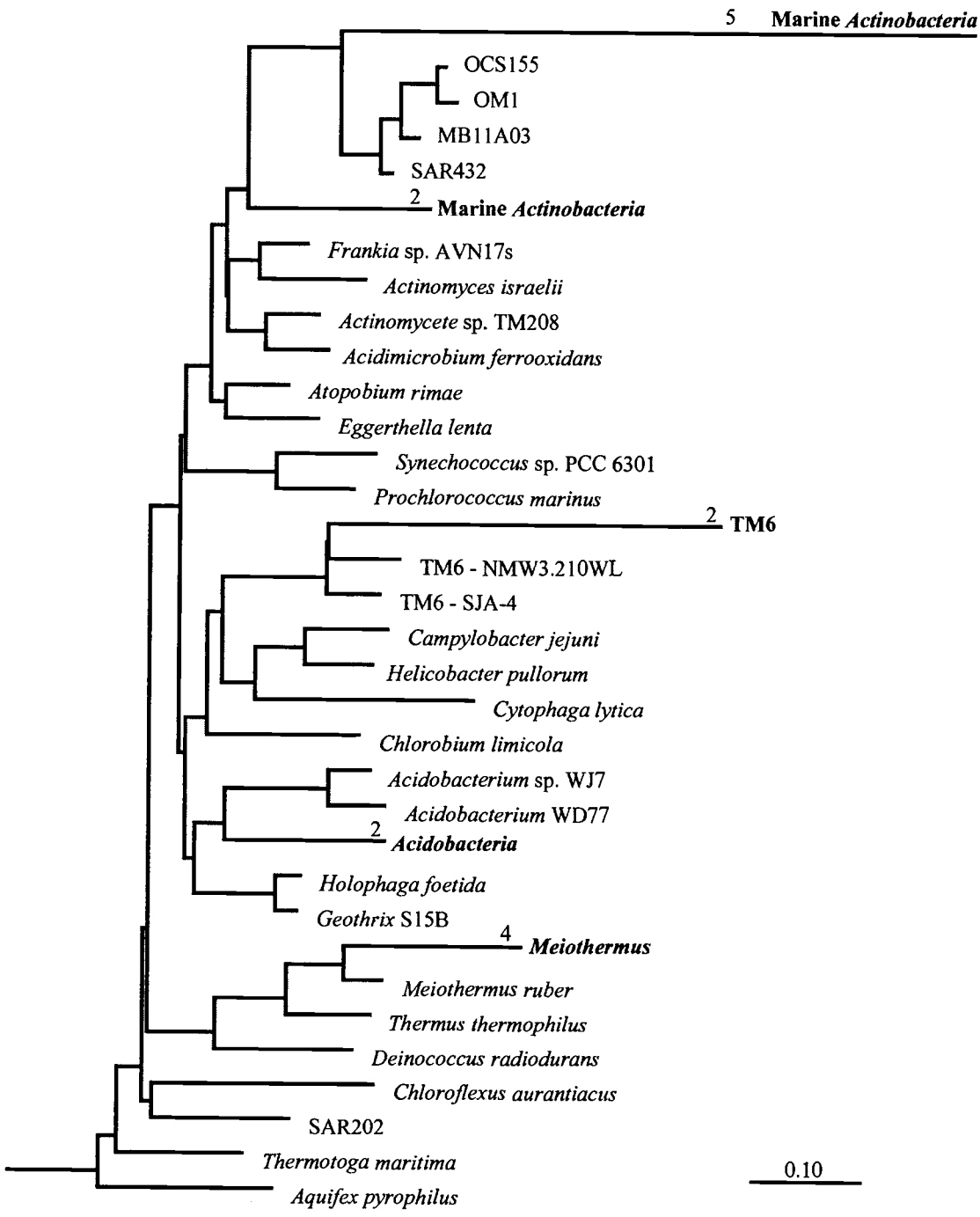

Figure 7-8 Maximum likelihood tree of the DGGE sequences indicating the phylogenetic affiliation of the sequences clustering with *Meiothermus*, the *Acidobacteria*, the Marine *Actinobacteria*, and the candidate group TM6 sequences. Archaeal sequences were used as the outgroup.

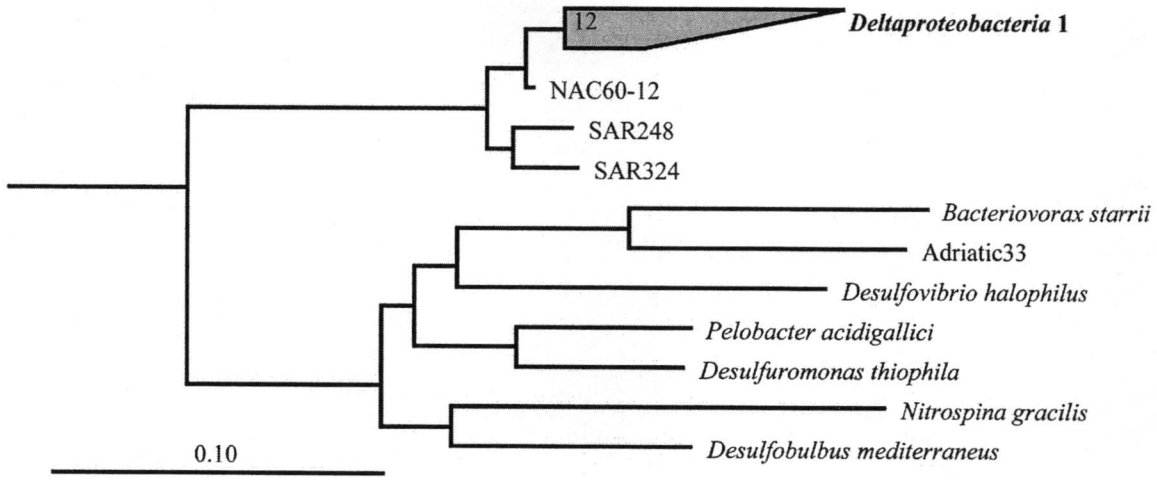

Figure 7-9 Maximum likelihood tree of the *Deltaproteobacteria* indicating the clustering of the sequences from the DGGE bands with the SAR324 sequences initially identified in the Sargasso Sea (Wright et al. 1997). Two *Betaproteobacteria* sequences were used as the outgroup.

7.2.4 Details on sequence distribution with depth

As discussed in Chapter 4, the distribution of the sequences did not vary greatly by depth, or by the depths sampled either within a station or between the three sampling stations. The pie graphs detailing the distribution by sampling depth and site are shown in Figure 7-10; the important details from the figure are summarized in Chapter 4.

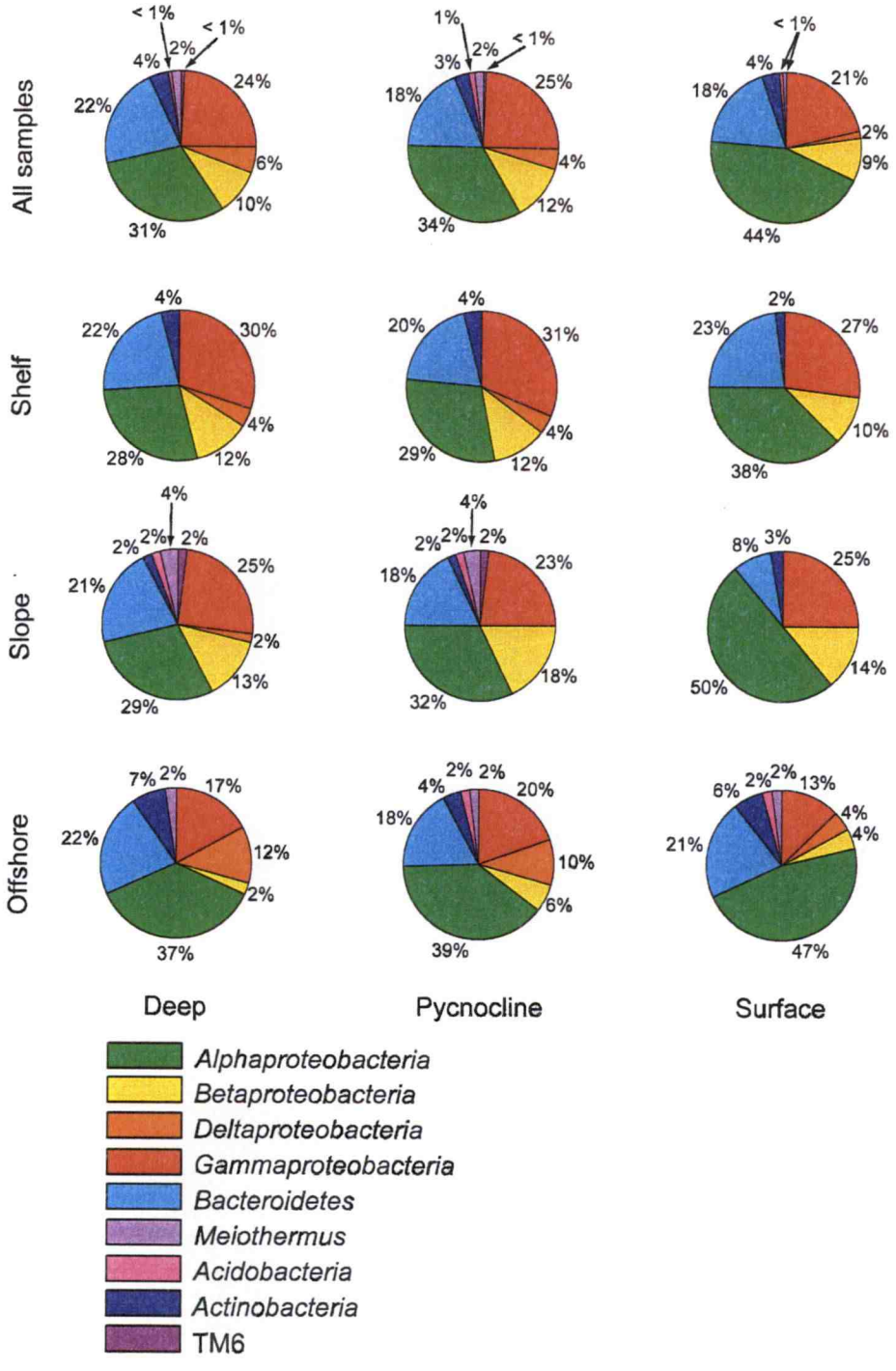

Figure 7-10. Pie graphs detailing the distribution of the sequences with sampling depth for all the stations, and for the shelf, slope and offshore station considered separately. The legend shown is the same legend used in Chapter 4.

7.3 Appendix literature cited

Wright, T.D., K.L. Vergin, P.W. Boyd and S.J. Giovannoni (1997). A novel δ-subdivision proteobacterial lineage from the lower ocean surface layer. *Applied and Environmental Microbiology* **63**: 1441-1448.

Zar, J.H. (1999). *Biostatistical Analysis*. Upper Saddle River, New Jersey, Prentice Hall.